

**TOWARDS UNDERSTANDING THE SPECTRAL AND TEMPORAL  
FLUORESCENCE BEHAVIOUR OF SOME ORGANIC SOLUTES IN  
CONVENTIONAL SOLVENTS AND ROOM TEMPERATURE IONIC LIQUIDS**

**A Thesis**

**Submitted for the Degree of  
DOCTOR OF PHILOSOPHY**

**by**

**Prasun Kumar Mandal**



**School of Chemistry  
University of Hyderabad  
Hyderabad 500 046  
INDIA**

**May 2006**

*To*

*My Family Members*

ॐ सह नाववतु ।  
सह नौ भुनक्तू ।  
सह वीर्यं करवावहै ।  
तेजस्वि नावधीतमस्तु ।  
मा विद्विषावहै ॥  
ॐ शान्तिः शान्तिः शान्तिः ॥

*I thank God for the most incredible adventure anyone could  
ever hope, wish or dream for – praise to you.*

## STATEMENT

I hereby declare that the matter embodied in the thesis entitled “*Towards Understanding The Spectral and Temporal Fluorescence Behaviour of Some Organic Solutes in Conventional Solvents and Room Temperature Ionic Liquids*” is the result of investigations carried out by me in the School of Chemistry, University of Hyderabad, Hyderabad, India under the supervision of **Prof. Anunay Samanta**.

In keeping with the general practice of reporting scientific investigations, due acknowledgements have been made wherever the work described is based on the findings of other investigators. Any omission or error that might have crept in is regretted.

**May 2006**

Prasun Kumar Mandal

SCHOOL OF CHEMISTRY  
UNIVERSITY OF HYDERABAD  
HYDERABAD-500 046, INDIA



Phone: +91-40-2301 1594 (O)  
+91-40-2301 0715 (R)  
Fax: +91-40-2301 2460  
Email: assc@uohyd.ernet.in  
anunay\_s@yahoo.com

---

Anunay Samanta, F.A.Sc.  
Professor

### CERTIFICATE

Certified that the work embodied in the thesis entitled ***“Towards Understanding The Spectral and Temporal Fluorescence Behaviour of Some Organic Solutes in Conventional Solvents and Room Temperature Ionic Liquids”*** has been carried out by **Mr. Prasun Kumar Mandal** under my supervision and that the same has not been submitted elsewhere for any degree.

Anunay Samanta  
(Thesis Supervisor)

Dean  
School of Chemistry  
University of Hyderabad

### *Acknowledgement*

*I would like to express my heartfelt gratitude to Prof. Anunay Samanta, my research supervisor, for his constant cooperation, encouragement, and kind guidance. I confess him as my true mentor in both academic and personal fronts.*

*I am gratified to Prof. M. Durgaprasad , for all his help and cooperation. Without his thought provoking discussions my research would not have been that easy.*

*I am quite thankful to Prof. P. Natarajan and Prof. P. Ramamurthy for the picosecond laser facility at National Centre for UltraFast Processes (NCUFP), Chennai. Special thanks are due to Mrs.V. K. Indirapriyadharsini for her help during decay measurement.*

*I would like to thank the former and present Dean(s), School of Chemistry, for their constant support, inspiration, and for the available facilities. I am extremely appreciative individually to all the faculty members of the school for their help, cooperation and encouragement at various stages.*

*I must express my heartfelt appreciation to dedicated teachers I got at different stages of my life. During school life Rezaul sir, Gurupada babu, and Subhash babu were much more than my teacher. The basis of being a good human being over a good student was implanted by them. In college Hrisikesh da and Asish Da (St. Xavier's College, Calcutta) impregnated the interest towards Physical Chemistry inside me. Arogya da, I just can't forget you for your dedication and self-sacrifice attitude towards the college. It is impossible for me to forget the discussion that you did with me after devastating result in B.Sc. part I. Satya da (Swami Suparnananda Ji Maharaj), your words are more than reality when I came out of the Narendrapur. I believe you as my life mentor. Dipankar da (Swami Sarbagananda Ji Maharaj), I am still following your advice despite strong attraction towards darker side of life. In University I got extremely good teachers like Dr. Sazzad Adnan , Dr. Subir Nath*

*Bhattacharya. Their teaching is much more than taking a class at the M.Sc. level. Theirs were one of the very few classes that I could enjoy. Dr. S. Mohanta's helpful advice on different domain of life is really encouraging.*

*My friends are real gem of my life. Starting from school level, Pradipta, Soumen, Pallab, Shanti, Santanu, Sudipta da, and Priya da were my chirping sparrows who used to cry and laugh together. In college life so many friends, I am scared to miss anyone, but definitely Debashis, Gautam, Tarun are still few of my best friends. In the university, Chaitali, Tanushree were much more than friends. I didn't really feel how the two apparently boring years passed by. If Tanushree was not there for taking class notes I wouldn't have passed M.Sc, frankly speaking. Sohaham da will always be remembered for being elder brother in different domain. Partha, Debu, and Amit were just like helpful brothers.*

*During doctoral work, my association with my senior colleagues like Saroja, Ramachandram, Satyen, Sankaran Rana, Sandip, Tamal is worth mentioning. I have learnt so many unwritten aspects, from them, both academically and non-academically in my research life. I acknowledge my junior friends, Moloy, Aniruddha, Bhaswati, and Ravi for maintaining a friendly and cooperative atmosphere in the lab. I would also like to thank three M. Sc. Project students, Narahari, Sreedhar, and Suresh, with whom I have spent wonderful time. I would really like to thank Sankaran for his help in learning instrument operation. Special thanks are due to Moloy and Bhaswati for their careful reading of the thesis. I cherish my association with Archan, Manab, Abhik, Sunirban, Binoy da, Masum, Bipul, Dinu da, Saikat, Prashant, Arindam, Tapta, Sandip, Pati, Shatabdi, Anindita, Rumpa, Subhash, Utpal, Tanmoy, Rakesh, Malla, Pavan, Venkatesh, Anoop da, Rashmi, Umar, Anand, Vinod, Harish, Pradeep, Sanjeeb, Abey while staying in the campus. I am scared whether I have missed some close people.*

*I thank all the non-teaching staff of the school for their time-to-time cooperation. They had all been quite helpful, Specially "Reagent" Shetty, Vijay Bhaskar, Bhaskar Rao, IR madam, were quite helpful.*

*Financial assistance from DST and CSIR, New Delhi is greatly acknowledged. Special thanks are due to CSIR and UPE programme of UGC for providing me the financial assistance for attending International Symposium on Methods and Applications of Fluorescence (MAF 9), Lisboa, Portugal, during September, 2005.*

*Due thanks to Sharath, Padmanabhan and Anoop da for helping me academically at times.*

*Joydeep, and Arnab, you both are such a pure and genuine soul, it is reflected in your attitude towards me.*

*I should acknowledge my wonderful parents for being so selfless and just offering me their complete understanding, love and support whenever I had asked for. Without your complete guidance I would not have been what I am now.*

*My incredibly supporting overprotective sisters, Mousumi, Gautami and Soumi, for taking me is such a pain. I truly appreciate it now!! (finally!)*

*My sweetest nieces, Srijanee and Oisee for being such a naughty yet beautiful. You both are sparkling young stars of my life.*

*Of course to my grand ma, for her blind love, and patience that she showed at the tender age of my life. Everyone should learn it from her how to pursue that much painful life of a widow yet loving everyone in the family.*

*Diya, of course for being so sweet. Your presence is just like music to me.*

*My parents in law, for being so much supportive and humorous and encouraging me on things I never thought of.*



*My two buddies of the HCU campus, Udit, who did try her level best to fill up the absence of my real life sisters, quite comfortably; and Kalyan, for being so much helpful whenever required. He is just a call away to help me. Thanks for the support you both have provided while my stay in Hyderabad.*

*When I am writing here twisting my hair, Ditipriya, my wife now and the then my best friend, might be thinking how come I have forgotten her. It's very difficult to forget you, for the space you have provided in these five years of apparently boring and frustrating life. The amount of patience and love you have kept for me, I just can't believe.*

*Prasun.*

### ***List of Publications***

1. "Evidence of Ground State Proton Transfer Reaction of 3-Hydroxyflavone in Neutral Alcoholic Solvents" **Prasun K. Mandal** and Anunay Samanta\* *J. Phys. Chem. A* (2003), **107**, 6334.
2. "Solvation Dynamics of Nile Red in a Room Temperature Ionic Liquid Using Streak Camera" S. Saha, **Prasun K. Mandal** and Anunay Samanta\* *Phys. Chem. Chem. Phys.* (2004), **6**, 3106.
3. "Excitation-Wavelength-Dependent Fluorescence Behavior of Some Dipolar Molecules in Room Temperature Ionic Liquids" **Prasun K. Mandal**, Moloy Sarkar and Anunay Samanta\* *J. Phys. Chem. A* (2004), **108**, 9048.
4. "How Transparent are the imidazolium ionic liquids? A case study with 1-methyl-3-butylimidazolium hexafluorophosphate, [bmim][PF<sub>6</sub>]" A. Paul, **Prasun K. Mandal** and Anunay Samanta\*, *Chem. Phys. Lett.* (2005), **402**, 375.
5. "On the optical properties of the imidazolium ionic liquids" A. Paul, **Prasun K. Mandal** and A. Samanta\*, *J. Phys. Chem. B* (2005) **109**, 9148.
6. "Fluorescence response of mono- and tetraazacrown derivatives of 4-aminophthalimide with and without some transition and post transition metal ions" N. B. Sankaran, **Prasun K. Mandal**, B. Bhattacharya and A. Samanta\* *J. Mater. Chem.* (2005), **15**, 2854.
7. "Fluorescence studies in environmentally benign solvents: Solvation dynamics of Coumarin 102 in [bmim][BF<sub>4</sub>]" **Prasun K. Mandal**, A. Paul and A. Samanta\*. *Res. Chem. Intermed.* (2005), **31**, 575.

8. "Fluorescence Studies in a Pyrrolidinium Room Temperature Ionic Liquid: Measurement of polarity and Solvation dynamics" **Prasun K. Mandal** and A. Samanta\*. *J. Phys. Chem. B* (2005), **109**, 15172.
9. "Solvation Dynamics in Room Temperature Ionic Liquids: Dynamic Stokes Shift Studies of Fluorescence of Dipolar Molecules" **Prasun K. Mandal**, S. Saha, R. Karmakar and A. Samanta\*. *Current Science* (2006), **90**, 301. (Review Article).
10. "Room Temperature Ionic Liquids as media for Photophysical Studies" **Prasun K. Mandal**, A. Paul and A. Samanta\*. *J. Chin. Chem. Soc.* (2006), **53**, 247.
11. "Excitation Wavelength Dependent Fluorescence Behavior of the Room Temperature Ionic Liquids and Dissolved Dipolar Solutes" **Prasun K. Mandal**, A. Paul and A. Samanta\*. *J. Photochem. Photobiol. A Chem.* In Press.
12. "Influence of Solvents with Hydrogen Bond Accepting Ability on the Photophysics of 2-(2'-hydroxyphenyl)benzoxazole, Revisited: Formation of Trans-Keto Species in the Ground State" **Prasun K. Mandal** and A. Samanta\*. (To be communicated).
13. "Solvent and Excitation Wavelength Dependent Photophysics of 4'-N, N-diethyl-3-hydroxyflavone: Emission from Higher Singlet Excited State, and Anion Formation" **Prasun K. Mandal**, K. Sridhar Reddy, and A. Samanta\*. (To be communicated).
14. "Synthesis and photophysical studies of a few Schiff bases based on 4-aminophthalimide." **Prasun K. Mandal** and A. Samanta\*. (To be communicated).

## ***Conference Proceedings***

### **Talk**

1. "Time-dependent Dynamic Stokes Shift of Fluorescence Emission: Solvation Dynamics in a Pyrrolidinium Room Temperature Ionic Liquid" **Indo-Japan Students Symposium**, University of Hyderabad, Hyderabad, January 10<sup>th</sup>, 2006.
2. "Unusual Red Edge Excitation Shift of Dipolar Solutes in Room Temperature Ionic Liquids" Chemfest, An In-house symposium of School of Chemistry, University of Hyderabad, Hyderabad, 4<sup>th</sup> March, 2006.

### **Poster Presentations**

1. "Photophysics in Room Temperature Ionic Liquids: Dual Fluorescence as Ratiometric Probe for Viscosity", **International Conference on Methods and applications of Fluorescence (MAF 9)**, Lisbon, Portugal, September 4<sup>th</sup> – 7<sup>th</sup>, 2005.
2. "Solvation Dynamics in Room Temperature Ionic Liquids", Discussion Meeting on Advances in Spectroscopy (**DMAS**), **Indian Institute of Science (IISc)**, Bangalore, February 21<sup>st</sup> – 24<sup>th</sup>, 2005.
3. "Solvent Dependent Photophysics of Second Excited State Singlet State and Red Edge effect (REE) of 4' - N, N-diethylamino derivative of 3-Hydroxyflavone", National Symposium on Radiation and Photochemistry (NSRP), University of Karnataka, Dharwad, January 17<sup>th</sup> - 19<sup>th</sup>, 2005.
4. "Edge Excitation Red shift of a Dipolar Probe in Room Temperature Ionic Liquids". Trombay Symposium on Radiation and Photochemistry (TSRP), **Bhaba Atomic Research Centre (BARC)**, Mumbai, January 8<sup>th</sup> – 12<sup>th</sup>, 2004.

## Thesis layout

The thesis has been divided into six chapters. **Chapter 1** provides a brief introduction of the excited state intramolecular proton transfer reactions, different properties of the room temperature ionic liquids, the molecular basis of the dynamic Stokes shift phenomenon and pertinent results of solvation dynamics studied in various media, and various examples and the underlying principles responsible for excitation wavelength dependent emission behaviour. **Chapter 2** provides procurement, synthesis, and purification of different chemicals, solvents, and room temperature ionic liquids. Moreover, the instrumentation and different methods employed in different investigations have also been outlined. **Chapter 3** depicts solvent mediated ground state proton transfer in 3-hydroxyflavone and thus the anion formation in neutral alcoholic solvents. **Chapter 4** describes the dynamic Stokes shift of fluorescence emission and thus measurement of solvation dynamics in an imidazolium and a pyrrolidinium cation based room temperature ionic liquids. **Chapter 5** discusses on the underlying reasons for the observation of excitation wavelength dependent fluorescence behaviour of some dipolar molecules in room temperature ionic liquids. **Chapter 6** summarizes the results of the investigations delineated in chapters 3-5. The scope of further studies based on the present work has also been outlined.

## Contents

Statement	i
Certificate	ii
Acknowledgement	iii
List of Publications	vii
Conference proceedings	ix
Thesis Layout	x
<b>Chapter 1    Introduction</b>	<b>1</b>
1.1.    Excited state intramolecular proton transfer	1
1.1.1.    Intrinsic intramolecular proton transfer	4
1.1.2.    Double proton transfer	5
1.1.3.    Catalysed proton transfer	5
1.1.4.    Proton transfer through relay	7
1.2.    Room Temperature Ionic Liquids	7
1.2.1.    A brief introduction	7
1.2.2.    Properties as alternative solvent	9
1.2.3.    Preparation	11
1.2.4.    Melting point	11
1.2.5.    Polarity	12
1.2.6.    Viscosity and density	13
1.2.7.    Thermal stability and volatility	14
1.2.8.    Conductivity	14
1.2.9.    Optical properties	15
1.2.10.    Structural organisation	15
1.2.11.    Applications	17
1.3.    Solvation dynamics	17
1.3.1.    Solvation in polar solvents	19

1.3.2.	High pressure solvation dynamics in alcoholic media	19
1.3.3.	Solvation dynamics in high temperature molten salts	20
1.3.4.	Solvation dynamics in ionic salt solution	20
1.3.5.	Solvation dynamics in confined environment	21
1.3.6.	Solvation dynamics in supercooled glasses	21
1.3.7.	Solvation dynamics in neat RTILs	22
1.4.	Excitation wavelength dependent fluorescence behaviour	26
1.4.1.	Initial background	26
1.4.2.	Theory of Red Edge Excitation Shifts	27
1.4.3.	Some examples of REE	29
1.4.3.1.	REE in proteins	29
1.4.3.2.	REE in polymer	29
1.4.3.3.	REE in micelles	30
1.4.3.4.	REE in phospholipid vesicles	30
1.4.3.5.	REE in low temperature glasses	31
1.4.3.6.	REE in different photophysical processes	31
1.4.4.	Molecular basis of REE	31
1.5.	Motivation of the present work	32
1.6.	References	35
<b>Chapter 2</b>	<b>Materials, Instrumentation and Methods</b>	<b>43</b>
2.1.	Materials	43
2.1.1.	Purification of conventional solvents	44
2.2.	Synthesis	46
2.2.1.	3-Methoxyflavone	46
2.2.2.	Room temperature ionic liquids	47

	2.2.2.1. Preparation of [bmim][BF <sub>4</sub> ] and [emim][BF <sub>4</sub> ]	47
	2.2.2.2. Preparation of [bmim][PF <sub>6</sub> ]	49
	2.2.2.3. Purification of the imidazolium RTILs	49
	2.2.2.4. Preparation of [bmpy][Tf <sub>2</sub> N]	50
	2.2.2.5. Purification of [bmpy][Tf <sub>2</sub> N]	50
2.3.	Instrumentation	51
2.3.1.	Picosecond time-correlated single photon counting setup	52
2.3.2.	Nanosecond time-correlated single photon counting setup	54
2.4.	Methods	55
2.4.1.	Sample preparation for spectral measurements	55
2.4.2.	Data analysis	56
2.4.3.	Construction of time resolved emission spectra	57
2.4.4.	Estimation of polarity in E <sub>T</sub> (30) and $E_T^N$ scale	59
2.4.5.	Standard error limits	61
2.4.6.	Theoretical calculation	61
2.5.	References	61
<b>Chapter 3</b>	<b>Solvent Mediated Ground State Proton Transfer in 3-hydroxyflavone: Anion Formation in Neutral Alcoholic Solvents</b>	<b>63</b>
3.1.	Introduction	63
3.2.	Results	65
3.2.1.	Spectral behaviour in aprotic solvents	65
3.2.2.	Spectral behaviour in protic solvents	67
3.2.2.1.	Absorption	67
3.2.2.2.	Fluorescence	70
3.3.	Discussion	73



	3.4. Conclusion	80
	3.5. References	80
<b>Chapter 4</b>	<b>Dynamic Stokes' Shift of Fluorescence: Solvation Dynamics in Room Temperature Ionic Liquids</b>	<b>83</b>
	4.1. Introduction	83
	4.2. Solvation dynamics in [bmim][BF <sub>4</sub> ] employing C102	87
	4.2.1. Steady state fluorescence studies	87
	4.2.2. Time-resolved fluorescence studies	89
	4.3. Solvation dynamics in a pyrrolidinium RTIL	92
	4.3.1. Steady state fluorescence studies	93
	4.3.2. Time-resolved fluorescence studies	95
	4.4. Conclusion	103
	4.5. References	103
<b>Chapter 5</b>	<b>Excitation Wavelength Dependent Fluorescence Behaviour of Some Dipolar Molecules in Room Temperature Ionic Liquids</b>	<b>107</b>
	5.1. Introduction	107
	5.2. Results	111
	5.3. Discussion	117
	5.3.1. Case of ANF	117
	5.3.2. Case of ANS and HNBD	119
	5.4. Conclusion	122
	5.5. References	123
<b>Chapter 6</b>	<b>Concluding Remarks</b>	<b>127</b>
	6.1. Overview	127
	6.2. Future prospects	131
<b>Appendix 1</b>		

## **Chapter 1**

### **Introduction**

---

A brief introduction to some of the photophysical processes, which the present thesis deals with, is presented in this chapter. Specifically, some fundamental information on excited state intramolecular proton transfer reactions has been provided briefly. Different physical properties of the room temperature ionic liquids have been described. The molecular basis of the dynamic Stokes' shift phenomenon has been discussed. Pertinent results on solvation dynamics in various media have also been concisely described. Various examples and the underlying principles responsible for excitation wavelength dependent emission behaviour, observed earlier for fluorophores embedded in highly viscous or rigid media, commonly termed as red edge effect, have been elaborated.

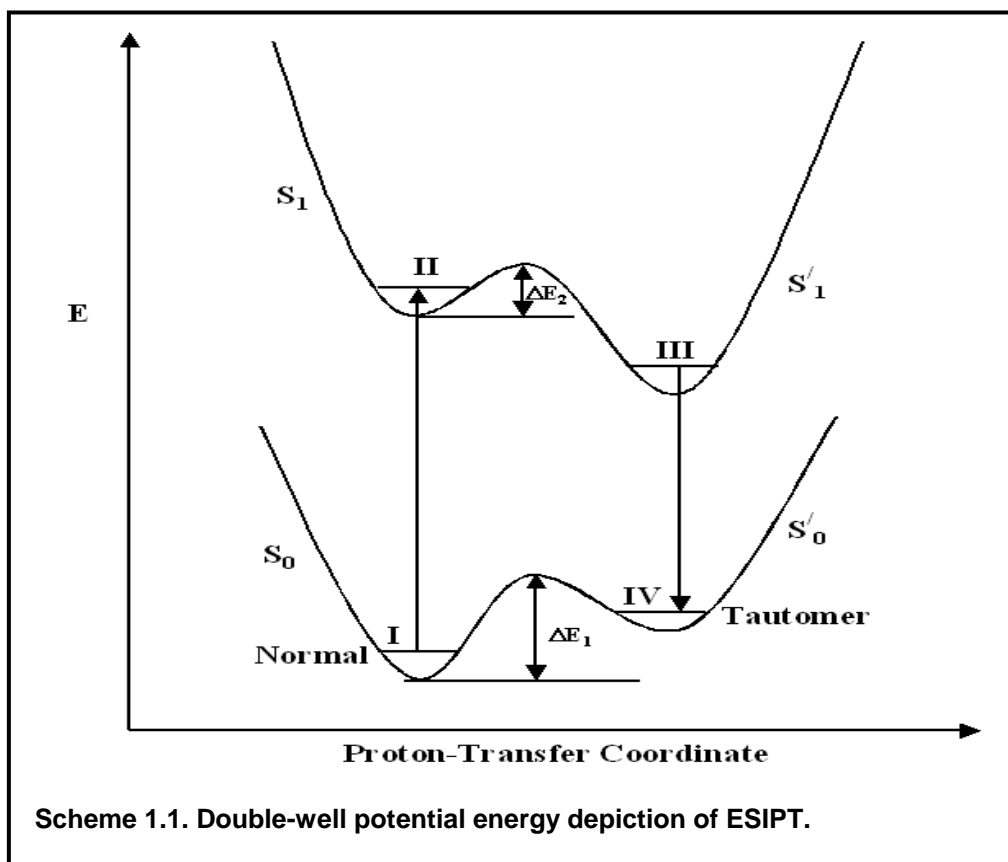
The motivation behind the projects undertaken winds up this chapter.

---

#### **1.1. Excited state intramolecular proton transfer**

Organic bi-functional molecules comprising both hydrogen bond donor and acceptor groups in close proximity form an intramolecular hydrogen-bonded structure in the ground state. Due to photonic excitation, there occurs a massive intramolecular redistribution of electronic charge and as a consequence the proton gets relocated from the hydrogen-bond donor group to the hydrogen bond acceptor group. This phenomenon is commonly termed as excited state intramolecular proton transfer (ESIPT). ESIPT reaction has been considered to be one of the simplest photoreactions of great importance in chemical and biological systems and has received a great deal of attention both experimentally

and theoretically.<sup>1-12</sup> ESIPT phenomenon is most commonly monitored using fluorescence technique. Excitation of an ESIPT system usually leads to dual fluorescence; one from the normal form of the molecule and another from the proton transferred i.e. tautomer form. The interplay between the molecular structure and potential energy surface has been shown to be quite important for an understanding of the mechanism of ESIPT.<sup>10</sup> Due to enormous change of the electronic distribution in the excited state, we observe that the tautomer fluorescence gets highly Stokes' shifted ( $6000 - 10000 \text{ cm}^{-1}$ ).<sup>3</sup> This phenomenon can be understood with the help of a double-well potential depicted in the following **Scheme 1.1**.



## *Introduction*

As can be seen from the above scheme, due to photonic excitation (from  $S_0 \rightarrow S_1$ ) there occurs huge electronic change and consequently the proton moves on a potential with double-well structure as shown above. In the ground state there exists significant energy barrier for the proton transfer, whereas, in the excited state the barrier becomes very small, but non-vanishing. The  $S_1 \rightarrow S_0$  energy gap of the tautomer is much lower than the normal form. Hence, large Stokes' shift is observed for the fluorescence originating from the tautomer.

ESIPT requires hydrogen bond formation between the proton donor (generally, a moiety containing  $-OH$  or  $-NH$  group) and the acceptor (generally, a moiety containing  $=N-$  or  $=O$  group). The dynamics of this ESIPT phenomenon, on a symmetrical double well potential, has been reviewed in literature.<sup>10,13</sup> The presence of an unsymmetrical double well potential is generally visualized as a representation of nearly barrierless proton transfer.<sup>7</sup> Quantum mechanical calculations have shown the impact of tunnelling effect and vibration dynamics of bonds involved in hydrogen bonded network on the proton transfer dynamics; thus the potential energy surfaces have shown to be dependent on the nature of the molecules.<sup>8,10</sup>

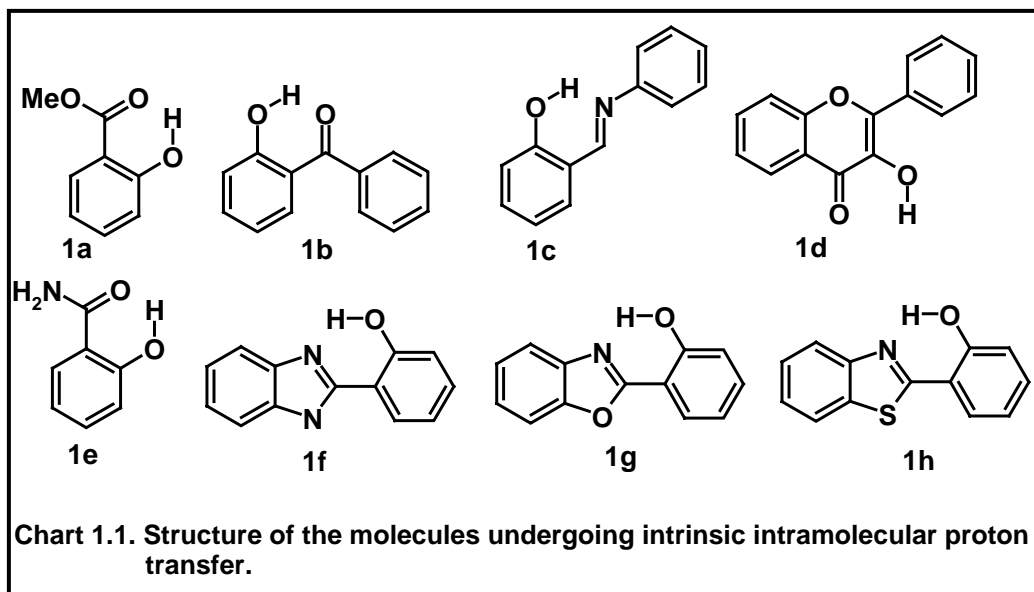
In aprotic solvents, where solvent perturbation is negligible, ESIPT phenomenon normally takes place through the pre-existing strong intramolecular hydrogen bonded structure. However, in protic solvents the solvent perturbation can become significant, particularly when the intramolecular hydrogen-bonding between the donor and acceptor moieties is less strong. In the latter cases, the intermolecular hydrogen bonded network inhibits to some extent the ESIPT phenomenon. The most striking feature of the proton transfer dynamics in aprotic solvents is its ultrafast nature, occurring in sub-picosecond to few femtoseconds timescale.

The ESIPT phenomenon has been utilised for various applications. Classical examples of these include four-level dye lasers, energy or data storage devices and optical switching,<sup>14-23</sup> Raman filters,<sup>24</sup> scintillation counters,<sup>25</sup> polymer stabilizers<sup>26,27</sup>. Moreover, different ESIPT molecules have been used in metal ion chelates.<sup>28</sup> These ESIPT molecules are known to possess photochemical stability, and are resistant to thermal degradation. Low self-absorption of the tautomer fluorescence has been utilised in electroluminescence.<sup>29</sup>

From the mechanistic point of view, the ESIPT phenomenon can be classified into four groups,<sup>3</sup> (i) intrinsic intramolecular proton transfer, (ii) double proton transfer, (iii) catalysed proton transfer, and (iv) proton transfer through relay. Each group is discussed separately as follows.

#### 1.1.1. Intrinsic intramolecular proton transfer

This is the simplest type of proton transfer, occurring in systems in which five/six-membered intramolecularly hydrogen bonded structure is present. Enormously studied, incomplete list of these molecules includes methyl salicylate (**1a**),<sup>30-32</sup> 2-hydroxybenzophenone (**1b**),<sup>33</sup> salicylidenaniline (**1c**),<sup>34</sup> 3-hydroxyflavone (**1d**),<sup>14,35-66</sup> salicylamide (**1e**),<sup>67</sup> 2-(2'-hydroxyphenyl)benzimidazole (**1f**),<sup>68-70</sup> 2-(2'-hydroxyphenyl)benzoxazole (**1g**),<sup>69,71,72</sup> and 2-(2'-hydroxyphenyl)benzothiazole (**1h**),<sup>73,74</sup> etc. (**Chart 1.1.**). In each case, specific molecular structure and conformation lead to specific behaviour. Environmental and/or solvent-cage perturbations have loomed large in the ESIPT studies of these molecules.



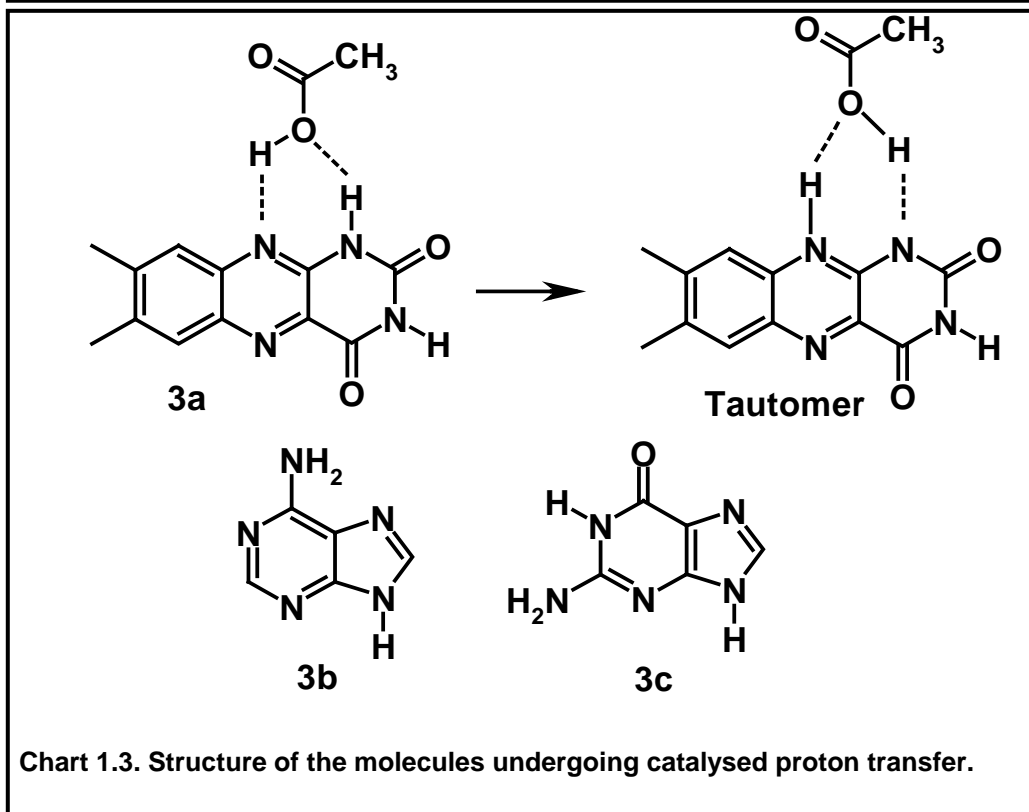
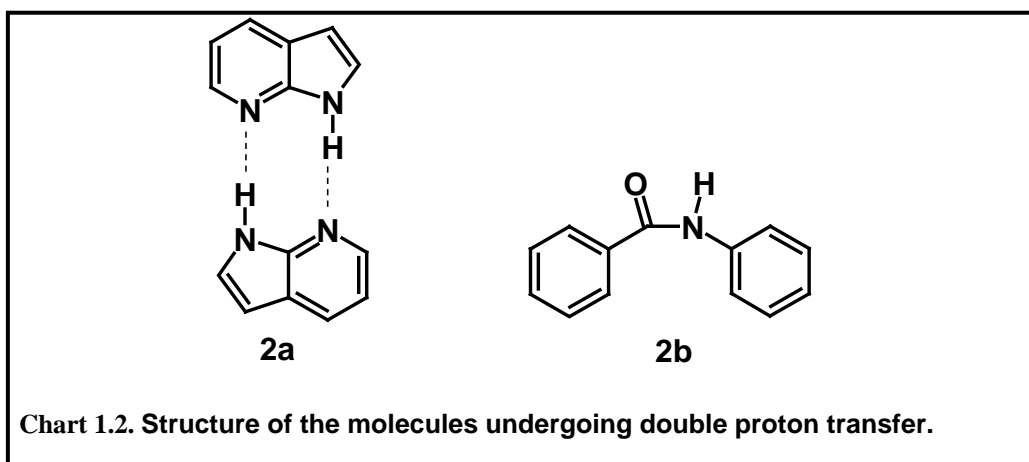
### 1.1.2. Double proton transfer

This type of proton transfer involves the formation of intermolecular hydrogen bonded network between two identical molecules. The first reported example of double proton transfer is 7-azaindole (**2a**).<sup>75-77</sup> At high probe concentration, in addition to the violet emission from the 'normal form' of the molecule, another green fluorescence is observed due to double proton transfer. Another molecule which shows similar biprotonic transfer is benzanilide (**2b**)<sup>78</sup> (Chart 1.2.).

### 1.1.3. Catalysed proton transfer

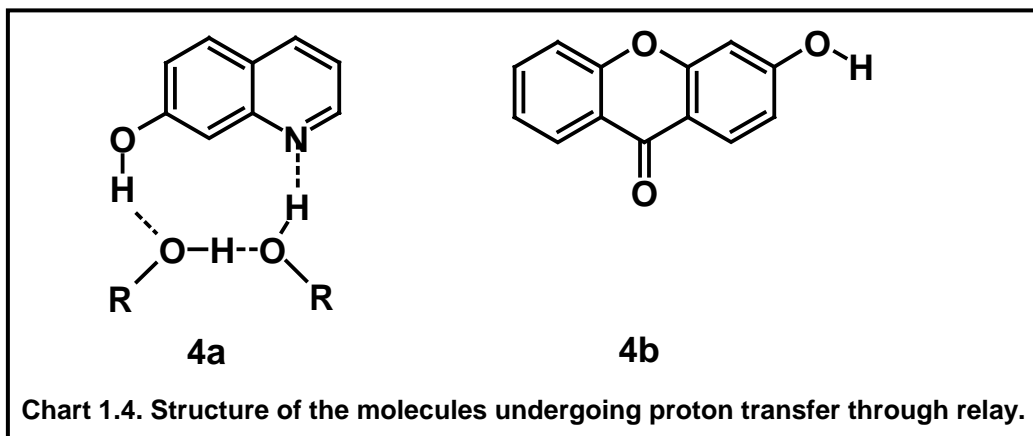
This is another type of double proton transfer, where the proton donor group is distal from the proton acceptor. A '*molecular companion*', (say acetic acid) must be involved in the form of a cyclic H-bonded complex, thus, acting as a '*catalyst*' for the proton transfer reaction of the reference molecule. 'Catalysed'

proton transfer has been reportedly observed in case of lumichrome (**3a**),<sup>79,80</sup> adenine (**3b**), and guanine (**3c**)<sup>3</sup> etc. (**Chart 1.3**).



#### 1.1.4. Proton transfer through relay

In this type of proton transfer the hydrogen bond donor and acceptor groups are quite distant, and two or more protons are transferred in a relay mechanism (say, with alcohol) via an extended H-bonded network, during the excited state lifetime of the fluorophore. Here the proton transfer is coupled through the electronic (inductive) effect of the cyclic complex. 7-hydroxyquiniline (**4a**),<sup>81</sup> 3-hydroxyxanthone (**4b**)<sup>82,83</sup> (**Chart 1.4.**) can be cited as examples of this type of proton transfer.



### 1.2. Room temperature ionic liquids

#### 1.2.1. A brief introduction

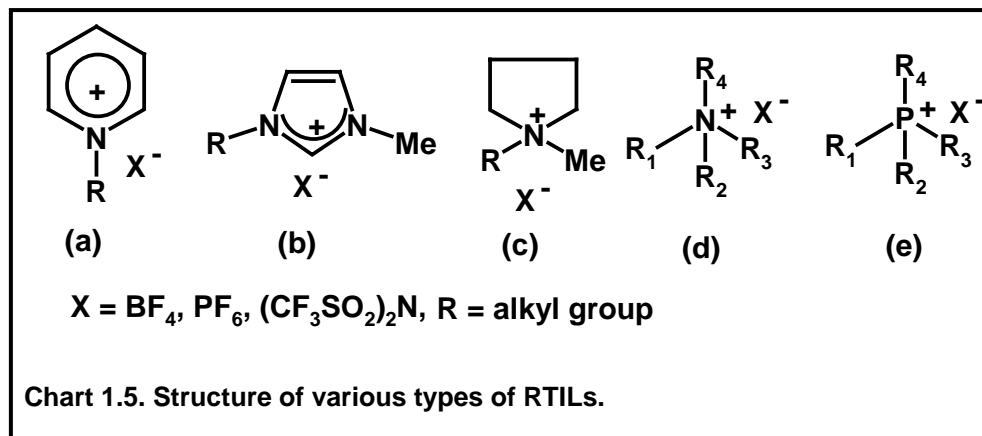
A significant effort in recent years has been directed towards finding suitable replacement for the conventional solvents, as these are volatile liquids used in large quantities for various purposes and are difficult to contain. The growing concern for increasing air and water pollution by these volatile organic compounds (VOCs) has brought forth a new branch in chemistry, namely **'green**



**chemistry**<sup>84</sup>. The quest for environmentally benign media has led to the realization of the importance of solvent free synthesis<sup>85</sup> and the use of water,<sup>86</sup> supercritical carbon dioxide<sup>87</sup> or room temperature ionic liquids (RTILs)<sup>88-96</sup>.

'Ionic liquids' are organic salts composed entirely of ions, which in their pure state are liquids below ca. 100<sup>0</sup>C. These are different from the 'molten inorganic salts', which are liquid at high temperatures (say, for NaCl the melting point is 803<sup>0</sup>C).<sup>92</sup> However, RTILs are liquid at ambient temperature and pressure. The lowest melting point reported so far for RTILs is -96<sup>0</sup>C.<sup>97</sup> First recognised RTIL, ([EtNH<sub>3</sub>][NO<sub>3</sub>]), was synthesized long ago in 1914.<sup>98</sup> However, the interest on RTILs started growing in the early '80s of the last century. Different types of RTILs based on pyridinium (**a**), imidazolium (**b**), pyrrolidinium (**c**), ammonium (**d**), phosphonium (**e**), etc. cations have been synthesized (**Chart 1.5.**).<sup>90</sup> Molten organic salts such as tetraalkylammonium and tetraalkylphosphonium salts were considered seriously for some time as a likely solvent system because of their relatively low melting points (between 50 – 250<sup>0</sup>C) and their ability to dissolve a wide variety of organic compounds. However, the moisture sensitivity, thermal decomposition and instability in acids of these salts have significantly restricted their usage.<sup>99-101</sup>

The discovery of air and water stable ionic liquids based on substituted imidazolium cation in 1992, has given a boost to the research activities on the ionic liquids.<sup>102</sup> Among the imidazolium salts, those involving [bmim] and [emim] (See **Chart 1.6.**) cations and [PF<sub>6</sub>], [BF<sub>4</sub>] and [(CF<sub>3</sub>SO<sub>2</sub>)<sub>2</sub>N] anions are most commonly studied.



### 1.2.2. Properties as alternative solvent

Some of the properties such as non-volatility, non-flammable nature, low reactivity, recyclable nature, wide liquid range and high thermal stability make these substances a neoteric alternative to the volatile organic solvents. Moreover, the RTILs dissolve a large variety of organic/inorganic substances. They also have high electrical conductivity and possess a wide electrochemical window<sup>103</sup>. Since the properties of the RTILs are largely dependent on the constituent ions, it is possible to obtain an RTIL having desired properties by proper choice of the two ionic components. It is therefore, not surprising, that the RTILs are termed as '**designer's solvent**'.<sup>88</sup> By virtue of iterative variations of available cations and anions,  $10^{18}$  numbers of RTILs (in comparison to  $\sim 500$  conventional solvents) have been visualized and thus, a large domain of physical and chemical properties could be available.<sup>88</sup> The concept of *task-specific ionic liquid* (**TSIL**) is also gradually becoming popular.<sup>104,105</sup> The *biphasic acid scavenging utilising ionic liquids* (**BASIL**) process has gained significant industrial attention.<sup>88</sup> The growing interest in RTILs is reflected in the enormous increase in the number of publications in recent years.

Table 1.1. Some physical properties of commonly known ionic liquids.

RTIL	T <sub>mp</sub> ( <sup>0</sup> C)	T <sub>d</sub> ( <sup>0</sup> C)	η(cP)	ρ(g/cc)	σ(ms/cm)	E <sub>T</sub> (30)
[emim][Cl]	86 <sup>a</sup>	-	s	s	-	-
[bmim][Cl]	65 <sup>a</sup>	-	s	s	-	-
[emim][BF <sub>4</sub> ]	6 <sup>a</sup>	447 <sup>b</sup>	66.5 <sup>c</sup>	1.25 <sup>c</sup>	13 <sup>d</sup>	49.1 <sup>e</sup>
[prmim][BF <sub>4</sub> ]	- 17 <sup>b</sup>	435 <sup>b</sup>	103 <sup>b</sup>	1.24 <sup>b</sup>	5.9 <sup>b</sup>	-
[bmim][BF <sub>4</sub> ]	- 81 <sup>f</sup>	435 <sup>b</sup>	154 <sup>c</sup>	1.2 <sup>c</sup>	3.5 <sup>b</sup>	48.9 <sup>e</sup>
[emim][PF <sub>6</sub> ]	60 <sup>g</sup>	-	s	s	5.2 <sup>d</sup>	s
[bmim][PF <sub>6</sub> ]	- 61 <sup>f</sup>	-	371 <sup>c</sup>	1.37 <sup>c</sup>	1.5 <sup>d</sup>	52.3 <sup>h</sup>
[emim][Tf <sub>2</sub> N]	- 3 <sup>i</sup>	-	34 <sup>i</sup>	1.52 <sup>i</sup>	8.8 <sup>i</sup>	47.7 <sup>j</sup>
[bmim][Tf <sub>2</sub> N]	- 4 <sup>i</sup>	>400 <sup>b</sup>	52 <sup>l</sup>	1.43 <sup>l</sup>	3.9 <sup>l</sup>	47.2 <sup>j</sup>
[bmpy][Tf <sub>2</sub> N]	-18 <sup>k</sup>	-	85 <sup>k</sup>	-	2.2 <sup>l</sup>	47.7 <sup>m</sup>

T<sub>mp</sub>: melting point; T<sub>d</sub>: decomposition temperature; s: solid; η: viscosity; ρ: density; σ: Specific conductivity; E<sub>T</sub>(30): microscopic solvent polarity parameter ref. 106

(a) ref. 91 ; (b) Nishida T. et al. *J. Fluorine Chem.* 2003, 120, 135.; (c) at 20<sup>0</sup>C, ref. 94; (d) at 25<sup>0</sup>C ref. 103; (e) ref. 107; (f) Watson, P. R. et al. *Langmuir*, 2001, 17, 6138.; (g) Haworth, D. et al. *Chem. Commun.* 1994, 299; (h) ref. 108; (i) at 20<sup>0</sup>C, ref. 109 ; (j) ref. 110; (k) (η at 25<sup>0</sup>C) ref. 111; (l) ref.111;(m) ref. 112.

### 1.2.3. Preparation

Synthesis of an RTIL involves two steps. The first step involves the reaction of 1-methylimidazole or 1-methylpyrrolidine with appropriate alkyl halide. This is followed by the replacement of the halide with the anion of choice. These steps have been elaborated in *Chapter 2*.

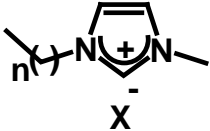
				
n =	1	2	3	5
X = BF <sub>4</sub>	[emim][BF <sub>4</sub> ]	[prmim][BF <sub>4</sub> ]	[bmim][BF <sub>4</sub> ]	
Tf <sub>2</sub> N	[emim][Tf <sub>2</sub> N]		[bmim][Tf <sub>2</sub> N]	
PF <sub>6</sub>	[emim][PF <sub>6</sub> ]		[bmim][PF <sub>6</sub> ]	[hmim][PF <sub>6</sub> ]

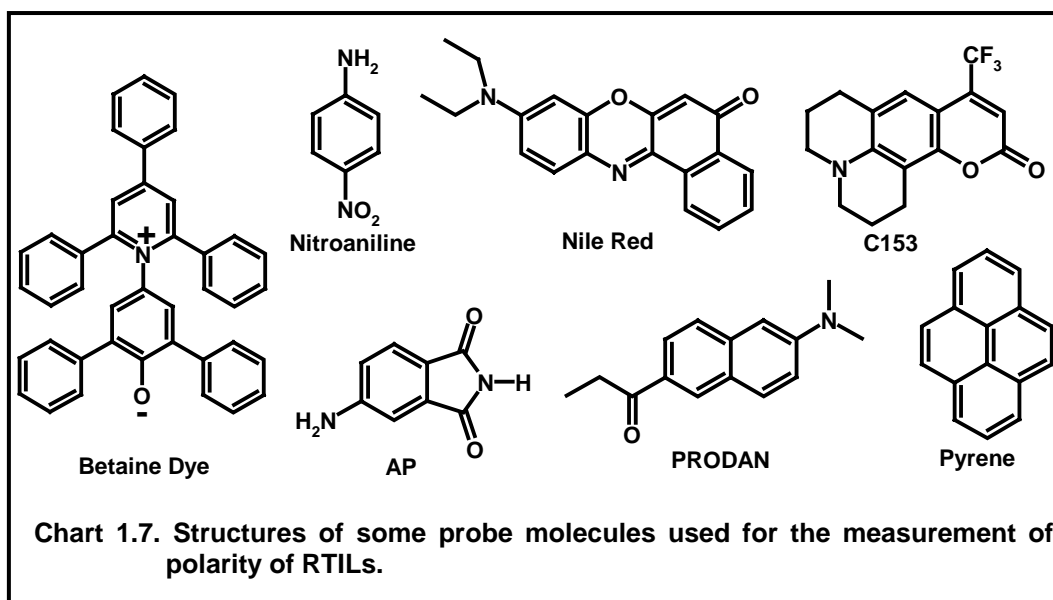
Chart 1.6. Structures and abbreviations of some imidazolium RTILs.

### 1.2.4. Melting point

Some of the physical properties of commonly used RTILs (**Chart 1.6**) have been put together in **Table 1.1**. As can be seen, the melting points of the commonly used RTILs are far below room temperature (25°C). The melting points of RTILs are uncertain, because they undergo considerable supercooling.<sup>96</sup> The temperature of the phase change can vary significantly, depending on whether the sample is being heated or cooled.

Several points have been put forward to answer the question *why do these RTILs have such a low melting point, in spite of being ionic in nature?* It has been established that the melting point decreases with increase in size and asymmetry of the cation. Moreover, the branching in the alkyl chain increases the

melting point.<sup>96</sup> Although the influence of the cation on the melting point is rather straightforward, the effect of anion is more difficult to rationalise. Lower melting point has been attributed to the more electron delocalisation and the relative inability of the anion to form hydrogen bonding with the hydrogens of the cations.<sup>96</sup> However, no simple correlation between the melting point and charge density of the anion and the number of C—H $\cdots$ X contacts could be derived till date.<sup>96</sup>



### 1.2.5. Polarity

Polarity of the RTILs has been measured by several groups,<sup>107-110,113-117</sup> mostly using steady state absorption or fluorescence techniques, in terms of the microscopic polarity parameter,  $E_T^{(30)}$  or  $E_T^N$ .<sup>106</sup> Different solvatochromic probes (See **Chart 1.7.**) have been employed for this purpose. The measured polarity of commonly used RTILs has been grouped in **Table 1.1.** As can be seen the RTILs

are more polar than acetonitrile but less polar than methanol. In fact, the polarity of most of the RTILs is similar to that of the short chain alcohols. The measured polarity of the same RTIL by different groups differs substantially in some cases.<sup>108</sup> This is presumably due to the fact that the purity of the RTILs, as used by different groups, is not the same.

#### **1.2.6. Viscosity and density**

The viscosity and density of some of the most commonly used RTILs (**Chart 1.6.**) have been provided in **Table 1.1.** The viscosity of the RTILs is generally much higher than that of the commonly used molecular solvents like hexane, acetonitrile or water. The viscosity of an RTIL has been shown to decrease with increase in the water content and temperature.<sup>96,97,118</sup> Generally, the viscosity follows a non-Arrhenius type of behaviour. However, most of the times the viscosity can be fitted to the Vogel-Tammann-Fulcher (VFT) equation.<sup>96</sup> Viscosity is shown to remain constant with the increasing shear rate.<sup>96</sup>

For RTILs with [Tf<sub>2</sub>N] anions the viscosity of the RTILs increases with increase in the number of carbon atoms in the alkyl chain. However the same is not the case of RTILs with [PF<sub>6</sub>] anions. Branching of the alkyl group of the imidazolium cation reduces the viscosity. The low viscosity of the perfluorinated anions has been attributed to the reduction of van der Waal interactions. Size of the anion, charge distribution, hydrogen bonding interactions, and sometimes symmetry of the anions plays a key role in determining the viscosity of the RTILs.<sup>96</sup>

The density of the RTILs is also much higher than the commonly used molecular solvents like hexane or water. The molar mass of the anions significantly affects the density. The density decreases with an increase in the anionic volume.<sup>96</sup>

### 1.2.7. Thermal stability and volatility

High thermal stability and nonvolatility are two of the interesting solvent properties of the RTILs that caught the attention of scientists. RTILs provide a wide liquid range (say from  $-10^{\circ}\text{C}$  till at least  $250^{\circ}\text{C}$ ). Beyond  $250^{\circ}\text{C}$ , some of the RTILs are reported to decompose.<sup>119</sup> The decomposition temperature decreases as the hydrophilicity of the anion increases. However, cations have no significant contribution in this regard.<sup>96</sup>

Until recently it was believed that RTILs have no vapour pressure and thus cannot be distilled. However, a recent report says that some of the RTILs have significant vapour pressure and thus, can be distilled under reduced pressure, without any decomposition.<sup>120</sup> Although the rate of distillation is very slow, it has been shown that both imidazolium and pyrrolidinium RTILs with  $[\text{Tf}_2\text{N}]$  anions do not decompose, even at  $300^{\circ}\text{C}$  (0.1 mbar) in the distillate or in the remaining portion. Therefore, distillation can also be used to purify the RTILs, especially those based on  $[\text{Tf}_2\text{N}]$  anions.

### 1.2.8. Conductivity

Since RTILs are composed entirely of ions, there is abundance of charge carriers, and thus large conductivity could be expected. However, as can be seen from **Table 1.1.**, the values are not large. The conductivity values of RTILs are similar to those of organic solvents with added inorganic electrolytes. The conductivity values generally decrease in the following order: 1-alkyl-3-methylimidazolium > N,N-dialkylpyrrolidinium > tetraalkylammonium.<sup>103</sup> This order has been attributed to the decrease in planarity of the cationic component. Among the RTILs having same cationic part but different anions, the conductivity values have been reported to be similar.<sup>121</sup>

### **1.2.9. Optical properties**

It was commonly accepted that RTILs are transparent beyond 300 nm and any absorption beyond this region is due to impurity present in the RTILs.<sup>109,122-124</sup> However, recent reports suggest that RTILs based on imidazolium moiety have significant absorption in the UV region and a long absorption tail extends into the visible region.<sup>125,126</sup> This absorption has been shown not to be due to any impurity, but inherent to the imidazolium moiety and different associated structures present in the system. More interestingly, these RTILs show dramatic excitation wavelength dependent fluorescence behaviour, which covers a large part of the visible region. This behaviour has been attributed to the different associated structures present in the RTILs and the inefficiency of the excited state energy transfer between these species.<sup>125,126</sup>

### **1.2.10. Structural organisation**

The structure of RTILs has been studied in the solid state as well as in solution using different spectroscopic techniques. A large number of theoretical studies have also been carried out in order to understand the structural organisation of the RTILs.

Imidazolium RTILs can be described as highly ordered polymeric hydrogen bonded supramolecules.<sup>127</sup> When the RTILs are mixed with other molecules they form nano-structured material with polar and nonpolar regions.<sup>127</sup> Hence RTILs should not be treated as homogeneous media.

X-ray crystallographic studies have shown  $\pi$ - $\pi$  stacking interaction among cation rings in case of imidazolium RTILs.<sup>128</sup> Moreover, weak C-H $\cdots$  $\pi$  interaction via the N-substituted methyl group and the imidazolium ring  $\pi$  system has also been detected.<sup>127,129</sup> In case of [emim][PF<sub>6</sub>], the interionic interactions are



dominated by cation-anion coulombic forces with minimal hydrogen bonding.<sup>130</sup> IR spectroscopic studies have revealed that the C-H...X hydrogen bonding remains intact even in the liquid state.<sup>131-135</sup> In case of octahedral [PF<sub>6</sub>] anion, it is the equatorial F atoms, whereas, in case of tetrahedral [BF<sub>4</sub>] anion only three of the four F atoms take part in the hydrogen bonding with protons attached to the 2<sup>nd</sup>, 4<sup>th</sup> and 5<sup>th</sup> carbon atoms.<sup>127</sup> Recoil spectrometry measurements with [bmim][PF<sub>6</sub>] have revealed that the bulk stoichiometry of cation and anions is maintained on the surface. The alkyl chain remains deeper in the surface and the plane of the ring remains vertically oriented.<sup>136</sup> Neutron diffraction analysis has shown significant charge ordering in the liquid state as well as in the solid state for dimethylimidazoliumhexafluorophosphate.<sup>127</sup> Deploying Raman spectroscopy it has been confirmed that the three-dimensional network is maintained in the liquid state also.<sup>137,138</sup> Multinuclear NMR experiments have proved the presence of contact ion pair, formed through hydrogen bonding between the imidazolium ring hydrogens and the halides, even in relatively polar molecular solvents such as propionitrile.<sup>96</sup> Quasistatic aromatic stacking of the imidazolium rings have also been observed in solvents like dichloromethane.<sup>131</sup> In dimethylsulfoxide (DMSO), the existence of solvent separated ion pairs has been reported even in dilute solutions. [bmim]Cl has been reported to form two different types of polymorphs.<sup>137,138</sup> Time-resolved Raman study on this RTIL revealed that the [bmim] cation forms two different types of '*mesoscopic local structures*'.<sup>137,138</sup> Optical Kerr effect,<sup>139</sup> small angle X-ray,<sup>140</sup> and sum frequency generation<sup>141</sup> experiments have also indicated the presence of '*local structures*'. The presence of different types of cation-cation, cation-anion local structures has been conclusively proved by the use of NOE and ROESY experiments.<sup>129,134,135</sup> A large volume of theoretical studies on the structural aspects of the RTILs have also

reported the variation of local structure present within RTIL.<sup>142-147</sup> Hence, RTILs cannot be treated as genuine liquids; rather these can be termed as “***nano-structured fluid***”.<sup>127</sup>

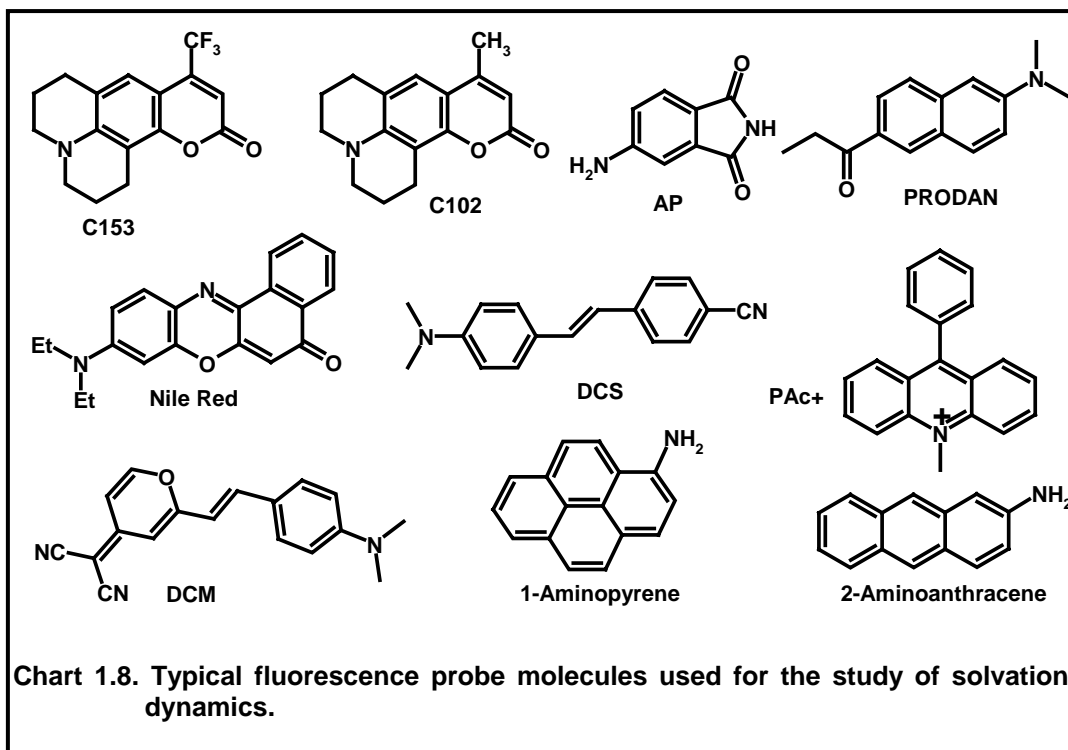
### **1.2.11. Applications**

An increasing usage of RTILs as media for organic synthesis,<sup>90-93</sup> liquid-liquid extraction,<sup>148</sup> electrochemical studies,<sup>103</sup> mass spectrometry,<sup>149</sup> biocatalysis,<sup>150</sup> solar cells,<sup>151</sup> synthesis of nanoparticles,<sup>152</sup> gas sensor,<sup>153</sup> etc. has been documented in literature. RTILs are also used as a stationary phase for gas chromatography.<sup>154</sup> Moreover, RTILs are known to provide proton transfer "support" properties when used as electrolytes for fuel<sup>155</sup> and solar<sup>156</sup> cells. They are also known to form “ionogels”<sup>157</sup> and inclusion compounds with aromatic molecules and also known to dissolve surfactants.<sup>158</sup> Different steric and electronic protecting properties for nanoparticles,<sup>159</sup> stabilization of enzymes<sup>160</sup> are also reported.

### **1.3. Solvation dynamics**

Solvation is an important phenomenon in chemistry and biology.<sup>161-190</sup> Solvation dynamics represents the rate at which the solvent dipoles or charged species get re-arranged surrounding a newly created photo-induced dipole of the solute. Instantaneous excitation with an ultra-short laser pulse, creates a change in electronic rearrangement of the probe molecule, and thus perturbs the equilibrium arrangement of the solvent dipoles around the probe molecule. Consequently, the solvent molecules reorient themselves around the newly created dipole. The time taken for this rearrangement of the solvent molecules to form a new equilibrium configuration around the excited probe molecule is generally referred to as the relaxation time of that solvent. This relaxation time

strongly depends on the viscosity, the molecular structure of the solvent as well as the temperature of the medium. In conventional molecular solvents, at room temperature, the excited state equilibrium is reached prior to emission because the solvent relaxation times are typically less than 100 picosecond, whereas the emission decay times are in the order of a few nanoseconds. However, the relaxation becomes much slower in a viscous solvent and in proteins or in membranes. In these cases, the emission occurs during the solvent relaxation and this results in a time-dependent shift in the emission spectra. This phenomenon is most pronounced when both probe (See **Chart 1.8.**) and the solvent are dipolar or charged species.



The dynamics of solvation is known to dictate the reaction rates of electron and proton transfer etc. in polar solvent. The method of studying solvation dynamics using dynamic Stokes' shift technique has been elaborated in *Chapter 2*.

### **1.3.1. Solvation in polar solvents**

The process of solvation is usually extremely fast in conventional solvents due to very fast reorientation of the solvent molecules. Using ultrafast time-resolved studies, it has been shown<sup>171</sup> that in majority of solvents, where specific interaction like hydrogen bonding is not important, the solvation times are in the sub picosecond time scale at room temperature. The result can well be explained using non-specific theories of solvation dynamics. The linear correlation between experimentally observed average relaxation time and longitudinal relaxation time, as predicted by simple continuum theory, depends primarily on the nature of solute-solvent interaction and temperature of the medium. Deviation from the above can be accounted for, considering the molecular nature of the solvent, translational contribution to the solvent relaxation and specific hydrogen bonding ability of the protic solvent.<sup>175,178,179</sup>

### **1.3.2. High-pressure solvation dynamics in alcoholic media**

Using picosecond dynamic Stokes' shift technique, Hara and co-workers have studied the effect of enhanced pressure on solvation dynamics in alcoholic solvents, with C153 as the fluorescence probe.<sup>191</sup> An excellent correlation between the high pressure average solvation time and the longest longitudinal relaxation time was observed. Huppert and co-workers made a similar observation while studying the solvation dynamics in ethanol using Coumarin 480 as the solvation probe, at much higher pressure.<sup>192</sup> At normal pressure, ethanol

shows usual monomeric relaxation process with a relaxation time of 35 ps. As the pressure is increased, ( $> 0.5$  GPa), the solvation becomes biexponential in nature. At 0.52 GPa the average of biexponential solvation times was measured to be 85 ps. For an applied pressure of 1.55 GPa, a biphasic solvation time of 110 ps and 500 ps, with an average relaxation time of 410 ps was observed. This slow dynamics has been explained on the basis of liquid-solid phase transition of ethanol at high pressure. Surprisingly, in solid phase, relaxation occurs at a relatively faster rate with an average time of 360 ps, quite similar to that in liquid phase at the same pressure. The faster relaxation process in solid crystalline alcohol has been ascribed to rapid reorientation of the ethanol molecule in the vicinity of the fluorophore.<sup>192</sup>

### 1.3.3. Solvation dynamics in high temperature molten salts

Huppert and co-workers have studied the solvation dynamics in different high temperature molten salts.<sup>188-190</sup> In all these cases, the solvation process was found to occur in two different time scales (picosecond and nanosecond). The average solvation time in molten salt was found to be higher than that observed in pure solvent or electrolyte solutions. Huppert and co-workers explained this slow solvation by taking into account the translational motion of the constituting ions present in the media. According to them, the fast component of the dynamics is due to the translational motion of the smaller species, i.e. the anion and the slower one is due to the larger cation. However, both the solvation times were found to be dependent on the cation size and the chosen probe molecule.

### 1.3.4. Solvation dynamics in ionic salt solution

The dynamics of solvation in ionic solution (metal perchlorate and halide salts in non-aqueous solvents with different polarity) has been studied using

common solvation probes.<sup>177</sup> The solvent response functions could be extracted, either by single exponential or biexponential decay function, depending on the salt concentration. The ionic solvation was observed to be rather slow (1-10 nanoseconds) compared to that in conventional solvents. Solvation rate was found to decrease with the solvent polarity and charge to size ratio of the cation.

### **1.3.5. Solvation dynamics in confined environment**

The relaxation in pure water is biexponential in nature with an ultrafast relaxation time of 126 fs and a relatively slower one, 880 fs.<sup>170</sup> According to Fleming et al., the faster component arises due to intramolecular vibration of the water molecule and the slower one because of librational motion.<sup>170</sup> Study of solvation dynamics in 'confined water' of various organized assemblies, which include model systems such as micelles and reverse micelles or real systems such as proteins, membranes, DNA etc., is a topic of considerable interest<sup>163,174,183-187</sup> Recent studies by different groups, have shown that the solvation dynamics in confined water bodies is drastically different from that in ordinary bulk water. The solvation response is found to be biphasic in nature. The faster sub-picosecond component is associated with a slower component, which can be as large as hundreds to thousands of picoseconds. The slow component has been attributed to the dynamic exchange between free and bound water molecules.<sup>163,174,183-187</sup>

### **1.3.6. Solvation dynamics in supercooled glasses**

In case of non-ionic glass forming liquids, it has been observed that the dynamics occur in two widely different timescales.<sup>193,194</sup> The faster component has been ascribed to the "phonon-induced" or "inertial motion", whereas the slower component has been ascribed to the "diffusive" or "structural relaxation".

The slower solvation component is observed to track the solvent viscosity and its magnitude, slows down further as the temperature is decreased and approaches the glass transition temperature ( $T_g$ ). As the temperature is reduced, the relaxation becomes more and more distributed and slowed down. Similar non-exponential dynamics has also been observed by other groups.<sup>195,196</sup> Although there is controversy between the homogenous vs. heterogeneous origin of such non-exponential relaxation in glass forming liquids, spatial heterogeneity is proposed to be the cause of the distribution kinetics in those systems.<sup>197,198</sup>

### 1.3.7. Solvation dynamics in neat RTILs

Since the RTILs are sufficiently polar, time-resolved fluorescence studies were expected to provide information on the reorganization of the constituent ions around the photoexcited dipolar probe molecule. This idea prompted the study of solvation dynamics in RTILs.<sup>110,115-117,199-205</sup> These studies have indicated the biphasic nature and slowness of the solvation dynamics in RTILs. Biphasic nature consists of a faster component of solvation, which is in picosecond time scale, and a slower component, which is in the nanosecond time scale. For moderately viscous imidazolium RTILs the faster component varies from 125 to 280 ps whereas the slower component varies from 0.65 to 3.98 ns.<sup>110,117</sup> The average solvation time is found to be consistent with the viscosity of the RTIL. The results of these studies have been presented in **Table 1.2**. The average solvation time is found to be dependent on probe molecules.

These studies have also shown that despite the high viscosity of these RTILs, nearly 50 % of the total spectral relaxation is too fast and cannot be measured accurately using setup having a time resolution of 25 ps,<sup>110,117</sup>. Interestingly, this ultrafast solvation component could not be observed in ammonium and phosphonium RTILs. This observation has been rationalised

proposing that the ultrafast component of dynamics in imidazolium RTILs arises due to small amplitude motions of one or more cations in close contact with the solute and is facilitated by the coplanar arrangements of the solute with the imidazolium nearest neighbours.<sup>200</sup>

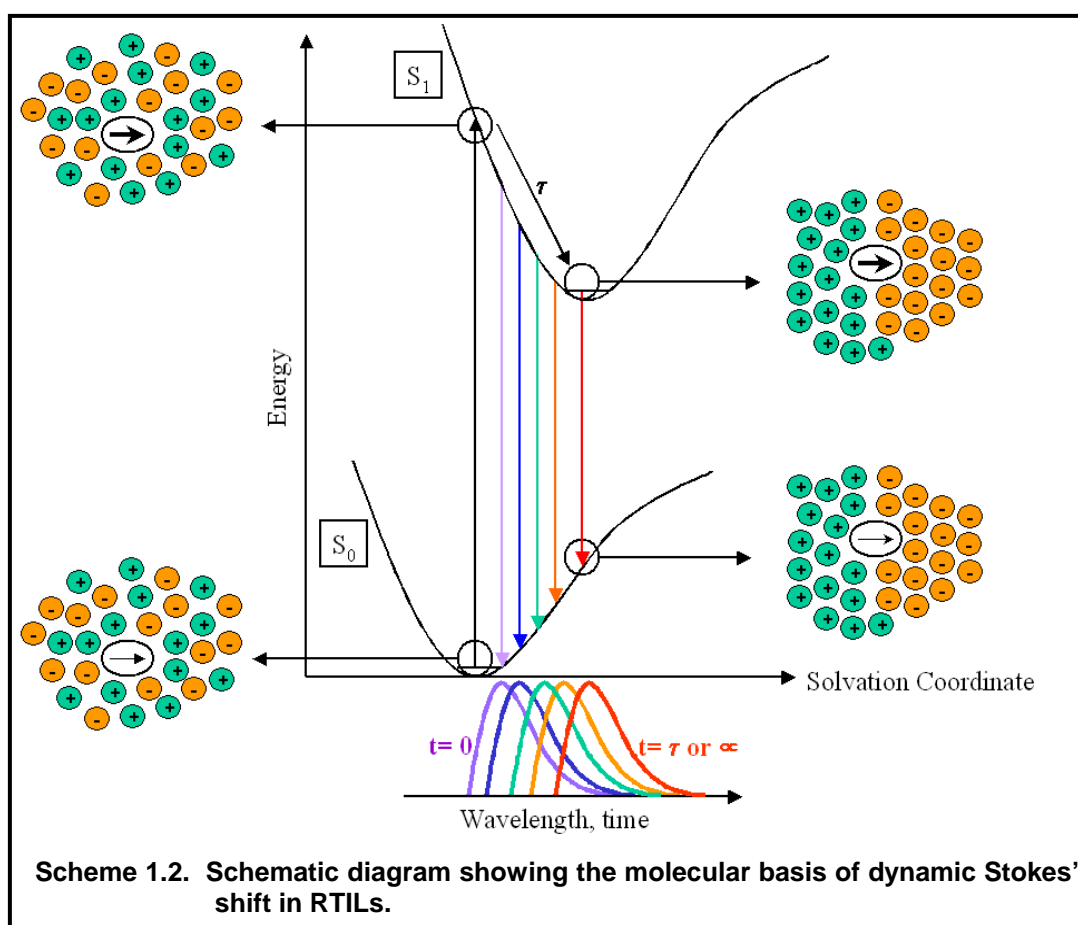
**Table 1.2. Measured average solvation time  $\langle\tau\rangle$ , in various imidazolium RTILs.**

RTIL	Viscosity (cP)	Probe	$\langle\tau\rangle$ (ps)	Reference
<b>[emim][BF<sub>4</sub>]</b>	66.5	C153	440	110
		PRODAN	680	110
<b>[bmim][BF<sub>4</sub>]</b>	154	C153	2130	110
		PRODAN	1440	110
		C153	460	204
		C102	850	206
<b>[emim][Tf<sub>2</sub>N]</b>	34	C153	280	117
		AP	370	117
		PRODAN	270	117
<b>[bmim][Tf<sub>2</sub>N]</b>	52	C153	480	117
		AP	380	117
		PRODAN	560	117
		C153	720	204
<b>[bmim][PF<sub>6</sub>]</b>	207 <sup>α</sup>	AP	1400	199
		C102	1800	199
		PRODAN	1800	200
		C153	1000	200
		AP	1600	200
		C153	1000	204
		C153	3350	202
		C152	2760	202
		Nile Red	1010	115
<b>[hmim][PF<sub>6</sub>]</b>	363	C153	6960	202
		C152	6090	202

<sup>α</sup> Viscosity of [bmim][PF<sub>6</sub>] in ref. 200 and 204 is reported to be 260 cP and 371 cP.



The polarizability of the cations is also thought to be responsible for the fast component.<sup>204</sup> Clearly, there is disagreement on the origin of the ultrafast components. There is also dispute on how fast the ultrafast component is. It was reported earlier that the ultrafast component is shorter than 5 ps.<sup>205</sup> However, with subpicosecond time resolution measurement, it has been suggested recently that the ultrafast time constant is around 40-70 ps.<sup>204</sup>



While in the case of molecular solvents, the reorientation of the solvent molecules around the photoexcited dipole is responsible for solvation; the

diffusional motion of the constituent ions mainly contributes to solvation in the case of RTILs. This has been illustrated using a simplified diagram (**Scheme 1.2.**).

Various theoretical molecular dynamics simulation studies have been performed by several groups to investigate the structure and dynamic properties of the RTILs.<sup>207-213</sup> Shim et al. have studied solvation using molecular dynamics simulation of [emim]Cl and [emim][PF<sub>6</sub>] using a *diatomic* probe molecule.<sup>207</sup> They found a sub-picosecond component of the solvation dynamics due to the anion translation. Kobrak et al., on the other hand, have shown that collective cation and anion motions are responsible for the fast component.<sup>211</sup> This disagreement can probably be attributed to the difference in the treatment of the probe molecules by the two groups. Shim et al. considered a diatomic molecule of 3.5 Å bond length, whereas Kobrak et al. used a much larger and more realistic, betaine dye as the probe molecule. Thus while the model of Shim et al. may be relevant to small molecule dynamics, the model of Kobrak et al. is more pertinent to studies involving large aromatic probe molecules used in solvation studies. The results of Kobrak et al. contradict the suggestion that cation and anion motions occur on different timescales and instead, these attribute the two different timescales of solvation to different length scales for solvation response. Shim et al. have recently examined the solvation structure and dynamics in RTILs using both diatomic and benzene like probes.<sup>212,213</sup> Both equilibrium and non-equilibrium solvation dynamics are characterized by a subpicosecond inertial regime and a slow diffusional regime.<sup>212,213</sup> Solvent region contributing to the subpicosecond dynamics is found to vary significantly with the inertial solvent configuration near the solute. In case of high local solvent density near the probe at the moment of excitation, the subpicosecond relaxation is governed mainly by

the motion of a few ions close to the probe molecule. However, for low initial density, the solvent ions, which are even farther away, contribute to the subpicosecond solvent relaxation process.

## **1.4. Excitation wavelength dependent fluorescence behaviour**

### **1.4.1. Initial background**

That the fluorescence of a polyatomic molecule in condensed media originates from the lowest vibrational level of the lowest electronic state of the same multiplicity, irrespective of the excitation energy is one of the most commonly accepted concepts, known as Kasha's rule.<sup>214</sup> Therefore the emission spectrum is expected to be independent of excitation wavelength.

However, shift of the fluorescence maximum of some systems towards longer wavelength with an increase in the excitation wavelength was observed as long as thirty years ago. Three groups independently and simultaneously reported this phenomenon.<sup>215-217</sup> In low temperature glasses, they found that when the excitation is performed at the longer wavelength slope of the absorption spectrum, the fluorescence spectra starts shifting towards the higher wavelength side with increase in the excitation wavelength.

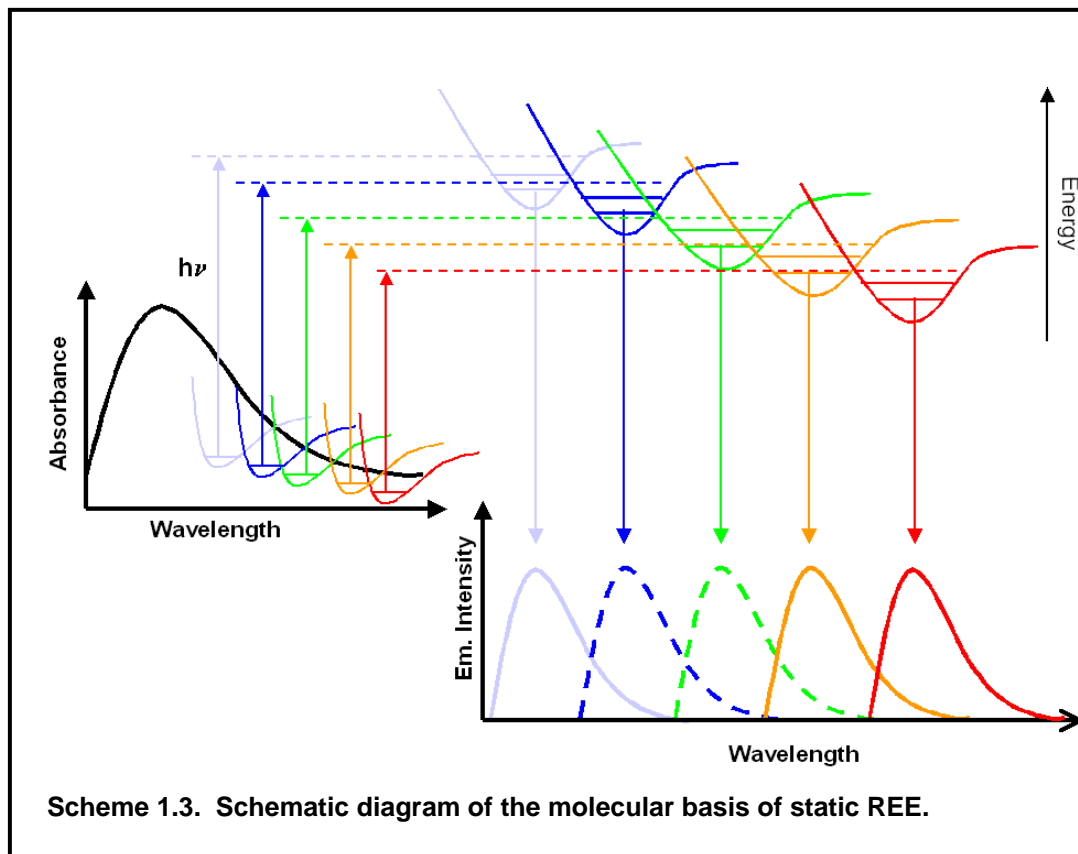
These unusual observations termed as 'Red Edge Effect' (REE) were shown to be the consequence of *inhomogeneous broadening* of the absorption band to a distribution of the solute-solvent interaction energy and the failure of the excited state energy transfer.<sup>218,219</sup>

Different acronyms other than REE are also used to describe this phenomenon. These are edge excitation shift (EES), edge excitation red shift (EERS) or red edge excitation shift (REES). Several researchers have exploited REE in biological systems and an excellent recent review on this topic is available.<sup>218</sup>

#### **1.4.2. Theory of Red Edge Excitation Shifts**

Some of the earlier interpretations of REE involved emission from multiple states or different conformers of the molecule.<sup>218</sup> However, it is now generally accepted that two conditions must be satisfied to observe REE. First, there must be a distribution of solute-solvent interaction energy leading to inhomogeneous broadening of the absorption spectrum.<sup>218,219</sup> This inhomogeneity, which always exists in condensed media, is particularly prominent for the dipolar systems in polar media. In organised assemblies, where REE is most common, the inhomogeneity also arises due to the spatial heterogeneity of these assemblies, which consist of the hydrophobic and hydrophilic pockets that allow multiple solvation sites and contribute to inhomogeneous broadening of the absorption spectra.<sup>218</sup> The presence of an ensemble of energetically different molecules in the ground state *alone* does not guarantee an excitation wavelength dependent fluorescence behaviour as rapid relaxation of the excited state is likely to result in fluorescence from the lowest excited state.<sup>218,219</sup>

Therefore, the second condition that must be met to observe REE is that the excited state relaxation of the fluorescent species, which can be solvation or energy transfer from the fluorescent state to a low lying energy state of the molecules, must be slower or comparable to the fluorescence lifetime of the species. This condition ensures that it is possible to observe emission from the unrelaxed photoexcited species rather than that from the lowest excited state.<sup>218,219</sup>



REE is observed only when the excitation is made at the red side of the absorption maximum. This is primarily because the molecules absorbing at the red side of the absorption band have stronger solute-solvent interaction.<sup>218</sup> The mechanism of the REE phenomenon has been depicted in **Scheme 1.3**.

However, it is now understood that the unusual excitation wavelength dependent emission behaviour does not really violate fundamental principles such as the Kasha's rule. Rather, this unusual observation is due to the operation in some specific conditions, whereby the molecules in the ensemble are distributed in different interaction energy domain with the surrounding molecules.

Thus, the fundamental assumptions based on which Kasha's rule was formulated do not hold here. Therefore, REE phenomenon should not be considered as the one, which contradicts Kasha's rule.<sup>218</sup>

#### **1.4.3. Some examples of REE**

REE phenomenon has been observed in different media for a variety of fluorophores, some of which are discussed below.

##### **1.4.3.1. REE in proteins**

Human serum albumin was the first protein for which REE has been reported.<sup>220</sup> Its tryptophan residue, when located in the ligand-binding pocket and is partially exposed to the solvent, negligible REE can be observed. However, due to isomerisation of the tryptophan residue at acidic pH or when the ligand-binding pocket is occupied by a hydrophobic ligand at neutral pH, a dramatic REE of 7-11 nm can be observed.<sup>220</sup> Systematic studies have revealed that those proteins having emission maximum in the range of 320-340 show REE phenomenon.<sup>221,222</sup> When the fluorescence maximum is beyond 340 nm, REE is not observed because of the high flexibility of those proteins and the access of the tryptophan residue to the rapidly relaxing solvent. Again when the emission maximum is below 320 nm, REE is not observed. This is because tryptophan environment is highly hydrophobic and the dielectric effects are not significant for the observation of REE.

##### **1.4.3.2. REE in polymer**

First reports of REE in polymer media were made with dimethylaminobenzonitrile (DMABN) in polymethyl methacrylate,<sup>223</sup> pyridine merocyanine dye in polyvinyl alcohol<sup>224</sup> and tert-butyl ester of anthroic acid in

different polymeric glasses<sup>225</sup>. The ground state heterogeneity is the primary cause for the observation of REE in these cases. Excitation at the red edge selects a subclass of conformers, which are more planar, and hence absorb lower energies than the other species.

Bianthryl in glassy polymer matrices exhibits REE.<sup>225</sup> In this case it is not the ground state heterogeneity that gives rise to REE. For those species, which interact strongly with the dielectric environment, the excited state electron transfer reactions are found to be more favourable than other species in the distribution. This is the cause of REE for bianthryl. Excitation at the red edge results in the loss of vibrational structure and a shift of the emission spectra towards the longer wavelengths is observed.

#### **1.4.3.3. REE in micelles**

7-nitrobenz-2-oxa-1,3-diazole(NBD)-phospholipid probes show REE phenomenon in micellar solutions of SDS, Triton X-100, CTAB etc.<sup>226,227</sup> These experiments support the fact that the properties of water molecules that remain inside the cavity (hydration water) were different from bulk water, provided earlier by the time resolved experiments. The mobility of the probe in the hydration water gets retarded by three or more orders of magnitude. Therefore, it is the probe distribution between the structurally dissimilar locations, which is the cause of REE in micelles.

#### **1.4.3.4. REE in phospholipid vesicles**

The first report of REE in phospholipid vesicles was made using the probe 1,8-naphthalene sulphonate (ANS).<sup>228</sup> This probe molecule contains a negative charge and is located between the polar lipid heads of the bilayer. If the relaxation is too fast (sub-nanosecond range) then REE will be observed. This

type of REE is known as dynamic REE. However, if the probe is deeply embedded in the bilayer, then the reorientational and translational motion towards the equilibration along the polarity gradient would be slower and thus REE will be observed. This type of REE is termed as static REE. The latter phenomenon occurs in case of neutral probe, phenylanthracene.<sup>229</sup> REE phenomenon has also been observed in case of phospholipid group modified by NBD.<sup>230,231</sup>

#### **1.4.3.5. REE in low temperature glasses**

Low temperature glasses are considered to be non-equilibrium structures, with many microscopic configurations, which are structurally different but nearly equivalent in energy. Since the viscosity of these media is very high, the relaxation process will be slow and consequently, both static and dynamic REE can be observed.

#### **1.4.3.6. REE in different photophysical processes**

REE phenomenon has been observed in different excited state processes, such as isomerisation, electron transfer, and proton transfer. DMABN exhibits REE due to excited state isomerisation in rigid polymeric matrices, like polyvinylacetate.<sup>223</sup> The characteristic example of REE phenomenon due to excited state electron transfer is anthracene.<sup>232,233</sup> REE phenomenon in the excited state proton transfer reaction has been observed in case of 4'-(diethylamino)-3-hydroxyflavone in protein (serum albumin).<sup>234</sup>

#### **1.4.4. Molecular basis of REE**

Some of the criteria to be fulfilled by the probe and solvent for the observation of REE are as follows:<sup>218</sup>



- (i) The probe molecules with large  $\Delta\mu$  values are the most suitable candidates to exhibit REE as inhomogeneous broadening, which dictates photoselection of the energetically different species, is directly proportional to  $\Delta\mu$ .
- (ii) Probe molecules with short fluorescence lifetime are more likely to exhibit REE than those with long lifetime.
- (iii) The larger the polarity and nuclear polarizability of the medium, the stronger is the interaction of the solvent with the probe molecule and hence, greater is the chance to observe REE.
- (iv) The more viscous is the medium, the slower is the intermolecular excited state relaxation process and hence, higher is the possibility to observe REE.
- (v) Specific interactions between the probe and solvent can sometime contribute to the inhomogeneous broadening and thus REE could be observed.

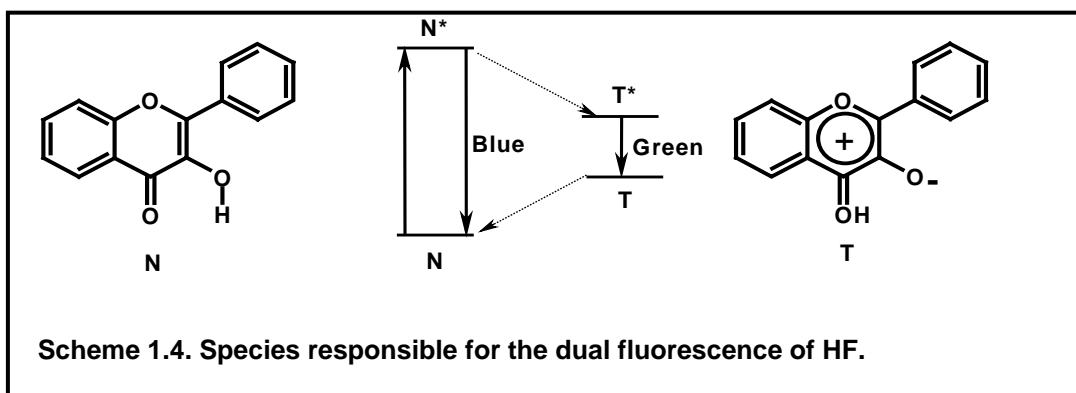
### 1.5. Motivation of the present work

3-Hydroxyflavone (HF) (**Chart 1.9.**) is undoubtedly one of the most extensively studied systems, for the understanding of the mechanism and dynamics of the intramolecular proton transfer reactions. HF is known to exhibit dual fluorescence; one originating from the normal isomer represented in **Scheme 1.4.** as **N** and another from the tautomer (**T**).

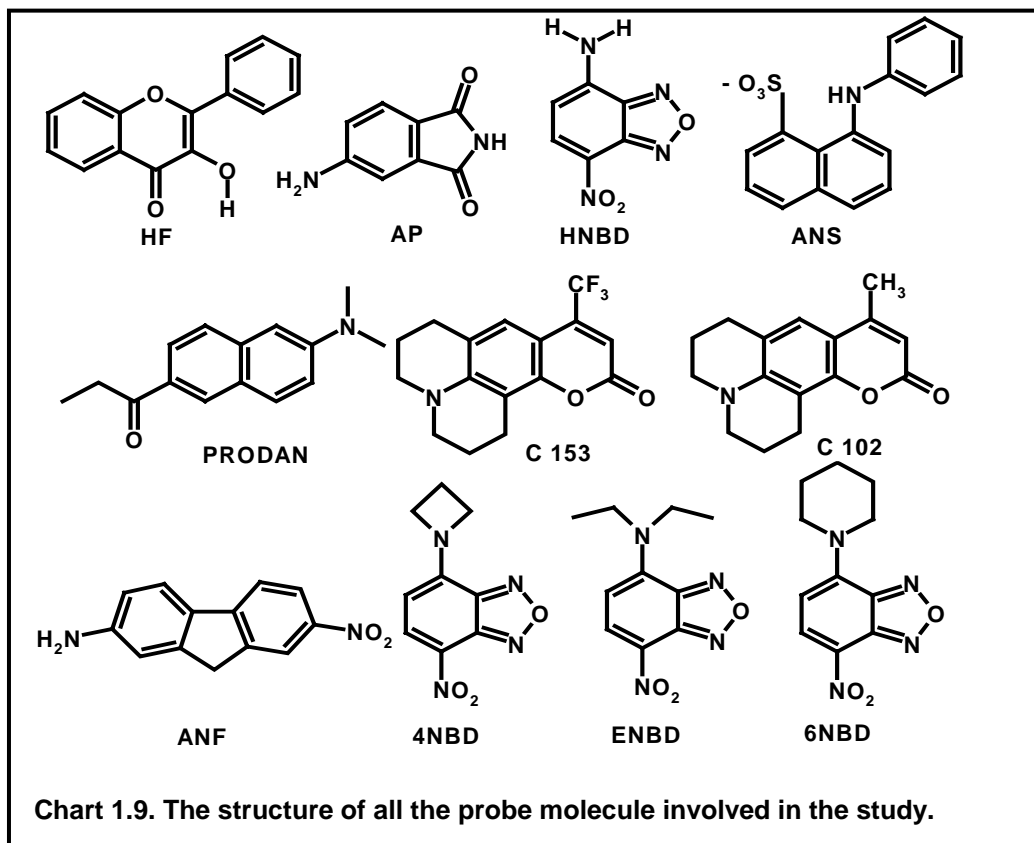
Although steady state and time-resolved fluorescence properties of HF in aprotic media are fairly well understood, the mechanism of the proton transfer reaction in hydrogen bond donating solvents is still far from clear. What we found difficult to comprehend is the fact that even though fluorescence measurements in hydroxylated solvents have clearly indicated the formation of complexes of

## Introduction

various stoichiometries between HF and the solvent molecules,<sup>38,40</sup> there is considerable ambiguity on the nature of the specific hydrogen bonded complexes and their spectral features. No specific absorption or emission due to the hydrogen-bonded complex has been reported. Hence, we thought it appropriate to reinvestigate the absorption and fluorescence behaviour of HF in alcoholic solvents.



Solvation dynamics in imidazolium RTILs have been reported to be biphasic in nature. The average solvation time is found to be dependent on the viscosity of the media. Different probes have been used in order to study this phenomenon and the average solvation time has been reported to be dependent on the probe molecule employed.<sup>200</sup> In order to investigate the probe dependence of the average solvation time, we have studied the solvation dynamics in [bmim][BF<sub>4</sub>] using Coumarin 102 (C102) (**Chart 1.9.**) as for this RTIL solvation dynamic has been studied using different solvation probes.<sup>110,116</sup>



Continued study of solvation dynamics in ammonium or phosphonium RTILs<sup>201,205</sup> has shown that although the solvation times are consistent with the viscosity, the ultrafast component of the solvation is completely absent in these RTILs. It was proposed that the ultrafast component of the dynamics in imidazolium RTILs arises due to small amplitude motions of one or more cations in close contact with the solute and is facilitated by coplanar arrangements of the solute with imidazolium nearest neighbours;<sup>200</sup> or due to the polarizability of the cation.<sup>204</sup> In order to verify this proposition we have studied the solvation

## Introduction

dynamics in a pyrrolidinium RTIL, [bmpy][Tf<sub>2</sub>N], because this RTIL is structurally similar to tetraalkylammonium RTILs, with a nonplanar cationic component. We have studied the dynamics employing three commonly used dipolar solvation probes, C153, AP, and PRODAN (**Chart 1.9.**) to investigate the probe dependence, if any.

Steady-state and time-resolved fluorescence experiments executed so far<sup>107,110,115-117</sup> in RTILs have reported that the latter behave normally towards most of the dipolar molecules. While studying the steady state fluorescence behaviour of the dipolar probe 2-amino-7-nitrofluorene (ANF) (**Chart 1.9.**), we quite surprisingly observed an excitation wavelength dependent shift of the fluorescence maximum. With a view to probing the possible reason(s) behind this excitation wavelength dependent emission behaviour, we have studied the spectral as well as temporal fluorescence behaviour of several dipolar molecules (See **Chart 1.9.**) in three imidazolium RTILs.

## 1.6. References

- (1) Klopffer, W. *Adv. Photochem.* **1977**, *10*, 311.
- (2) Huppert, D.; Gutman, M.; Kaufmann, M. J. *Adv. Chem. Phys.* **1981**, *47*, 643.
- (3) Kasha, M. *J. Chem. Soc., Faraday Trans. 2* **1986**, *82*, 2379.
- (4) Barbara, P. F.; Walsh, P. K.; Brus, L. E. *J. Phys. Chem.* **1989**, *93*, 29.
- (5) Special issue (Spectroscopy and Dynamics of Elementary Proton Transfer in Polyatomic Systems, Barbara, P. F.; Trommsdorff, H. D., Eds.) *Chem. Phys.* **1989**, *136*, 153-360.
- (6) Special Issue (M. Kasha Festschrift) *J. Phys. Chem.* **1991**, *95*, 10220-10524.
- (7) Chou, P. T. *J. Chin. Chem. Soc.* **2001**, *48*, 651.
- (8) Scheiner, S. *J. Phys. Chem. A* **2000**, *104*, 5898.
- (9) Arnaut, L. G.; Formosinho, S. J. *J. Photochem. Photobiol. A : Chem.* **1993**, *75*, 1.
- (10) Douhal, A.; Lahmani, F.; Zewail, A. *Chem. Phys.* **1996**, *207*, 477.
- (11) Aquino, A. J. A.; Lischka, H.; Christof, H. *J. Phys. Chem. A* **2005**, *109*, 3201.
- (12) Agmon, N. *J. Phys. Chem. A* **2005**, *109*, 13.
- (13) Shida, N.; Almlof, J.; Barbara, P. F. *J. Phys. Chem.* **1991**, *95*, 10457.

- (14) Chou, P. T.; McMorro, D.; Aartsma, T. J.; Kasha, M. *J. Phys. Chem.* **1984**, *88*, 4596.
- (15) Nishiya, T.; Yamauchi, S.; Hirota, N.; Baba, M.; Hanazaki, I. *J. Phys. Chem.* **1986**, *90*, 5730.
- (16) Nagaoka, S.; Fujita, M.; Takemura, T.; Baba, M. *Chem. Phys. Lett.* **1986**, *123*, 489.
- (17) Ernsting, N. P.; Nikolaus, B. *Appl. Phys. B* **1986**, *39*, 155.
- (18) Kasha, M. *Molecular Electronic Devices*; Elsevier Science: New York, 1988.
- (19) Ferrer, M. L.; Acuna, A. U.; Amat-Guerri, F.; Costela, A.; Figuera, J. M.; Florido, F.; Sastre, R. *Appl. Opt.* **1994**, *33*, 2266.
- (20) Jones, G.; Rahman, M. A. *J. Phys. Chem.* **1994**, *98*, 13028.
- (21) Liphardt, M.; Gooneskera, A.; Jones, B. E.; Ducharme, S.; Takacs, J. M.; Zhang, L. *Science* **1994**, *263*, 367.
- (22) Douhal, A.; Sastre, R. *Chem. Phys. Lett.* **1994**, *219*, 91.
- (23) Kuldova, K.; Corval, A.; P., T. H.; Lehn, J. M. *J. Phys. Chem. A* **1997**, *101*, 6850.
- (24) Chou, P. T.; Studer, S. L.; Martinez, M. L. *Appl. Spectrosc.* **1991**, *45*, 513.
- (25) Renschler, C. L.; Harrah, L. A. *Nucl. Inst. Methods Phys. Res. U.S.*, 1985; Vol. A 235, Sept.; pp 636.
- (26) Williams, D. L.; Heller, A. *J. Phys. Chem.* **1970**, *74*, 4473.
- (27) Heller, H. J.; Blattmann, H. R. *Pure Appl. Chem.* **1973**, *36*, 141.
- (28) Roshal, A. D.; Grigorovich, A. V.; Doroshenko, A. O.; Pivovarenko, V. G.; Demchenko, A. P. *J. Phys. Chem. A* **1998**, *102*, 5907.
- (29) Tarkka, R. M.; Zhang, X.; Jenekhe, S. A. *J. Am. Chem. Soc.* **1996**, *118*, 9438.
- (30) Weller, A. *Z. Elektrochem.* **1956**, *60*, 1144.
- (31) Smith, K. K.; Kaufmann, K. J. *J. Phys. Chem.* **1978**, *82*, 2286.
- (32) Helmbrook, L.; Kenny, J. E.; Kohler, B. E.; Scott, G. W. *J. Phys. Chem.* **1983**, *87*, 280.
- (33) Lamola, A. A.; Sharp, L. J. *J. Phys. Chem.* **1966**, *70*, 2634.
- (34) Barbara, P. F.; Rentzepis, P. M.; Brus, L. E. *J. Am. Chem. Soc.* **1980**, *102*, 2786.
- (35) Sengupta, P. K.; Kasha, M. *Chem. Phys. Lett.* **1979**, *68*, 382.
- (36) Woolfe, G. J.; Thistlethwaite, P. J. *J. Am. Chem. Soc.* **1981**, *103*, 6916.
- (37) Itoh, M.; Tokumara, K.; Tanimoto, Y.; Okada, Y.; Takeuchi, H.; Obi, K.; Tanaka, I. *J. Am. Chem. Soc.* **1982**, *104*, 4146.
- (38) Strandjord, A. J. G.; Courtney, S. H.; Friedrich, D. M.; Barbara, P. F. *J. Phys. Chem.* **1983**, *87*, 1125.
- (39) Strandjord, A. J. G.; Barbara, P. F. *Chem. Phys. Lett.* **1983**, *98*, 21.
- (40) McMorro, D.; Kasha, M. *J. Am. Chem. Soc.* **1983**, *105*, 5133.
- (41) McMorro, D.; Kasha, M. *J. Phys. Chem.* **1984**, *88*, 2235.
- (42) Strandjord, A. J. G.; Barbara, P. F. *J. Phys. Chem.* **1985**, *89*, 2355.
- (43) Strandjord, A. J. G.; Smith, D. E.; Barbara, P. F. *J. Phys. Chem.* **1985**, *89*, 2362.
- (44) Schwartz, B. J.; Peteanu, L. A.; Harris, C. B. *J. Phys. Chem.* **1992**, *96*, 3591.

## Introduction

- (45) Ameer-Beg, S.; Ormson, S. M.; Brown, R. G.; Matousek, P.; Towrie, M.; Nibbering, E. T. J.; Foggy, P.; Neuwahl, F. V. R. *J. Phys. Chem. A* **2001**, *105*, 3709.
- (46) Bader, A. N.; Ariese, F.; Gooijer, C. *J. Phys. Chem. A* **2002**, *106*, 2844.
- (47) Swinney, T. C.; Kelley, D. F. *J. Chem. Phys.* **1993**, *99*, 211.
- (48) Itoh, H.; Tanimoto, Y.; Tokumara, K. *J. Am. Chem. Soc.* **1983**, *105*, 3339.
- (49) Dick, B.; Ernsting, N. P. *J. Phys. Chem.* **1987**, *91*, 4261.
- (50) Itoh, H.; Fujiwara, Y.; Sumitani, M.; Yoshihara, K. *J. Phys. Chem.* **1986**, *90*, 5672.
- (51) Brucker, G. A.; Swinney, T. C.; Kelly, D. F. *J. Phys. Chem.* **1991**, *95*, 3190.
- (52) Premvardhan, L. L.; Peteanu, L. A. *J. Phys. Chem. A* **1999**, *103*, 7506.
- (53) Brewer, W. E.; Studer, S. L.; Chou, P. T.; Orton, E. *Chem. Phys. Lett.* **1989**, *158*, 345.
- (54) Sarkar, M.; Sengupta, P. K. *Chem. Phys. Lett.* **1991**, *179*, 68.
- (55) Salman, O. A.; Drickamer, H. G. *J. Chem. Phys.* **1981**, *75*, 572.
- (56) McMorrow, D.; Kasha, M. *Proc. Natl. Acad. Sci. USA* **1984**, *81*, 3375.
- (57) Ernsting, N. P.; Dick, B. *Chem. Phys.* **1989**, *136*, 181.
- (58) Khan, A. U.; Kasha, M. *Proc. Natl. Acad. Sci. USA* **1983**, *80*, 1767.
- (59) Ormson, S. M.; LeGourrierec, D.; Brown, R. G.; Foggi, P. *Chem. Commun.* **1995**, 2133.
- (60) Rulliere, C.; Declémy, A. *Chem. Phys. Lett.* **1987**, *134*, 64.
- (61) Dick, B. *J. Phys. Chem.* **1990**, *94*, 5752.
- (62) Perthenopoulos, D. A.; Kasha, M. *Chem. Phys. Lett.* **1990**, *173*, 303.
- (63) Ormson, S. M.; Brown, R. G.; Vollmer, F.; Rettig, W. *J. Photochem. Photobiol. A : Chem.* **1994**, *81*, 65.
- (64) McMorrow, D.; Dzugan, T. P.; Aartsma, T. J. *Chem. Phys. Lett.* **1984**, *103*, 492.
- (65) Brucker, G. A.; Kelley, D. F. *J. Phys. Chem.* **1987**, *91*, 2856.
- (66) Brucker, G. A.; Kelley, D. F. *J. Phys. Chem.* **1989**, *93*, 5179.
- (67) Woolfe, G. J.; Thistlethwaite, P. J. *J. Am. Chem. Soc.* **1980**, *102*, 6917.
- (68) Sinha, H.; Dogra, S. K. *Chem. Phys.* **1986**, 337.
- (69) Das, K.; Sarkar, N.; Ghosh, A. K.; Majumdar, D.; Nath, D. N.; Bhattacharyya, K. *J. Phys. Chem.* **1994**, *98*, 9126.
- (70) Mosquera, M.; Penedo, J. C.; Rodriguez, M. C. R.; Prieto, F. R. *J. Phys. Chem.* **1996**, *100*, 5398.
- (71) Woolfe, G. J.; Melzig, M.; Schneider, S.; Dorr, F. *Chem. Phys. Lett.* **1983**, *77*, 213.
- (72) Itoh, H.; Fujiwara, Y. *J. Am. Chem. Soc.* **1985**, *107*, 1561.
- (73) Barbara, P. F.; Brus, L. E.; Rentzepis, P. M. *J. Am. Chem. Soc.* **1980**, *102*, 5631.
- (74) Potter, C. A. S.; Brown, R. G. *Chem. Phys. Lett.* **1988**, *153*, 7.
- (75) Taylor, C. A.; El-Bayoumi, M. A.; Kasha, M. *Proc. Natl. Acad. Sci. USA* **1969**, *63*, 253.
- (76) Ingham, K. C.; Abu-Elgeith, M.; El-Bayoumi, M. A. *J. Am. Chem. Soc.* **1971**, *93*, 5023.

- (77) Hetherington, W. H.; Micheels, R. H.; Eisenthal, K. B. *Chem. Phys. Lett.* **1979**, 66, 230.
- (78) Tang, G. Q.; Macinnis, J.; Kasha, M. *J. Am. Chem. Soc.* **1987**, 109, 2531.
- (79) Song, P. S.; Sun, M.; Koziolawa, A.; Koziol, J. *J. Am. Chem. Soc.* **1974**, 96, 4319.
- (80) Choi, J. D.; Fugate, R. D.; Song, P. S. *J. Am. Chem. Soc.* **1980**, 102, 5293.
- (81) Itoh, M.; Adachi, T.; Tokumara, K. *J. Am. Chem. Soc.* **1983**, 105, 4828.
- (82) Schipfer, R.; Wolfbeis, O. S.; Knierzinger, A. *J. Chem. Soc., Perkin Trans. 2* **1981**, 1443.
- (83) Itoh, M.; Yoshida, N.; Takashima, M. *J. Am. Chem. Soc.* **1985**, 107, 4819.
- (84) Nelson, W. M. In *Green Chemistry*; Anastas, P. T., Williamson, T. C., Eds.; Oxford University Press: Oxford, 1998.
- (85) Tanaka, K.; Toda, F. *Chem. Rev.* **2000**, 100, 1025.
- (86) Hang, C. T.; Lianhai, L.; Yang, Y.; Wenshuo, L. Developing green chemistry: Organometallic reactions in aqueous media. In *Clean Solvents: Alternative Media for Chemical Reactions and Processing*; Abraham, M., Moens, L., Eds.; ACS Symposium Series 819: Washington DC, 2002; pp 166.
- (87) Kajimoto, O. *Chem. Rev.* **1999**, 99, 355.
- (88) Rogers, R. D.; Seddon, K. R. *Science* **2003**, 302, 792.
- (89) Seddon, K. R. *Nature (Materials)* **2003**, 2, 363.
- (90) Welton, T. *Chem. Rev.* **1999**, 99, 2071.
- (91) Dupont, J.; Souza, R. F. D.; Suarez, P. A. Z. *Chem. Rev.* **2002**, 102, 3667.
- (92) Wasserscheid, P.; Keim, W. *Angew. Chem., Int. Ed.* **2000**, 39, 3772.
- (93) *Ionic Liquids in Synthesis*; Welton, T. W., P., Ed.; VCH-Wiley: Weinheim, 2002.
- (94) Seddon, K. R.; Stark, A.; Torres, M. J. In *Clean Solvents: Alternative Media for Chemical Reactions and Processing*; Abraham, M., Moens, L., Eds.; ACS Symposium Series 819: Washington DC, 2002.
- (95) *Ionic Liquids, Industrial Applications for Green Chemistry*; Rodgers, R.; Seddon, K. R., Eds.; ACS Symposium Series 818: Washington DC, 2002.
- (96) Chiappe, C.; Pieraccini, D. *J. Phys. Org. Chem.* **2005**, 18, 275.
- (97) Seddon, K. R.; Stark, A.; Torres, M. *Pure Appl. Chem.* **2000**, 72, 2275.
- (98) Walden, P. *Bull. Acad. Imper. Sci. (St. Petersburg)* **1914**, 1800.
- (99) Starks, C. M. *J. Am. Chem. Soc.* **1971**, 93, 195.
- (100) Gordon, J. E.; Subbarao, G. N. *J. Am. Chem. Soc.* **1978**, 100, 7445.
- (101) Sun, J.; Forsyth, M.; MacFarlane, D. R. *J. Phys. Chem. B* **1998**, 102, 8858.
- (102) Wilkes, J. S.; Zaworotko, M. J. *Chem. Commun.* **1992**, 965.
- (103) Buzzeo, M. C.; Evans, R. G.; Compton, R. G. *Chem. Phys. Chem.* **2004**, 5, 1106.
- (104) Davis, J. H. *J. Chem. Lett.* **2004**, 33, 1072.
- (105) Lee, S. *Chem. Commun.* **2006**, 1049.
- (106) Reichardt, C. *Solvents and Solvent Effects in Organic Chemistry*; VCH: Weinheim, Germany, 1988.
- (107) Aki, S. N. V. K.; Brennecke, J. F.; Samanta, A. *Chem. Commun.* **2001**, 413.
- (108) Reichardt, C. *Green Chem.* **2005**, 7, 339.

## Introduction

- (109) Bonhote, P.; Dias, A.; Papageorgiou, N.; Kalyanasundaram, K.; Gratzel, M. *Inorg. Chem.* **1996**, *35*, 1168.
- (110) Karmakar, R.; Samanta, A. *J. Phys. Chem. A* **2002**, *106*, 6670.
- (111) MacFarlane, D. R.; Meakin, P.; Sun, J.; Amini, N.; Forsyth, M. *J. Phys. Chem. B* **1999**, *103*, 4164.
- (112) Mandal, P. K.; Samanta, A. *J. Phys. Chem. B* **2005**, *109*, 15172.
- (113) Muldoon, M. J.; Gordon, C. M.; Dunkin, I. R. *J. Chem. Soc., Perkin Trans. 2* **2001**, 433.
- (114) Carmichael, A. J.; Seddon, K. R. *J. Phys. Org. Chem.* **2000**, *13*, 591.
- (115) Saha, S.; Mandal, P. K.; Samanta, A. *Phys. Chem. Chem. Phys.* **2004**, *6*, 3106.
- (116) Karmakar, R.; Samanta, A. *J. Phys. Chem. A* **2002**, *106*, 4447.
- (117) Karmakar, R.; Samanta, A. *J. Phys. Chem. A* **2003**, *107*, 7340.
- (118) Widegren, J. A.; Laesecke, A.; Magee, J. W. *Chem. Commun.* **2005**, 1610.
- (119) Jeapes, A. J. Process for recycling ionic liquids. World Patent WO 01/15175, 2001.
- (120) Earle, M. J.; Esperanca, J. M. S. S.; Gilea, M. A.; Lopes, J. N. C.; Rebelo, L. P. N.; Magee, J. W.; Seddon, K. R.; Widegren, J. A. *Nature* **2006**, *439*, 831.
- (121) Every, H. A.; Bisop, A. G.; MacFarlane, D.; Oradd, G.; Forsyth, M. *Phys. Chem. Chem. Phys.* **2004**, *6*, 1758.
- (122) Billard, I.; Moutiers, G.; Labet, A.; Azzi, A. E.; Gaillard, C.; Mariet, C.; Lutzenkirchen, K. *Inorg. Chem.* **2003**, *42*, 1726.
- (123) Muldoon, M. J.; McLean, A. J.; Gordon, C. M.; Dunkin, I. R. *Chem. Commun.* **2001**, 2364.
- (124) Lancaster, N. L.; Salter, P. A.; Welton, T.; Young, G. B. *J. Org. Chem.* **2002**, *67*, 8855.
- (125) Paul, A.; Mandal, P. K.; Samanta, A. *Chem. Phys. Lett.* **2005**, *402*, 375.
- (126) Paul, A.; Mandal, P. K.; Samanta, A. *J. Phys. Chem. B* **2005**, *109*, 9148.
- (127) Dupont, J. *J. Braz. Chem. Soc.* **2004**, *15*, 341.
- (128) Holbrey, J. D.; Reichert, W. M.; Nieuwenhuyzen, M.; Sheppard, O.; Hardacre, C.; Rogers, R. D. *Chem. Commun.* **2003**, 476.
- (129) Dupont, J.; Suarez, P. A. Z.; Souza, R. F. D.; Burrow, R. A.; Kintzinger, J. *Chem. Eur. J.* **2000**, *6*, 2377.
- (130) Fuller, J.; Carlin, R. T.; Long, H. C. D.; Haworth, D. *Chem. Commun.* **1994**, 299.
- (131) Avent, A. G.; Chaloner, P. A.; Day, M. P.; Seddon, K. R.; Welton, T. *J. Chem. Soc., Dalton Trans.* **1994**, 23, 3405.
- (132) Tait, S.; Osteryoung, R. A. *Inorg. Chem.* **1984**, *23*, 4352.
- (133) Dieter, K. M.; Dymek, C. J.; Heimer, N. E.; Rovang, J. W.; Wilkes, J. S. *J. Am. Chem. Soc.* **1988**, *110*, 2722.
- (134) Mele, A.; Tran, C. D.; Lacerda, S. H. P. *Angew. Chem., Int. Ed.* **2003**, *42*, 4364.
- (135) Mele, A.; Romano, G.; Giannone, M.; Ragg, E.; Fronza, G.; Raos, G.; Marcon, V. *Angew. Chem., Int. Ed.* **2006**, *45*, 1123.
- (136) Gannon, T. J.; Law, G.; Watson, P. R.; Carmichael, A. J.; Seddon, K. R. *Langmuir* **1999**, *15*, 8429.



- (137) Hayashi, S.; Ozawa, R.; Hamaguchi, H. *Chem. Lett.* **2003**, 32, 498.
- (138) Ozawa, R.; Hayashi, S.; Saha, S.; Kobayashi, A.; Hamaguchi, H. *Chem. Lett.* **2003**, 32, 948.
- (139) Hyun, B.; Dzyuba, S. V.; Bartsch, R. A.; Quitevis, E. L. *J. Phys. Chem. A* **2002**, 106, 7579.
- (140) Moutiers, B. G.; Labet, A.; Azzi, A. E.; Gaillard, C.; Mariet, C.; Lutzenkirchen, K. *Inorg. Chem.* **2003**, 42, 1726.
- (141) Iimori, T.; Iwahashi, T.; Ishii, H.; Seki, K.; Ouchi, Y.; Ozawa, R.; Hamaguchi, H.; Kim, D. *Chem. Phys. Lett.* **2004**, 389, 321.
- (142) Popolo, M. G. D.; Voth, G. A. *J. Phys. Chem. B* **2004**, 108, 1744.
- (143) Urahata, S. M.; Ribeiro, M. C. C. *J. Chem. Phys.* **2004**, 120, 1855.
- (144) Harper, J. B.; Lynden-Bell, R. M. *Molecular Physics* **2004**, 102, 85.
- (145) Hanke, C. G.; Lynden-Bell, R. M. *J. Phys. Chem. B* **2003**, 107, 10873.
- (146) Hanke, C. G.; Johansson, A.; Harper, J. B.; Lynden-Bell, R. M. *Chem. Phys. Lett.* **2003**, 374, 85.
- (147) Hu, Z.; Margulis, C. J. *Proc. Natl. Acad. Sci. USA* **2006**, 103, 831.
- (148) Huddleston, J. G.; Willauer, H. D.; Swatoski, R. P.; Visser, A. E.; Rogers, R. D. *Chem. Commun.* **1998**, 1765.
- (149) Armstrong, D. W.; Zhang, L. K.; He, L.; Gross, M. L. *Anal. Chem.* **2001**, 73, 3679.
- (150) van Rantwijk, F.; Lau, R. M.; Sheldon, R. A. *Trends Biotechnol.* **2003**, 21, 131.
- (151) Wang, P.; Zakeeruddin, S. M.; Moser, J.; Gratzel, M. *J. Phys. Chem. B* **2003**, 107, 13280.
- (152) Itoh, H.; Naka, K.; Chujo, Y. *J. Am. Chem. Soc.* **2004**, 126, 3026.
- (153) Buzzeo, M. C.; Hardacre, C.; Compton, R. G. *Anal. Chem.* **2004**, 76, 4583.
- (154) Anderson, J. L.; Armstrong, D. W. *Anal. Chem.* **2003**, 75, 4851.
- (155) de Suza, R. F.; Padilha, J. C.; Goncalves, R. S.; Dupont, J. *Electrochem. Commun.* **2003**, 5, 728.
- (156) Wang, P.; Zakeeruddin, S. M.; Comte, P.; Exnar, I.; Gratzel, M. *J. Am. Chem. Soc.* **2003**, 125, 1166.
- (157) Kimizuka, N.; Nakashima, T. *Langmuir* **2001**, 17, 6759.
- (158) Baker, G. A.; Pandey, S. In *Ionic Liquids IIIA: Fundamentals, Progress, Challenges, and Opportunities. Properties and Structure*; Rogers, R. D., Seddon, K. R., Eds. Washington DC, 2005; Vol. ACS Symposium Series 901.
- (159) Fonseca, G. S.; Umpierre, A. P.; Fichtner, P. F. P.; Teixeira, S. R.; Dupont, J. *Chem. Eur. J.* **2003**, 9, 3263.
- (160) Park, S.; Kazlauskas, R. J. *Curr. Opin. Biotech.* **2003**, 14, 432.
- (161) Bagchi, B.; Oxtoby, D. W.; Fleming, G. R. *Chem. Phys.* **1984**, 86, 257.
- (162) Bagchi, B. *Annu. Rev. Phys. Chem.* **1989**, 40, 115.
- (163) Bagchi, B. *Chem. Rev.* **2005**, 105, 3197.
- (164) Fleming, G. R.; Cho, M. *Annu. Rev. Phys. Chem.* **1996**, 47, 109.
- (165) Hutterer, R.; Schneider, F. W.; Lanig, H.; Hof, M. *Biochim. Biophys. Acta* **1997**, 1323, 195.

## Introduction

- (166) Sykora, J.; Mudogo, V.; Hutterer, R.; Nepras, M.; Vanerka, J.; Kapusta, P.; Fidler, V.; Hof, M. *Langmuir* **2002**, 18, 9276.
- (167) Sykora, J.; Kapusta, P.; Fidler, V.; Hof, M. *Langmuir* **2002**, 18, 571.
- (168) Koti, A. S. R.; Krishna, M. M. G.; Periasamy, N. *J. Phys. Chem. A* **2001**, 105, 1767.
- (169) Rossky, P. J.; Simon, J. D. *Nature* **1994**, 370, 263.
- (170) Jimenez, R.; Fleming, G. R.; Kumar, P. V.; Maroncelli, M. *Nature* **1994**, 369, 471.
- (171) Horng, M. L.; Gardecki, J. A.; Papazyan, A.; Maroncelli, M. *J. Phys. Chem.* **1995**, 99, 17311.
- (172) Horng, M. L.; Gardecki, J. A.; Maroncelli, M. *J. Phys. Chem. A* **1997**, 101, 1030.
- (173) van der Zwan, G.; Hynes, J. T. *J. Phys. Chem.* **1985**, 89, 4181.
- (174) Nandi, N.; Bhattacharyya, K.; Bagchi, B. *Chem. Rev.* **2000**, 100, 2013.
- (175) Castner, E. W.; Maroncelli, M.; Fleming, G. R. *J. Chem. Phys.* **1987**, 86, 1090.
- (176) Castner, E. W.; Fleming, G. R.; Bagchi, B.; Maroncelli, M. *J. Chem. Phys.* **1988**, 89, 3519.
- (177) Chapman, C. F.; Maroncelli, M. *J. Phys. Chem.* **1991**, 95, 9095.
- (178) Chapman, C. F.; Fee, R. S.; Maroncelli, M. *J. Phys. Chem.* **1995**, 99, 4811.
- (179) Chapman, C. F.; Fee, R. S.; Maroncelli, M. *J. Phys. Chem.* **1990**, 94, 4929.
- (180) Su, S. G.; Simon, J. D. *J. Phys. Chem.* **1986**, 90, 6475.
- (181) Su, S. G.; Simon, J. D. *J. Phys. Chem.* **1987**, 91, 2693.
- (182) Jarzeba, W.; Barbara, P. F. *Adv. Photochem.* **1990**, 15, 1.
- (183) Bhattacharyya, K.; Bagchi, B. *J. Phys. Chem. A* **2000**, 104, 10603.
- (184) Bhattacharyya, K. *Acc. Chem. Res.* **2003**, 36, 95.
- (185) Pal, S. K.; Peon, J.; Zewail, A. *Proc. Natl. Acad. Sci. USA* **2002**, 99, 1763.
- (186) Pal, S. K.; Peon, J.; Bagchi, B.; Zewail, A. *J. Phys. Chem. B* **2002**, 106, 12376.
- (187) Pal, S. K.; Zhao, L.; Zewail, A. *Proc. Natl. Acad. Sci. USA* **2003**, 100, 8113.
- (188) Bart, E.; Meltsin, A.; Huppert, D. *J. Phys. Chem.* **1994**, 98, 3295.
- (189) Bart, E.; Meltsin, A.; Huppert, D. *J. Phys. Chem.* **1994**, 98, 10819.
- (190) Bart, E.; Meltsin, A.; Huppert, D. *J. Phys. Chem.* **1995**, 99, 9253.
- (191) Kometani, N.; Kajimoto, O.; Hara, K. *J. Phys. Chem. A* **1997**, 101, 4916.
- (192) Molotsky, T.; Koifman, N.; Huppert, D. *J. Phys. Chem. A* **2002**, 106, 12185.
- (193) Berg, M. *J. Phys. Chem. A* **1998**, 102, 17.
- (194) Fourkas, J. T.; Berg, M. *J. Chem. Phys.* **1993**, 98, 7773.
- (195) Ediger, M. D.; Angell, C. A.; Nagel, S. R. *J. Phys. Chem.* **1996**, 100, 13200.
- (196) Ediger, M. D. *Annu. Rev. Phys. Chem.* **2000**, 51, 99.
- (197) Yang, M.; Richert, R. *J. Chem. Phys.* **2001**, 115, 2676.
- (198) Richert, R. *J. Chem. Phys.* **2001**, 114, 7471.
- (199) Ingram, J. A.; Moog, R. S.; Ito, N.; Biswas, R.; Maroncelli, M. *J. Phys. Chem. B* **2003**, 107, 5926.
- (200) Ito, N.; Arzhantsev, S.; Maroncelli, M. *Chem. Phys. Lett.* **2004**, 396, 83.
- (201) Ito, N.; Arzhantsev, S.; Heitz, M.; Maroncelli, M. *J. Phys. Chem. B* **2004**, 108, 5771.

- (202) Chakrabarty, D.; Hazra, P.; Chakraborty, A.; Seth, D.; Sarkar, N. *Chem. Phys. Lett.* **2003**, 381, 697.
- (203) Chakrabarty, D.; Chakraborty, A.; Seth, D.; Sarkar, N. *J. Phys. Chem. A* **2005**, 109, 1764.
- (204) Chowdhury, P. K.; Halder, M.; Sanders, L.; Calhoun, T.; Anderson, J. L.; Armstrong, D. W.; Song, X.; Petrich, J. W. *J. Phys. Chem. B* **2004**, 108, 10245.
- (205) Arzhantsev, S.; Ito, N.; Heitz, M.; Maroncelli, M. *Chem. Phys. Lett.* **2003**, 381, 278.
- (206) Mandal, P. K.; Paul, A.; Samanta, A. *Res. Chem. Intermed.* **2005**, 31, 575.
- (207) Shim, Y.; Duan, J.; Choi, M. Y.; Kim, H. J. *J. Chem. Phys.* **2003**, 119, 6411.
- (208) Margulis, C. J.; Stern, H. A.; Berne, B. J. *J. Phys. Chem. B* **2002**, 106, 12017.
- (209) Popolo, M. G. D.; Lynden-Bell, R. M.; Kohanoff, J. *J. Phys. Chem. B* **2005**, 109, 5895.
- (210) Lynden-Bell, R. M.; Kohanoff, J.; Popolo, M. G. D. *Faraday Discuss.* **2005**, 129, 57.
- (211) Kobrak, M. N.; Znamenskiy, V. *Chem. Phys. Lett.* **2004**, 395, 127.
- (212) Shim, Y.; Choi, M. Y.; Kim, H. J. *J. Chem. Phys.* **2005**, 122, 044510.
- (213) Shim, Y.; Choi, M. Y.; Kim, H. J. *J. Chem. Phys.* **2005**, 122, 044511.
- (214) Birks, J. B. *Photophysics of Aromatic Molecules*; Wiley-Inter-science: London, 1970.
- (215) Galley, W. C.; Purkey, R. M. *Proc. Natl. Acad. Sci. USA* **1970**, 67, 1116.
- (216) Rubinov, A. N.; Tomin, V. *Opt. Spekt.* **1970**, 29, 1082.
- (217) Weber, G.; Shinitzky, M. *Proc. Natl. Acad. Sci. USA* **1970**, 65, 823.
- (218) Demchenko, A. P. *Luminescence* **2002**, 17, 19.
- (219) Demchenko, A. P. In *Topics in Fluorescence Spectroscopy*; Lakowicz, J. R., Ed.; Plenum Press: New York, 1991; Vol. 3.
- (220) Demchenko, A. P. *Ukr. Biochim. Zh.* **1981**, 53, 22.
- (221) Demchenko, A. P. *Eur. Biophys. J.* **1988**, 16, 121.
- (222) Demchenko, A. P. *Ultraviolet Spectroscopy of Proteins*; Springer-Verlag: Heidelberg: New York, 1986.
- (223) Al-Hassan, K. A.; Rettig, W. *Chem. Phys. Lett.* **1986**, 126, 273.
- (224) Al-Hassan, K. A.; El-Bayoumi, M. A. *J. Polymer Sci. B* **1987**, 25, 495.
- (225) Al-Hassan, K. A.; Azumi, T. *Chem. Phys. Lett.* **1988**, 150, 344.
- (226) Rawat, S.; Mukherjee, S.; Chattopadhyay, A. *J. Phys. Chem. B* **1997**, 101, 1922.
- (227) Rawat, S.; Chattopadhyay, A. *J. Fluoresc.* **1999**, 9, 233.
- (228) Lakowicz, J. R.; Nakamoto, S. K. *Biochemistry* **1984**, 23, 3013.
- (229) Gakamsky, D. M.; Demchenko, A. P.; Nemkovich, N. A.; Rubinov, A. N. *Biophys. Chem.* **1992**, 42, 49.
- (230) Chattopadhyay, A.; Mukherjee, S. *Biochemistry* **1993**, 32, 3804.
- (231) Chattopadhyay, A.; Mukherjee, S. *J. Phys. Chem. B* **1999**, 103, 8180.
- (232) Demchenko, A. P.; Sytnik, A. S. *Proc. Natl. Acad. Sci. USA* **1991**, 88, 9311.
- (233) Demchenko, A. P.; Sytnik, A. S. *J. Phys. Chem.* **1991**, 95, 10518.
- (234) Demchenko, A. P. *Biochim. Biophys. Acta* **1994**, 1209, 149.

### **Materials, Instrumentation and Methods**

---

This chapter provides the details on the procurement, preparation, and purification of different materials used in this study. The time-correlated-single-photon-counting technique based picosecond and nanosecond setups including the laser system have been described in detail. The methods of analysis of data including the spectral reconstruction of the time-resolved emission spectra from the decay curves have also been discussed.

---

#### **2.1. Materials**

HF was procured from Tokyo Kasei Co. and was recrystallised several times from methanol. The recrystallised sample was vacuum sublimed prior to photophysical measurements. Laser-grade C102 (Eastman Kodak) was used without any purification. AP was obtained from TCI and was recrystallised twice from ethanol in the presence of active charcoal. C153 (laser grade) and PRODAN were procured from Eastman Kodak and Molecular probes respectively, and were used as obtained. ANF was a generous gift from Dr. G. Saroja and was used as received. ANS was procured from Molecular probes, and was recrystallised from doubly distilled water. NBD derivatives, HNBD, ENBD, 4NBD, and 6NBD were received from Dr. S. Saha. The details of synthesis of these compounds can be found elsewhere.<sup>1</sup> These compounds were recrystallised further from ethanol. The purity of all the compounds was checked

by single spot in TLC, as well as by matching the absorption and emission spectra with literature.

Silica gel, and neutral and acidic alumina for column chromatography were obtained from Acme Scientific Chemicals, India. The various drying agents,  $\text{CaH}_2$ ,  $\text{MgSO}_4$ ,  $\text{KOH}$ ,  $\text{NaOH}$ ,  $\text{P}_2\text{O}_5$ ,  $\text{CaO}$  and  $\text{Mg}$  turnings, used at different stages of the purification procedure, were purchased from local chemical companies.

1-methylimidazole (99%), sodium tetrafluoroborate ( $\text{NaBF}_4$ ) (97%), and hexafluorophosphoric acid ( $\text{HPF}_6$ ) (65% solution in water) required for the synthesis of the RTILs were procured from Lancaster, whereas, 1-methylpyrrolidine and lithium bis(trifluoromethanesulfonyl)imide were procured from Acros and Aldrich respectively, and were used as received. 1-chlorobutane (HPLC grade), and 1,1,1-trichloroethane (99%) were obtained from Aldrich. Bromoethane (extra pure) was purchased from Loba. Both 1-chlorobutane and bromoethane were distilled over  $\text{P}_2\text{O}_5$ . 1-methylimidazole was vacuum distilled with  $\text{KOH}$  prior to synthesis. Glycerol was procured from Aldrich and was used as received.

The deuteriated solvents,  $\text{CDCl}_3$  (Isotec, Inc), methanol- $\text{d}_4$  (Acros Organic), acetonitrile- $\text{d}_3$  (Merck), and  $\text{DMSO-d}_6$  (Merck) used for NMR analysis were used as received.

### 2.1.1. Purification of conventional solvents

All the solvents used for spectroscopic measurements were procured from local companies and were rigorously purified by following standard literature procedures.<sup>2</sup>

***n*-Hexane, Cyclohexane, Toluene, 1,4-Dioxane, Tetrahydrofuran, Diethylether:** Dried by refluxing with metallic sodium and benzophenone until

### *Materials, Instrumentation, and Methods*

the solution became deep blue due to formation of disodium benzophenone complex (ketyl radical) during reflux and its persistence on cooling. Finally, the dry solvent was fractionally distilled and collected in a dry reagent bottle.

**Ethylacetate:** The solvent was treated with  $P_2O_5$  for a couple of hours and then fractionally distilled. The first fraction was discarded and the remaining amount was collected.

**Acetonitrile:** Maximum water was eliminated by adding coarse blue silica gel in the solvent with occasional shaking in nitrogen atmosphere for at least 3 hr. Finally the solvent was fractionally distilled over dry  $CaH_2$ .

**1-Butanol, 2-Propanol, Ethanol:** GR grade 1-Butanol, 2-Propanol and ethanol were refluxed with freshly ignited  $CaO$  (250 g/L) for at least 6 hr, standing overnight and distilled cautiously to exclude moisture. For further dehydration magnesium alkoxide was used. This was prepared by mixing 5 g of clean dry magnesium turnings and 0.5 g of iodine in a round-bottomed flask, followed by 50-75 mL of alcohol, and warming the mixture until a vigorous reaction occurs. The heating was continued until the entire amount of magnesium was converted to the alkoxide. The remaining alcohol was added slowly and refluxed for an hour and distilled to collect the final dry alcohol to be used in spectroscopic studies.

**Methanol:** After the initial drying over  $CaH_2$  by keeping overnight, 50-75 mL of methanol was added to clean dry magnesium turnings (5 g) and iodine (0.5 g) and warmed until the entire amount of magnesium was converted into magnesium methoxide. About 1 L of methanol was added to this, refluxed for 2-3 hr and distilled out.

**Water:** De-ionised water, collected from an ion exchange resin column, was first treated with sodium hydroxide and a little potassium permanganate and distilled. Thus obtained water was distilled twice to obtain the water to be used for the spectroscopic study.

In order to prevent any decomposition by light or prolonged storage, all the solvents were freshly distilled prior to use. The extent of dryness of each solvent was checked by measuring the  $E_T(30)$  value of the solvent (See Section 1.x) and comparing this value with the literature value. The polarity scale that has been adopted in the whole thesis is the  $E_T(30)$  scale of solvent polarity proposed by Dimorth and Reichardt.<sup>3</sup> The calculated  $E_T(30)$  value of the solvent, estimated from the longest wavelength peak of the absorption spectrum of betaine dye was then compared with the literature value of the respective solvent. The betaine dye was received as a generous gift from Prof. Christian Reichardt of Philips University (Germany) and was used without further purification. All the dried conventional solvents were found to be optically transparent in the wavelength range (300 - 600 nm) of our interest.

## 2.2. Synthesis

### 2.2.1. 3-Methoxyflavone

3-methoxyflavone was synthesised following a literature procedure<sup>4</sup> by the methylation of the hydroxy group of the parent 3-hydroxyflavone in the following manner. 3-hydroxyflavone (2.15 g, 0.009 mol) was dissolved in 30 mL acetone and the mixture was transferred to a round-bottomed flask containing potassium carbonate (2.5 g, 0.018 mol). To this mixture was added dimethylsulphate (2.27 g, 0.018 mol) dropwise and the solution mixture was heated under refluxing condition for 6 hr. While refluxing, the yellow colour of the solution changed to colourless. Excess dilute ammonia was added in order to

destroy the dimethylsulphate that remained in the mixture. Then the solvent was removed under vacuum in a rotary evaporator. The white solid was filtered and extracted. Following this, the white solid was washed several times until the filtrate was neutral (checked by litmus paper). Finally, the white solid was recrystallised from methanol to get white needles. The melting point of the recrystallised sample was checked to be 116<sup>0</sup>C, matching quite well with the literature value.<sup>4</sup> The purity of the sample was checked by the single spot in TLC and by NMR.

### **2.2.2. Room temperature ionic liquids**

Methods for the preparation of imidazolium RTILs have been depicted in **Scheme 2.1**.

#### **2.2.2.1. Preparation of [bmim][BF<sub>4</sub>] and [emim][BF<sub>4</sub>]**

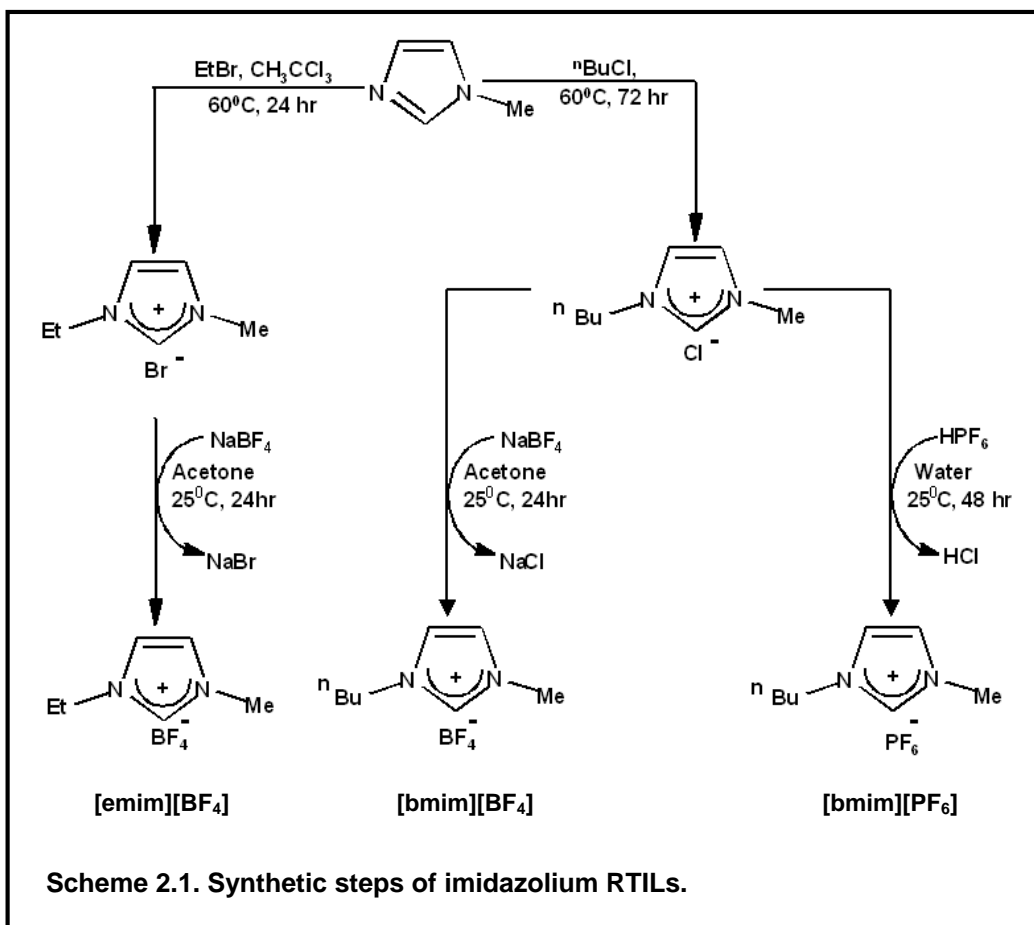
[bmim][BF<sub>4</sub>] was prepared from its chloride salt, [bmim]Cl following standard procedure.<sup>5</sup> The latter was first prepared by treating a mixture of freshly distilled 1-methylimidazole and n-chlorobutane (1:2 mole ratio) in 1,1,1-trichloroethane at 70<sup>0</sup>C for 72 hr under nitrogen atmosphere. The solution was cooled down to room temperature and was washed several times with dry ethylacetate until the washing was free from unreacted 1-methylimidazole. This was spectroscopically ensured by the absence of the strong absorption peak due to 1-methylimidazole at around 275 nm, in the washing. The halide was then recrystallised from ethylacetate:acetonitrile mixture before proceeding to the next reaction step.

Triply distilled acetone solution of a mixture of [bmim]Cl and NaBF<sub>4</sub> (in 1:1.2 mole ratio) was stirred for 24 hr at room temperature. The resulting solution



of [bmim][BF<sub>4</sub>] was filtered through a plug of celite and the volatiles were removed under reduced pressure.

[emim][BF<sub>4</sub>] was prepared from the corresponding bromide salt, [emim]Br, following a procedure similar to that adopted for the preparation of [bmim][BF<sub>4</sub>].



#### **2.2.2.2. Preparation of [bmim][PF<sub>6</sub>]**

[bmim][PF<sub>6</sub>] was also prepared following a literature procedure.<sup>6</sup> A dilute aqueous solution of [bmim]Cl was prepared in a plastic box. To this ice-cold solution, was added ice-cold HPF<sub>6</sub> (65% solution in water) (in 1:1.5 molar proportion) drop wise over an hour, with constant stirring. This slow addition prevented the rise in temperature significantly and thus avoided rapid exothermic reaction. The reaction mixture was then stirred for 24 hr at room temperature. After decanting the upper acidic layer, the lower viscous ionic liquid portion was washed with triply distilled water until it was free from acid (checked by a pH paper).

#### **2.2.2.3. Purification of the imidazolium RTILs**

The [BF<sub>4</sub>] salts were prepared in triply distilled acetone as solvent, keeping in mind the fact that the solubility of the halides in dry acetone is very low.<sup>7</sup> It is reported<sup>8</sup> that the solubility of NaCl in acetone is  $5.5 \times 10^{-6}$  mol lit<sup>-1</sup>. The [PF<sub>6</sub>] salt, on the other hand, was prepared in and washed several times with conductivity water. The removal of the halide impurities from the RTILs was confirmed by making sure that the RTILs or the final washing did not form any precipitate of silver halide when treated with an aqueous silver nitrate solution.

All the RTILs were eventually diluted with acetone or acetonitrile and then treated with activated charcoal for 48 hr and filtered a couple of times by passing through a plug of celite. The liquids thus prepared were then transferred to clean and dry reagent bottles and kept in high vacuum (pressure  $10^{-2}$  –  $10^{-3}$  mbar) for 12 hr at 60-65°C for the removal of any organic impurities or water.<sup>9</sup> The purified RTILs were characterized by both IR and NMR spectroscopy and stored in a desiccator under dry nitrogen atmosphere wrapped in aluminum foils.

#### 2.2.2.4. Preparation of [bmpy][Tf<sub>2</sub>N]

This RTIL was prepared following a standard procedure<sup>10</sup> that involved two steps (**Scheme 2.2.**). The first step consisted of the preparation of the iodide salt and the second one involved the replacement of the anion.

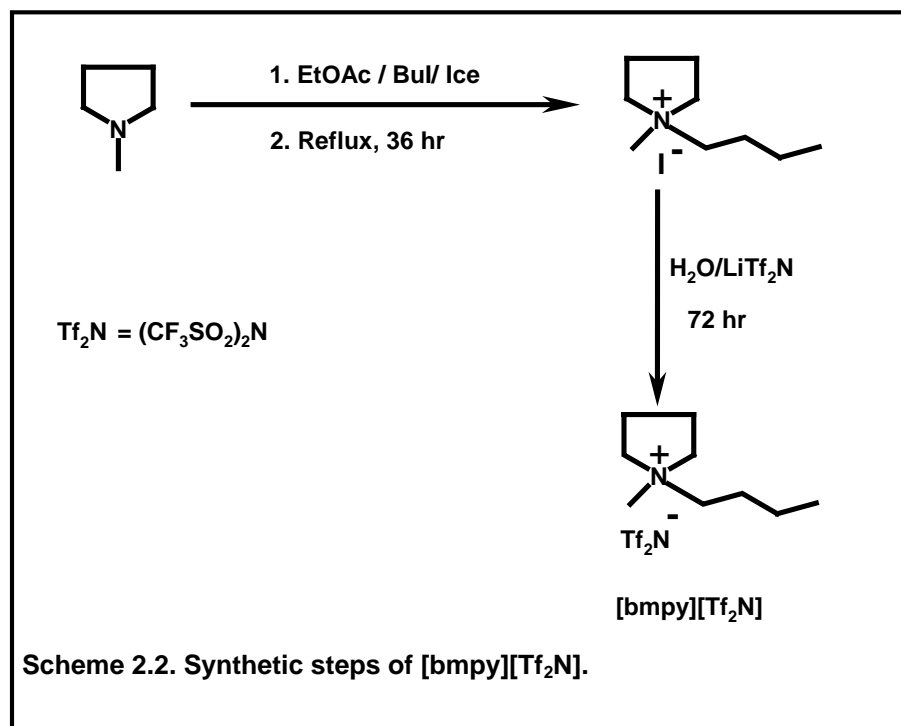
**Step 1:** 1-Methylpyrrolidine was added to ethyl acetate taken in a round-bottomed flask and was cooled with ice. To this ice-cold solution, was added 1-iodobutane drop wise for an hour. On completion of the addition, ice was removed and the solution was allowed to attain room temperature and then refluxed for 36 hr. The solution was further cooled to room temperature and the liquid portion was decanted. The colourless powder was recrystallised from acetone/ethyl acetate mixture and was washed with ethyl acetate and then dried under vacuum.

**Step 2:** The iodide salt prepared in the first step was added to triply distilled water, taken in a round-bottomed flask. To this solution, was added an aqueous solution of lithium bis(trifluoromethanesulfonyl)imide with constant stirring. The resulting solution was allowed to stir for 72 hr and then filtered.

#### 2.2.2.5. Purification of [bmpy][Tf<sub>2</sub>N]

The RTIL thus prepared, was washed several times with triply distilled water, until the washing was free from any halide (confirmed by the silver nitrate test). The resulting solution was dissolved in acetone and was treated with activated charcoal for 48 hr and then filtered through a pad of acidic alumina. The resulting colourless liquid was then kept in a dry reagent bottle and dried under high vacuum (pressure of  $10^{-2}$ -  $10^{-3}$  mbar) for 18 hr at 60-65°C for the removal of any organic impurity or water. The purified RTIL was characterized by NMR

spectroscopy (compared with the literature data),<sup>11,12</sup> and were stored in a desiccator under dry nitrogen atmosphere, wrapped in aluminium foil.



### 2.3. Instrumentation

The IR and NMR spectra of the compounds synthesized as well as RTILs prepared were measured using Jasco FTIR 5300 spectrometer and Bruker AV 400 MHz NMR spectrometer, respectively. Steady state absorption and fluorescence spectra were recorded on UV-Vis-NIR scanning spectrophotometer (Shimadzu, Model no. UV-3101PC) and on SPEX FluoroMax-3 or FluoroLog-3

spectrofluorometer, respectively. All the fluorescence spectra were corrected for the instrumental response.

### **2.3.1. Picosecond time-correlated single photon counting setup**

Time-resolved fluorescence measurements were carried out employing a picosecond laser as the excitation source, a micro-channel plate (MCP) photomultiplier tube (PMT) as the detector and a time correlated single photon counting (TCSPC) setup.<sup>13</sup> (**Fig. 2.1.**)

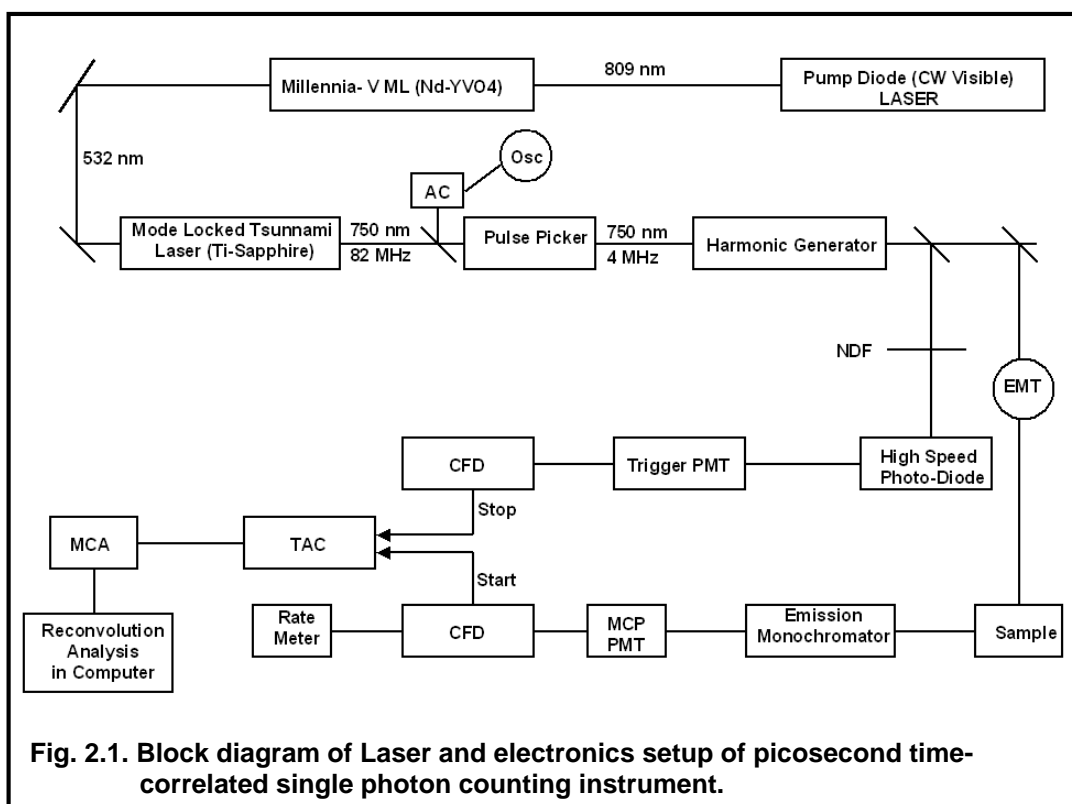
A diode-pumped Millennia (5 W) CW laser (Spectra Physics) having an output at 532 nm was used to pump the Titanium–Sapphire rod in Tsunami picosecond mode-locked laser system (Spectra Physics, Model no. 4960 M3S). The Titanium–Sapphire rod was oriented at Brewster's angle to the laser beam. The tuning of the wavelength range that could be afforded by this laser system was 720–850 nm. The pulse repetition rate was 82 MHz. A scanning auto correlator (AC, Model 409-08, Spectra Physics) was used to monitor the shape and width of the pulse from Tsunami in real-time on an oscilloscope (Osc). The laser pulse was then focussed onto the pulse picker (Model 3980, Spectra Physics), which selected the pulse from the 82 MHz train at a maximum pulse selection rate of 4 MHz. The output from the pulse picker was frequency-doubled using a flexible harmonic generator (FHG–23, Spectra Physics). The frequency-doubled 375 nm output, chosen by computer controlled excitation monochromator turret (EMT), was used to excite the sample. The emission monochromator was in Seya–Namioka configuration with 10 cm focal length and f/3 aperture. The wavelength selection in the monochromator was achieved automatically via the personal computer. The emission was detected at right angle to the excitation beam using a Hamamatsu R3809U MCP photomultiplier (160 – 850 nm).

A part of the incident picosecond pulse train selected from a quartz plate via a neutral density filter (NDF) was focused on a high-speed photodiode (PD). The output of the PD signal was triggered and fed into a constant fraction discriminator (CFD, ORTEC) to discriminate the background noise and to generate a voltage ramp, and thus, a precise timing pulse. The output of the CFD *normally* serves as the START pulse of the time-to-amplitude converter (TAC). However, since the experiment was performed in “reverse” mode (in order to get more fluorescence signal),<sup>13</sup> the photodiode signal was used as STOP signal for the TAC. Detection of the first emitted photon by the MCP photomultiplier generates a pulse, which was then fed into the CFD. The output from the CFD served as a START signal (in the “reverse” mode) for the TAC. The MCP output could be directly read on a ratemeter. The time difference between the START and STOP pulse was due to the time taken by the pulses to travel through the cables/electronics and for the excited state to relax and emit a photon. The TAC converts this time difference into a voltage ramp, and thus a particular voltage was saved in a particular channel. Repetitive laser pulsing and hence piling up of emitted photon produces a histogram of counts versus time channel. The channel axis could then be transformed into a time axis by appropriate multiplication of the time calibration factor per channel.

IBH 5000U fluorescence spectrophotometer was used for picosecond excitation and detection system attached with MCP photomultiplier tube, NIM (Nuclear Instrument Modules) timing electronics and multi channel analyser (MCA) utility software. The final instrument response time was ~ 50 ps.

Thus, the time profile of the fluorescence signal was provided. The fluorescence decay of the sample was further analysed using IBH data analysis software for Windows (version 6.1.36). Picosecond TCSPC setup was used while

measuring wavelength dependent decay for solvation dynamics measurement, and for measuring the lifetime of ANF.



### 2.3.2. Nanosecond time-correlated single photon counting setup

This system consisted of IBH 5000 single photon counting spectrophotometer, along with a PMT (Hamamatsu 3235) with a spectral range of 190-650 nm. The instrument was operated with a thyatron-gated flash lamp filled with hydrogen at a pressure of 0.5 atmosphere. The gap between the electrodes was kept at 1 mm and the operating synchronised PMT voltage was 550 Volt. The lamp frequency (repetition rate) was tuned to 40 kHz and the full-width at half-maxima of the lamp under the operating condition was  $\sim 1.4$  ns.

Unlike the previous picosecond setup, here the output of CFD served as the START pulse for TAC (Tennelec, Model TC 863) and the fluorescence photon recorded by the emission photomultiplier, as determined by CFD (ORTEC, Model 584), generated a pulse that served as the STOP signal for TAC. The same software provided by IBH was used here also for further analysis of data. The instrumental response was measured using a colloidal suspension of Ludox<sup>#</sup>, served as a scatterer, in a quartz cuvette. Nanosecond TCSPC setup was used while measuring lifetime of the samples, which are greater than 1 ns.

## **2.4. Methods**

### **2.4.1. Sample preparation for spectral measurements**

In conventional solvents, dilute solutions of the probe molecules were used for both absorption and fluorescence measurements. The optical densities of the solutions employed for all measurements, were always maintained below 0.2, at the exciting wavelength.

The sample preparation in RTILs was not so straightforward. Each time before performing any experiment the required RTILs were kept in high vacuum at 60°C for at least 12 hour to remove any moisture trapped in these media. Such treated liquids were slowly allowed to cool down to room temperature under vacuum, prior to the addition of the probe molecule. 2.5 mL of RTIL at room temperature, taken in a quartz cuvette, was used to prepare the sample solution in each case, and after the addition of solute, the quartz cuvette was sealed immediately, with septum and parafilm. Proper precaution was adopted in every step to avoid moisture contamination from atmosphere. The cuvette with the sample was kept in sealed condition at least for 24 hr with occasional shaking to

---

<sup>#</sup> Ludox is the trade name of a special type of silica made by Dupont Inc.



overcome the slow dissolution of the probe in RTILs. Each sample in the cuvette was then deoxygenated by bubbling dry nitrogen gas for a period of minimum 30 minutes prior to any measurement. The purging of nitrogen gas not only removed the dissolved oxygen, but also helped the dissolution of the solute. The sealed sample solutions were found to be stable for months under dark condition. The optical density of the probe for solvation dynamics calculation was kept below 0.3 at the excitation wavelength (375 nm), whereas for Red Edge Excitation studies the optical density at the absorption maximum was kept below 0.5.

#### 2.4.2. Data analysis

The lifetime of the samples were estimated from the measured fluorescence decay curves and the instrumental profiles using a non-linear least-squares iterative fitting procedure (IBH Decay analysis software, version 6.1.36). This programme uses a reconvolution method for the analysis of the experimental data.<sup>14</sup> When the decay time is long compared to the decay time of the excitation pulse, the excitation may be described as a  $\delta$ -function. However, when the lifetime is short, distortion of the experimental data occurs by the finite decay time of the instrumental pulse and the response time of the photomultiplier and associated electronics. Since the measured decay function is a convolution of the true fluorescence decay and the instrumental pulse, it is necessary to deconvolute the measured data from the latter in order to get the actual fluorescence lifetime. The mathematical expression of this procedure is given by the equation,

$$D(t) = \int_0^t P(t')G(t-t')dt' \dots\dots\dots(2.1)$$

where,  $D(t)$  is the fluorescence intensity at any time  $t$ ;  $P(t')$  is the intensity of the exciting light at time  $t'$ ;  $G(t-t')$  is the response function of the experimental system. The experimental data  $D(t)$  and  $P(t')$  from the MCA are fed into a personal computer to determine the lifetime. The deconvolution has been achieved by mixing the instrumental profile and a projected decay to form a new reconvoluted set. The data is compared with the experimental set and the difference between the data points summed that produced  $\chi^2$  function for fitting. The deconvolution proceeds through a series of iterations until an insignificant change of  $\chi^2$  occurs between two successive iterations. The goodness of the fit was evaluated from the reduced  $\chi^2$  values and the plot of the weighted residuals.

#### **2.4.3. Construction of time resolved emission spectra**

The time-resolved emission spectra (TRES) were constructed indirectly<sup>15</sup> by measuring a series of fluorescence decay profiles at every 5/10 nm wavelength intervals across the entire steady state emission spectrum of the probe molecule in a particular RTIL. Each intensity decay curve was then fitted to a tri-exponential decay function to obtain a  $\chi^2$  value between 1 and 1.2. This procedure deconvoluted the measured decay from its instrumental response and increased the effective time-resolution of the experiments to ~25 ps. The impulse response function  $I(\lambda, t)$  was calculated from those best-fitted curve. To make the time-integrated intensity at each wavelength equal to the steady state intensity at that particular wavelength, a set of  $H(\lambda)$  values were calculated using,

$$H(\lambda) = \frac{I_{ss}(\lambda)}{\sum_i \alpha_i(\lambda) \tau_i(\lambda)} \dots\dots\dots (2.2)$$

where,  $I_{ss}(\lambda)$  is the steady state intensity,  $\alpha_i(\lambda)$  is the pre-exponential coefficient and  $\tau_i(\lambda)$  is the decay time at that wavelength with  $\sum \alpha_i(\lambda) = 1$ . The time-resolved emission spectra at different times were calculated from the appropriately normalized intensity decay (impulse response) function  $I'(\lambda, t)$  for different wavelengths at different times, where  $I'(\lambda, t) = H(\lambda) \times I(\lambda, t)$ . The emission maximum (wavenumber scale) at each time  $t$ ,  $(\bar{\nu}(t))$  was obtained by fitting the spectra to lognormal line shape function known for its better representation of the emission spectrum in polar solvents. The lognormal function<sup>16,17</sup> can be expressed as,

$$F(\bar{\nu}, t) = h \exp\left\{-\ln(2)[\ln(1 + \alpha)/\gamma]^2\right\}, \quad \text{for } \alpha > -1 \quad \text{.....(2.3)}$$

$$= 0, \quad \text{for } \alpha \leq -1$$

where,  $\alpha \equiv \frac{2\gamma [\bar{\nu} - \bar{\nu}_p]}{\Delta}$ ,  $h$  is the peak height,  $\bar{\nu}_p$  is the peak frequency,  $\gamma$

is the asymmetry parameter and  $\Delta$  is the width of the curve. While fitting our spectral data all the above four parameters were allowed to vary freely and a non-linear least square fitting was used to extract the best-fitted curve until successive iterations gave the identical  $\chi^2$  value.

Apart from using  $\bar{\nu}_p$ , obtained directly from the lognormal fits, several researchers have used the average frequency (first moment) of the spectrum, the average of the half-height points or the high-frequency half-height points.<sup>17-21</sup>

The solvation dynamics, described by the normalized Stokes' shift correlation function  $C(t)$ , defined as,<sup>22,23</sup>

$$C(t) = \frac{\bar{\nu}(t) - \bar{\nu}(\infty)}{\bar{\nu}(0) - \bar{\nu}(\infty)} \quad \text{.....(2.4)}$$

was calculated using the peak frequency of the time-resolved emission spectra, where,  $\bar{\nu}(0)$ ,  $\bar{\nu}(t)$  and  $\bar{\nu}(\infty)$  are the peak frequencies instantly after excitation, at an intermediate time ( $t$ ) and at infinite time after excitation (when the spectrum does not show any time dependent Stokes' shift), respectively. The method of determination of  $\bar{\nu}(0)$  from the time-resolved data is dependent on the finite time-resolution of the instrumental setup.<sup>24-26</sup> Hence, the initial response of the solvent that occurs within the first ~25 ps (time-resolution of the picosecond single photon count setup, after deconvolution of the fitted decay curves) would not be included in the so obtained  $C(t)$  function.

In all the cases, the obtained  $C(t)$  functions can be fitted well with a simple bi-exponential decay function,  $C(t) = a_1 \exp^{-t/\tau_1} + a_2 \exp^{-t/\tau_2}$  where  $\tau_1$  and  $\tau_2$  are the two relaxation times having amplitudes of  $a_1$  and  $a_2$  respectively. As the time dependence of  $C(t)$  consists of more than one component, the relaxation time is generally expressed as an average. The average relaxation time,  $\langle \tau \rangle$  is defined as,  $\langle \tau \rangle = a_1 \tau_1 + a_2 \tau_2$ , where  $a_1$ ,  $a_2$  are the corresponding amplitudes of the relaxation time,  $\tau_1$ ,  $\tau_2$  respectively and  $(a_1 + a_2) = 1$ .

Research groups of Barbara and Huppert have used a stretched exponential factor  $\beta$ , in order to improve their bi-exponential fitting parameters.<sup>27-29</sup> However, in our case, no significant improvement, to the quality of the fit, has been noticed by varying the  $\beta$  value from 0.4 to 0.9.

#### **2.4.4. Estimation of polarity in $E_T(30)$ and $E_T^N$ scale**

The solvatochromic visible absorption of the betaine dye has been used as a solvent dependent reference probe to define empirically a solvent polarity scale, namely  $E_T(30)$  scale.<sup>3</sup> The  $E_T(30)$  values are defined as the molar

transition energies of the betaine dye measured in solvents of different polarity at room temperature (25°C) and normal pressure (1 bar). Thus,

$$E_T(30) = hc \bar{\nu}_{\max} N_A = (2.8591 \times 10^{-3}) \bar{\nu}_{\max} / \text{cm}^{-1} \\ = 28591 / \lambda_{\max} (\text{nm}) \dots\dots\dots (2.5)$$

where,  $\bar{\nu}_{\max}$  is the wavenumber and  $\lambda_{\max}$  is the wavelength corresponding to the maximum of longest wavelength, solvatochromic, intramolecular charge transfer absorption of the betaine dye; 'h' is the Planck's constant, 'c' is the velocity of light in vacuum and 'N<sub>A</sub>' is the Avogadro number. This is the direct way of measurement of solvent polarity.

Instead of measuring the  $E_T(30)$  value of the solvent from the longest wavelength absorption maximum of betaine dye in that particular solvent, it is often measured in an indirect way, described as follows. The wavenumber corresponding to the fluorescence maximum,  $\bar{\nu}_{\max}^{flu}$ , of each probe molecule, in various conventional solvents, was experimentally measured from its steady state emission spectra at room temperature. The emission maximum values ( $\text{cm}^{-1}$ ) were then plotted against known  $E_T(30)$  values of the solvent to obtain a linear relationship between the two quantities. Using this plot and the measured  $\bar{\nu}_{\max}^{flu}$  value of the probe in RTIL, the  $E_T(30)$  value of the particular RTIL was estimated.

The normalized microscopic solvent polarity parameter,  $E_T^N$  (a dimensionless number), for each RTIL can be calculated from the following relation, using the estimated  $E_T(30)$  value of RTIL and the same of tetramethylsilane (TMS) and water as a reference solvent.<sup>3</sup>

$$E_T^N = [E_T(\text{RTIL}) - E_T(\text{TMS})] / [E_T(\text{water}) - E_T(\text{TMS})] \dots\dots\dots (2.6)$$

#### 2.4.5. Standard error limits

The estimated error limits in different measurements are:

$\lambda_{\max}$ (fluo/abs)	$\pm 1$ nm
$\tau$ (higher than 1ns)	$\pm 5$ %
$\tau$ (lower than 1ns)	$\pm 5$ %
Equilibrium constant	$\pm 10$ %
Polarity of RTILs in $E_T(30)$ scale	$\pm 5$ %
Relaxation time	$\pm 5$ -10 %

#### 2.4.6. Theoretical calculation

The molecular structure of different fluorophores in gas phase and their dipole moments were calculated using quantum mechanical calculation based on semiempirical AM1 (Austin Model 1) Hamiltonian.<sup>30,31</sup> The calculations were performed in a personal computer using HyperChem package (Release 6.0) for Windows obtained from Hypercube, Inc. The unrestricted geometry optimisation of the molecular structure was done by using AM1 Hamiltonian in view of its superiority over other semi-empirical methods.<sup>30-32</sup> This was achieved using conjugate gradient (Polak-Ribiere) type of algorithm with root mean square (rms) gradient as the convergence criterion. The rms gradient was kept below 0.001 kcal/(Åmol) in all the cases. The ground state dipole moments were calculated from single point calculation on the optimised geometry.

#### 2.5. References

- (1) Saha, S.; Samanta, A. *J. Phys. Chem. A* **1998**, *102*, 7903.
- (2) Perrin, D. D.; Armarego, W. L. F.; Perrin, D. R. *Purification of Laboratory Chemicals*; Pergamon Press: New York, 1980.
- (3) Reichardt, C. *Solvents and Solvent Effects in Organic Chemistry*; VCH: Weinheim, Germany, 1988.

- (4) Ormson, S. M.; Brown, R. G.; Vollmer, F.; Rettig, W. *J. Photochem. Photobiol. A : Chem.* **1994**, *81*, 65.
- (5) Suarez, P. A. Z.; Dullius, J. E. L.; Einloft, S.; Souza, R. F. D.; Dupont, J. *Polyhedron* **1996**, *15*, 1217.
- (6) Huddleston, J. G.; Willauer, H. D.; Swatoski, R. P.; Visser, A. E.; Rogers, R. D. *Chem. Commun.* **1998**, 1765.
- (7) Fuller, J.; Carlin, R. T.; Osteryoung, R. A. *J. Electrochem. Soc.* **1997**, *144*, 3881.
- (8) Holbrey, J. D.; Seddon, K. R. *J. Chem. Soc., Dalton Trans.* **1999**, 2133.
- (9) Seddon, K. R.; Stark, A.; Torres, M. J. In *Clean Solvents: Alternative Media for Chemical Reactions and Processing*; Abraham, M., Moens, L., Eds.; ACS Symposium Series 819: Washington DC, 2002.
- (10) Henderson, W. A.; Passerini, S. *Chem. Mater.* **2004**, *16*, 2881.
- (11) MacFarlane, D. R.; Meakin, P.; Sun, J.; Amini, N.; Forsyth, M. *J. Phys. Chem. B* **1999**, *103*, 4164.
- (12) Lancaster, N. L.; Salter, P. A.; Welton, T.; Young, G. B. *J. Org. Chem.* **2002**, *67*, 8855.
- (13) O'Connor, D. V.; Phillips, D. *Time-Correlated Single Photon Counting*; Academic Press: New York, 1984.
- (14) Bevington, P. R. *Data Reduction and Error Analysis for the Physical Sciences.*; McGraw-Hill: New-York, 1969.
- (15) Lakowicz, J. R. *Principles of Fluorescence Spectroscopy*, 2nd ed.; Plenum Press: New York, 1999.
- (16) Fraser, R. D. B.; Suzuki, E. In *Spectral Analysis*; Blackburn, J. A., Ed.; Marcel Dekker: New York, 1970.
- (17) Horng, M. L.; Gardecki, J. A.; Papazyan, A.; Maroncelli, M. *J. Phys. Chem.* **1995**, *99*, 17311.
- (18) Siano, D. B.; Metzler, D. E. *J. Chem. Phys.* **1969**, *51*, 1856.
- (19) Maroncelli, M.; Fleming, G. R. *J. Chem. Phys.* **1988**, *89*, 875.
- (20) Maroncelli, M.; Fleming, G. R. *J. Chem. Phys.* **1988**, *89*, 5044.
- (21) Maroncelli, M.; Fleming, G. R. *J. Chem. Phys.* **1990**, *92*, 3251.
- (22) Bagchi, B.; Oxtoby, D. W.; Fleming, G. R. *Chem. Phys.* **1984**, *86*, 257.
- (23) van der Zwan, G.; Hynes, J. T. *J. Phys. Chem.* **1985**, *89*, 4181.
- (24) Fee, R. S.; Maroncelli, M. *Chem. Phys.* **1994**, *183*, 235.
- (25) Chapman, C. F.; Fee, R. S.; Maroncelli, M. *J. Phys. Chem.* **1995**, *99*, 4811.
- (26) Fee, R. S.; Milsom, J. A.; Maroncelli, M. *J. Phys. Chem.* **1991**, *95*, 5170.
- (27) Bart, E.; Meltsin, A.; Huppert, D. *J. Phys. Chem.* **1994**, *98*, 3295.
- (28) Bart, E.; Meltsin, A.; Huppert, D. *J. Phys. Chem.* **1994**, *98*, 10819.
- (29) Bart, E.; Meltsin, A.; Huppert, D. *J. Phys. Chem.* **1995**, *99*, 9253.
- (30) Dewar, M. J. S.; Zebisch, E. G.; Healy, E. F.; Stewart, J. J. P. *J. Am. Chem. Soc.* **1985**, *107*, 3902.
- (31) Dewar, M. J. S.; Dieter, K. M. *J. Am. Chem. Soc.* **1986**, *108*, 8075.
- (32) Dewar, M. J. S.; Thiel, W. *J. Am. Chem. Soc.* **1977**, *99*, 4899.

### Solvent Mediated Ground State Proton Transfer in 3-hydroxyflavone: Anion Formation in Neutral Alcoholic Solvents

---

This chapter describes the photophysical behaviour of 3-hydroxyflavone in hydrogen bond donating solvents. In neat alcohols and in acetonitrile-methanol mixture a long wavelength absorption band ( $\lambda_{\text{max}} \approx 410$  nm) has been observed. Selective excitation of this band does not produce the characteristic fluorescence of the 'normal' form or the tautomer of the molecule; instead, an emission characterized by a featureless band ( $\lambda_{\text{max}} \approx 480$  nm) is observed. Based on the control experiments, the long-wavelength absorption band of HF has been attributed to its anionic form, generated in the alcoholic media by solvent mediated deprotonation of the 3-hydroxy group of the molecule in the ground state.

---

#### 3.1. Introduction

Excited state intramolecular proton transfer (ESIPT) reaction is considered to be one of the simplest photoreactions of great importance in chemical and biological systems and is of great interest from both experimental and theoretical points of view.<sup>1-12</sup> 3-Hydroxyflavone (HF) is one of the most extensively studied systems to understand the mechanism and dynamics of the intramolecular proton transfer reactions.<sup>13-47</sup> HF is known to exhibit dual fluorescence; one originating from the 'normal' isomer and another from the tautomer (**T**) (as represented earlier in **Scheme 1.4.** as **N**). HF exists in the ground state as **N** and on photonic excitation, it undergoes an adiabatic ESIPT reaction resulting in the formation of **T\***. The fluorescence that occurs from **N\*** is



referred to as 'blue' fluorescence, while that, which originates from  $T^*$  is termed as 'green' one.<sup>13</sup>

Time-resolved fluorescence studies by different groups have shown that ESIPT dynamics depends on the nature of the solvent and temperature.<sup>14,15</sup> Two different forms of N in the excited state, undergoing proton transfer reaction at different rates have been suggested by the proton transfer kinetics.<sup>16</sup> ESIPT in HF is reported to be so rapid in dry hydrocarbon solvents that the fluorescence from  $N^*$  could not be observed even in frozen solvent at 77K. Interestingly, a third fluorescence band ( $\lambda_{\text{max}} = 497 \text{ nm}$ ) in methyl cyclohexane at 77K, has been attributed to the anionic form (**A**) of HF (**Chart 3.1.**), formed due to the presence of trace amount of water as impurity in the solvent.<sup>20</sup> In order to understand the mechanism of proton transfer reaction in alcoholic media the photophysics of HF have been studied in a series of alcohols. Various solvated structures of HF have been invoked to account for the different fluorescence bands of HF in hydroxylic solvents. A direct correlation between the slow proton transfer rate constant with the hydrogen bond donating ability of the solvent is revealed. A mechanistic model for the proton transfer reaction has been proposed assuming the formation of 1:1 complex with the alcohol molecules.<sup>21</sup> The rate constant for the slow proton transfer process is found to be independent of the viscosity of the solvent. Further studies on several HF derivatives suggested that ESIPT mechanism in these systems is governed primarily by the energetic factors of the solute:solvent complex, rather than by the solvent reorganization dynamics.<sup>22</sup> Employing femtosecond absorption and fluorescence technique, the presence of both subpicosecond and picosecond components of proton transfer dynamics has been observed in all solvents. The fast and slow components in alcohol have been attributed to the mono-solvated and di-solvated HF molecules respectively.

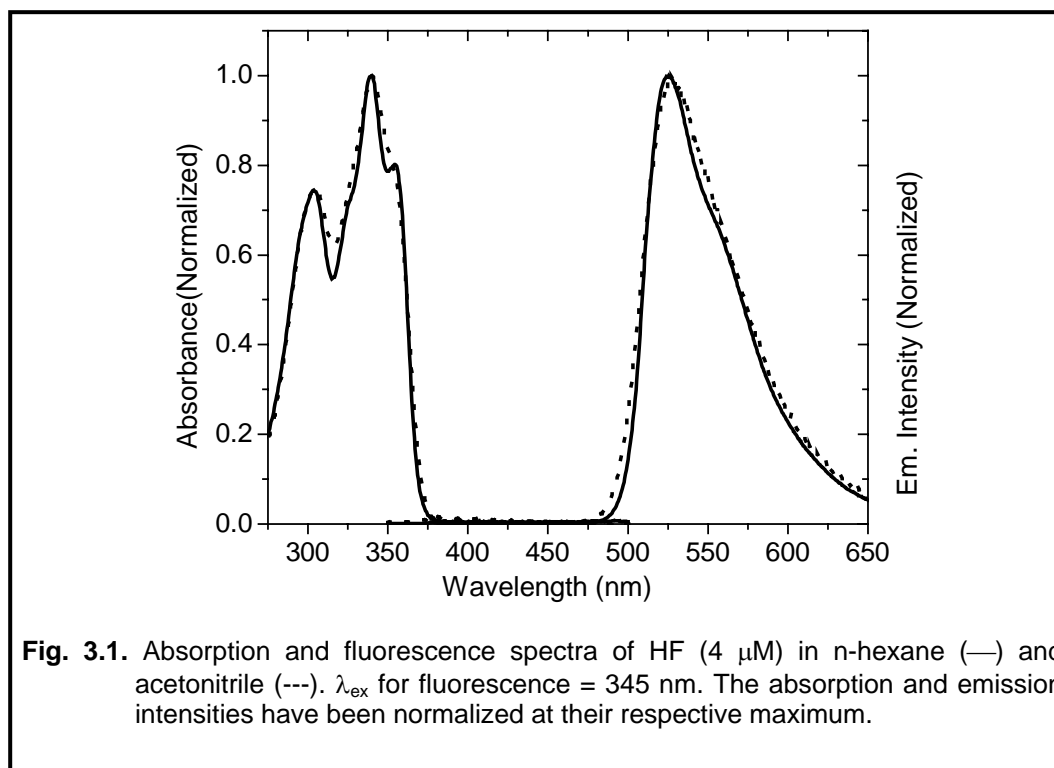
However, there is controversy on how fast the proton transfer is. In methanol, a fast rise component ( $<125$  fs) has been observed, whereas in ethanol, a 60 fs component has been reported. In aprotic solvents such as methyl cyclohexane and acetonitrile, ESPT was found to be even faster. From a recent analysis of the homogeneous bandwidth of the emission spectra of HF and its deuterated derivative in Shpol'skii matrixes (n-octane and n-octane/octanol mixtures) at 10 K, the time constant for excited state proton transfer reaction has been estimated to be  $39 \pm 10$  fs.<sup>25</sup>

Therefore, it is evident that while steady state and time-resolved fluorescence properties of HF in aprotic media are fairly well understood, the mechanism of the proton transfer reaction in hydrogen bond donating solvents is still far from clear. What is difficult to comprehend is the fact that even though fluorescence measurements in hydroxylated solvents have clearly indicated the formation of hydrogen bonded complexes of various stoichiometries between HF and the solvent molecules, no light has been thrown on the exact nature of the hydrogen-bonded complex and the specific absorption or emission due to the hydrogen bonded complex has not been reported. Since identification of specific absorption due to the hydrogen-bonded complex allows selective excitation of this species, we thought it appropriate to reinvestigate the absorption and fluorescence behaviour of HF in alcoholic solvents.

## **3.2. Results**

### **3.2.1. Spectral behaviour in aprotic solvents**

The steady state absorption and fluorescence behaviour of HF in nonpolar media such as n-hexane and in polar media such as acetonitrile has been depicted in **Fig. 3.1**.



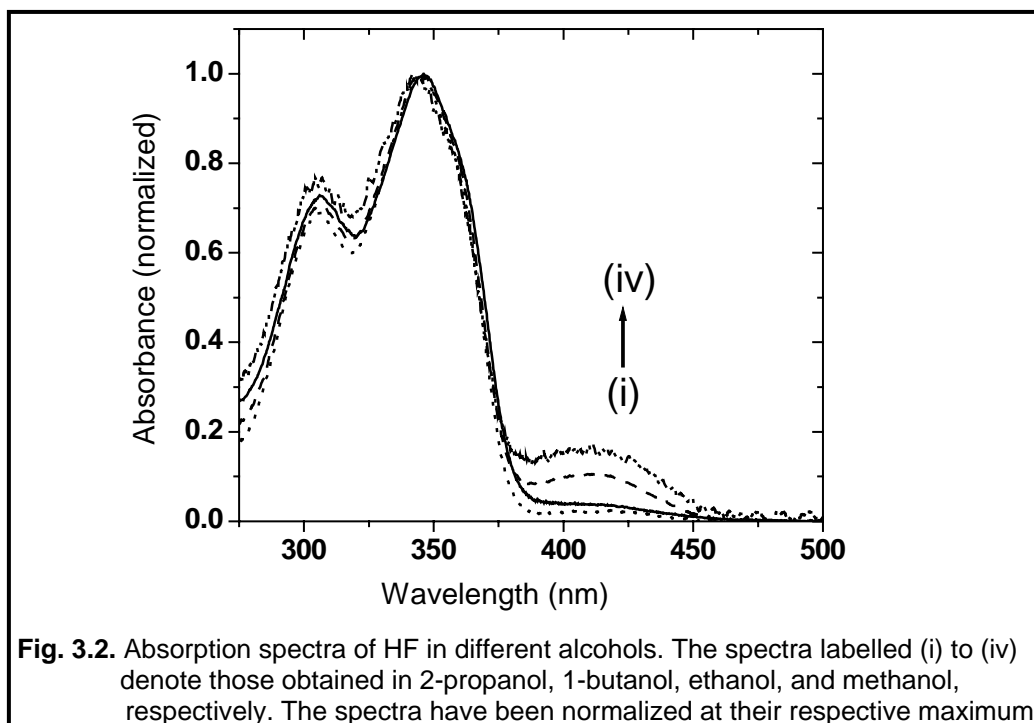
Except for the fact that the absorption spectrum is relatively more resolved in non-polar n-hexane, the spectral behaviour of the system is very similar in both the solvents. The onset of the absorption is observed at around 375 nm and the absorption peaks are observed at 355, 340, and 304 nm.

On the other hand, the fluorescence spectrum is characterized by a highly Stokes'-shifted band ( $\lambda_{\text{max}} \sim 527$  nm) in both the solvents. This spectral behaviour of HF is consistent with what is reported in literature, according to which the absorption band is due to excitation of the form N and the Stokes'-shifted fluorescence originates from  $T^*$ .<sup>13</sup>

### 3.2.2. Spectral behaviour in protic solvents

#### 3.2.2.1. Absorption

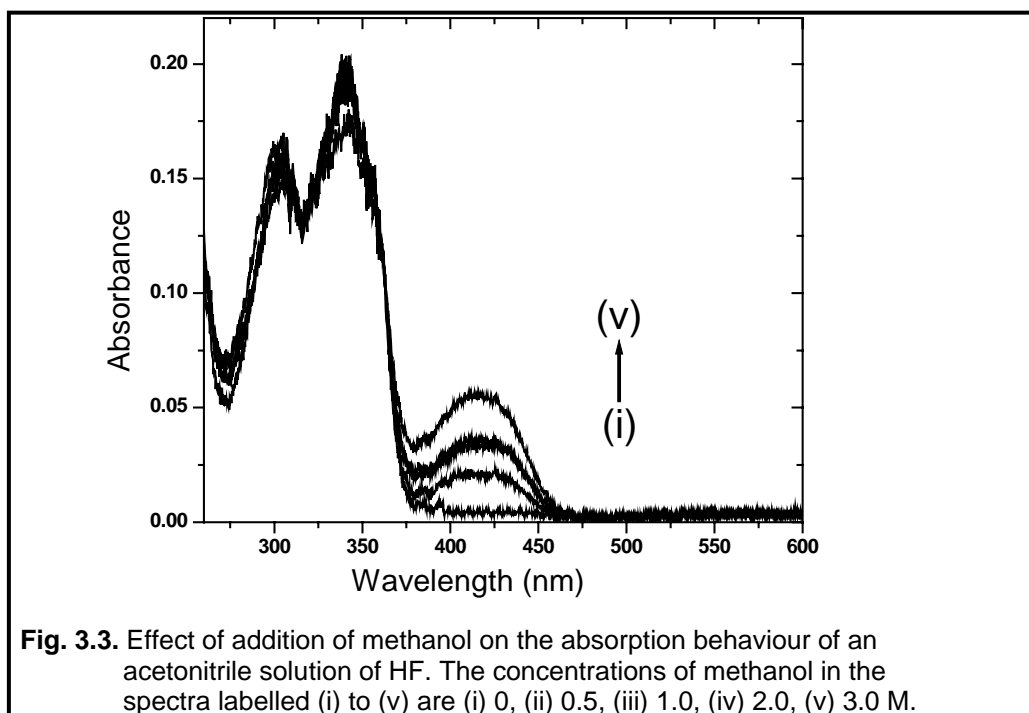
Quite surprisingly, the absorption and fluorescence behaviour of HF in alcoholic media is found to be significantly different from what is reported in the literature. In methanol, in addition to the absorption features observed in aprotic solvents, a broad absorption band is observed between 400 and 450 nm ( $\lambda_{\text{max}} \approx 410$  nm). This has been depicted in **Fig. 3.2**.



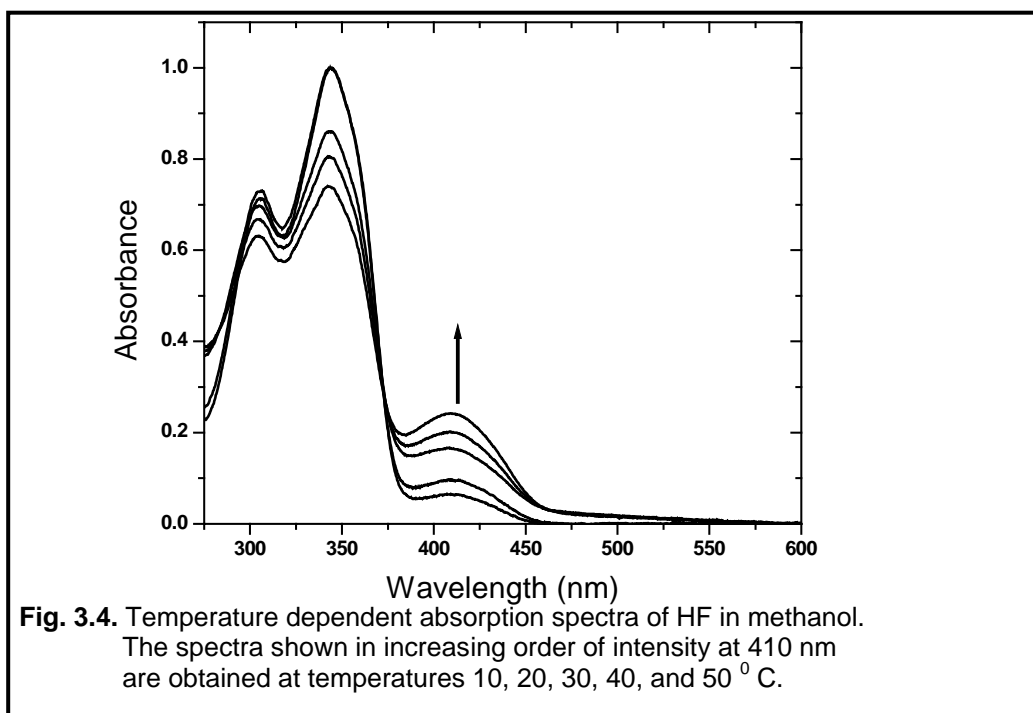
The fact that this absorption band is not due to any impurity present in HF is evident from the fact that it showed a single spot in TLC. This is further supported by the absence of this new absorption band in protic solvents.

Moreover, in order to nullify the possibility that this new absorption band is due to any impurity present in methanol, we have examined the absorption behaviour of the system in a few other alcohols, such as ethanol, 2-propanol and 1-butanol. As can be seen, this hitherto unobserved absorption band of HF above 400 nm appears in all the alcoholic solvents, although less prominently in other alcohols. Thus, the new absorption band is not due to any impurity present in either the compound or the solvents.

A long-wavelength absorption band similar to that observed in pure alcoholic solvents, is also observed on addition of methanol (or other alcohols) to an acetonitrile solution of HF. The presence of an isosbestic point around 362 nm is suggestive of the existence of more than one species in the solution. This feature has been depicted in **Fig. 3.3**.

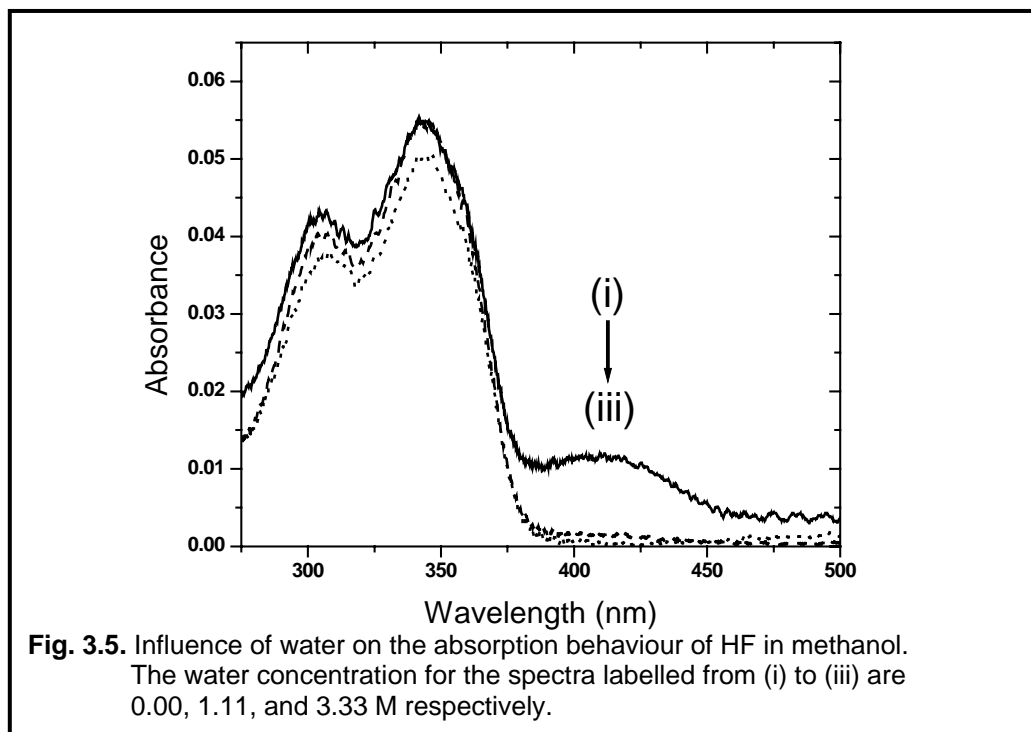


In order to probe into the species responsible for the 410 nm absorption band we have performed some control experiments. The temperature dependence of steady state absorption behaviour is one of them. The results have been depicted in **Fig. 3.4**. With an increase in the temperature, the optical density (OD) at 410 nm gradually increases with concomitant decrease of the OD in the 300 - 350 nm region of the spectra. An isosbestic point can be observed at ~372 nm.



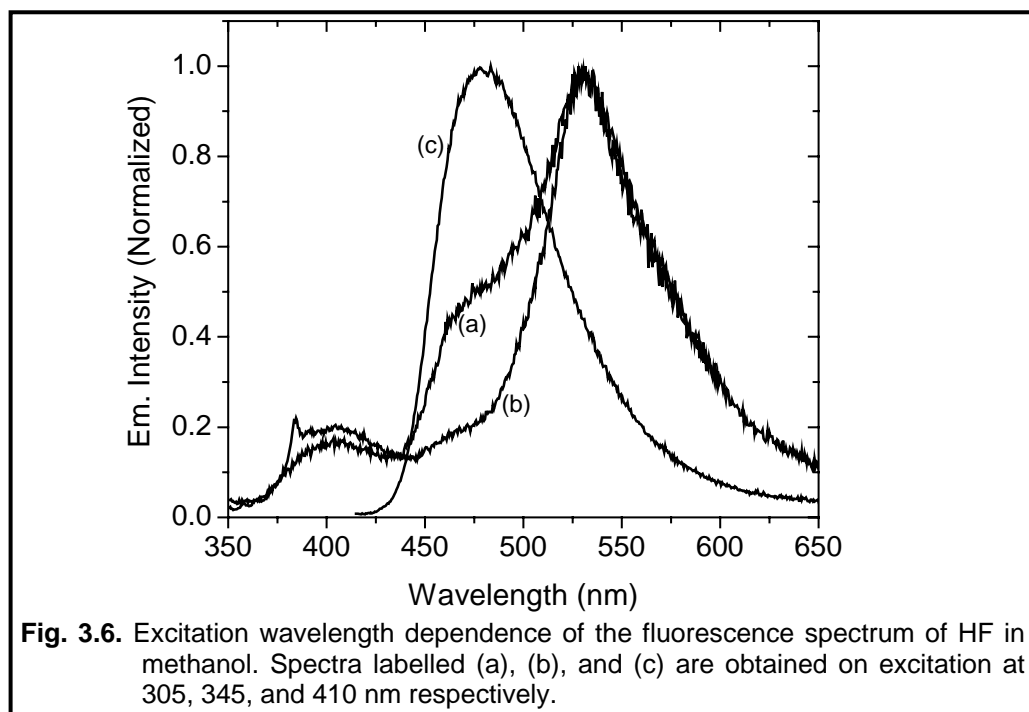
Another control experiment is the study of influence of addition of water on the steady state absorption and emission behaviour of HF in alcoholic media. The influence of water on the long wavelength absorption band is found to be quite interesting. In the presence of a small concentration of water (~1M), the

new absorption band disappears almost completely. **Fig. 3.5.** illustrates the influence of water on the absorption behaviour of HF in methanol medium.



### 3.2.2.2. Fluorescence

The steady state fluorescence behaviour of HF in alcoholic media is also found to be surprising. We have found an excitation wavelength dependent emission behaviour of HF in alcoholic media. **Fig. 3.6.** depicts the excitation wavelength dependence of the fluorescence spectrum of HF in methanol.



On excitation at 305 nm, HF shows, dual emission bands with maxima at 405 and 527 nm, quite similar to that observed in aprotic solvents. However, a third emission band, appearing as a shoulder at around 480 nm can also be observed. On excitation at 410 nm, neither the 405 nm band nor the 530 nm band can be observed. Instead, a single emission band having maximum at 480 nm could be observed.

The excited state lifetime of this emitting species in methanol, monitoring the decay profile at 480 nm, ( $\lambda_{\text{ex}} = 410$  nm), is estimated to be  $\sim 2.0$  ns. The decay profile corresponding to the 480 nm emission is also examined by exciting the sample at 305 nm. However, we cannot resolve any rise time, which might suggest that 480 nm species is produced on excitation of a second species.



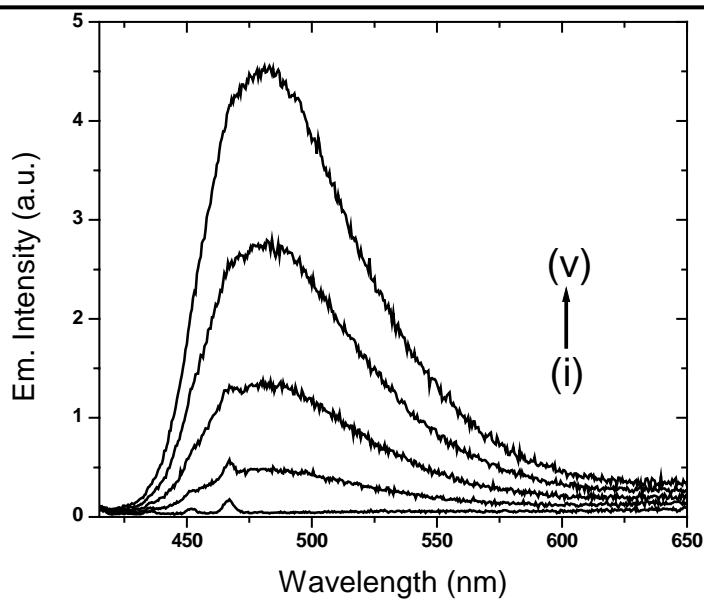


**Fig. 3.7.** Effect of addition of methanol on the fluorescence behaviour of HF in acetonitrile ( $\lambda_{\text{ex}} = 410$  nm). The concentrations of methanol in the spectra labelled (i) to (v) are as follows: (i) 0, (ii) 0.5, (iii) 0.7, (iv) 1.0, and (v) 1.2 M.

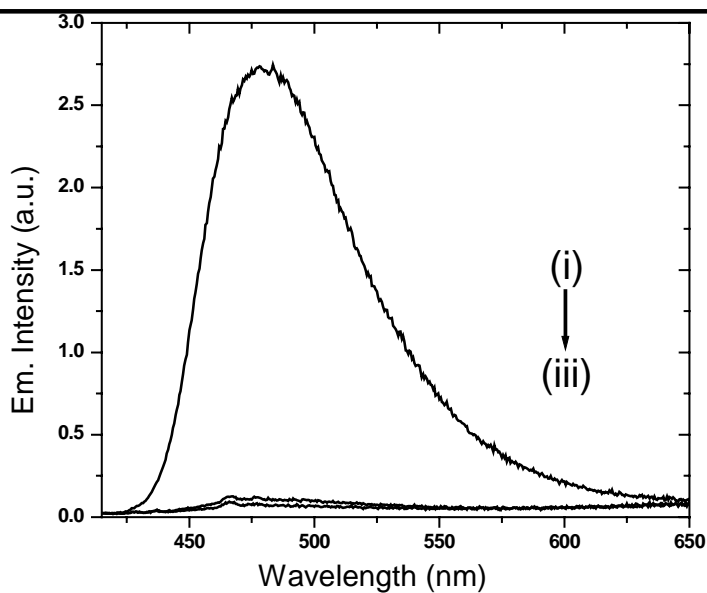


**Fig. 3.8.** Effect of addition of water on the fluorescence spectrum of HF in methanol ( $\lambda_{\text{ex}} = 410$  nm). The concentration of water in the spectra labelled from (i) to (iii) are 0.00, 2.22, and 3.33 M, respectively.

Although, only the green fluorescence due to the tautomer ( $T^*$ ) is observed in acetonitrile, addition of methanol (or any other alcohol) in this medium, indeed produces the 480 nm emission band, which is observed in neat alcoholic solutions. This effect has been illustrated in **Fig. 3.7**.

As a part of our control experiments, the influence of trace amount of water on the fluorescence behaviour of HF in alcoholic media, is illustrated in **Fig. 3.8**. As can be seen, the 480 nm emission band disappears almost completely in the presence of 1 M water.

### **3.3. Discussion**

We were a bit puzzled, initially to make out how a simple absorption band (though weak in intensity) in alcoholic media, could be missed by others, considering such a large volume of investigations made on the current system.<sup>13-47</sup> Thus, we had to carry out several control experiments to rule out the possibility that the new absorption band at 410 nm, is not due to any impurity present in the sample/solvent and to convince ourselves that this absorption band, which can be crucial to the dynamics and mechanism of excited state proton transfer reaction in alcoholic solvent, is indeed a real one. Only when we observed that the new absorption vanishes completely in the presence of trace amount of water, we realized that others might have missed this absorption because of the presence of a small amount of water in the alcohol. It is clearly evident from the literature that although utmost care was taken to ensure that the hydrocarbon solvents were free from hydroxylic impurities, no purification procedure was adopted for methanol.<sup>20</sup>

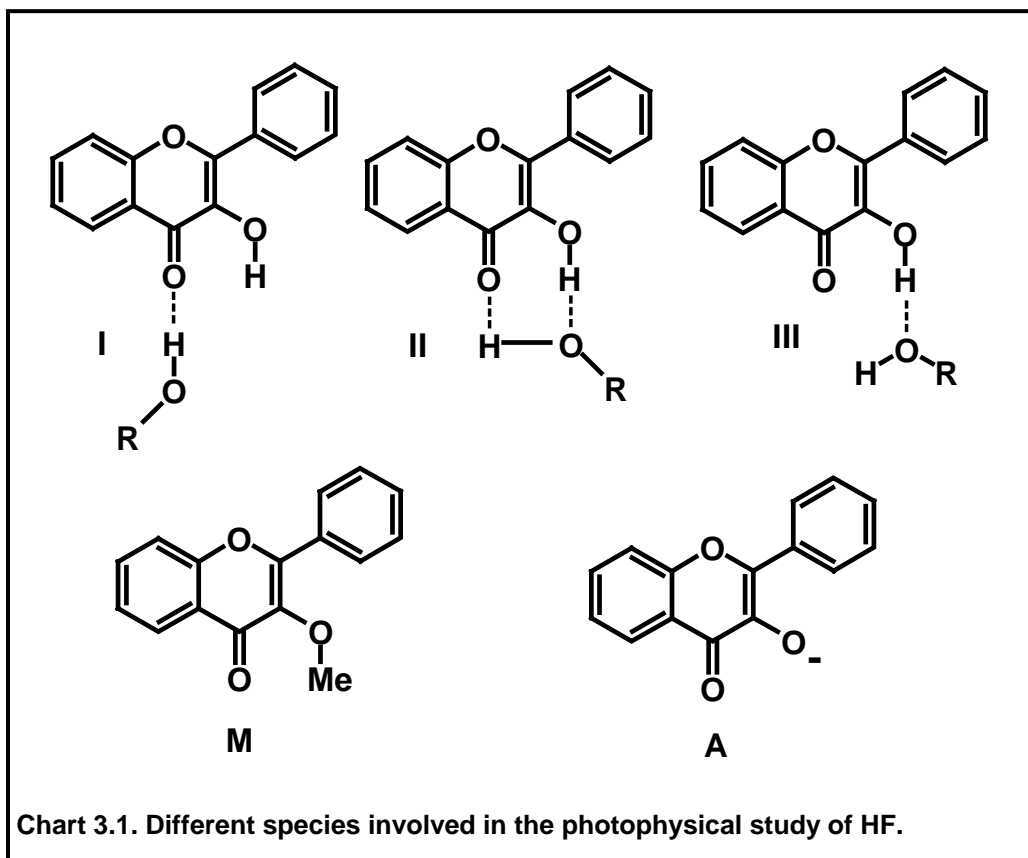
Since the long-wavelength absorption band can only be observed in alcoholic solvents (either pure alcohol or binary solvent containing alcohol), the hydrogen bond donating ability of the solvent can be responsible for the

formation of the species that contributes to this new absorption. This is corroborated by the fact that this long-wavelength absorption could not be observed in solvents that are well-known hydrogen bond acceptors (such as diethyl ether and ethyl acetate). Further support to this conjecture comes from the observation that the intensity of the 410 nm band decreases as follows: methanol>ethanol>1-butanol>2-propanol. This order, is in fact, identical with the hydrogen bond donating ability<sup>48</sup> of these solvent molecules.

Now, we would like to look upon what type of hydrogen-bonded complex could be responsible for this type of behaviour. Taking note of the isosbestic point in acetonitrile-methanol mixed solvent and the discussion in the earlier paragraph, one can perhaps attribute the 410 nm absorption to a 1:1 hydrogen-bonded complex formed between HF and alcohol molecules and speculate structures such as **I** or **II** (**Chart 3.1.**) for the complex. **III** (**Chart 3.1.**) is ruled out as a possibility, because in this species, the solvent molecule does not play the role of a hydrogen bond donor.

However, there are a few problems in attributing the 410 nm absorption band to one of the two 1:1 complexes. The main difficulty is the following: we have observed that the methoxy derivative of HF (**M**) (**Chart 3.1.**) does not show the long-wavelength absorption band in alcoholic solvents. Had the 410 nm absorption band been due to a 1:1 complex, in which the solvent acts as a hydrogen bond donor (as in **I** or **II**), **M** should have exhibited similar absorption in alcoholic solvents. A second difficulty is the interpretation of the observed effect of the temperature on the absorption spectrum of HF, as mentioned earlier. An increase in temperature should have led to the dissociation of the complex (**I** or **II**), resulting in a reduction in the intensity of the long-wavelength band. However, the effect of temperature on the absorption intensity at 410 nm is exactly

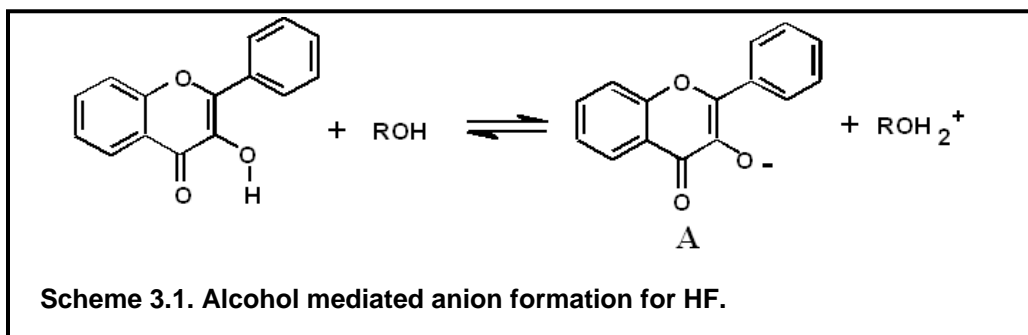
opposite to what is expected from the hydrogen-bonded complex. A third difficulty is to find a suitable explanation for the disappearance of the 410 nm absorption and 480 nm emission bands in the presence of water. Since water is a better hydrogen bond donor (*vide* later) than the alcohols, one would have expected a more intense 410 nm band in water.



Clearly, 1:1 complexation between HF and hydrogen bond donating solvents can not account for some of the crucial observations made in this study and thus, a different assignment for the 410 nm absorbing species is needed. We take into consideration that the species, which absorbs at 410 nm emits at

around 480 nm. Although no absorption band of the kind observed here has been reported in the past, a number of researchers have reported an emission band similar to the one described here. McMorrow and Kasha<sup>20</sup> attributed this type of emission, observed in MCH glass (at 77 K), to the anion (**A**) of HF, formed as a result of the presence of water as impurity in the solvent. Brucker and Kelly,<sup>46</sup> on the other hand, attributed a similar emission band of 3HF in argon:methanol matrix at 30K to a monosolvated tautomer. Interestingly, while studying the proton transfer reaction in HF/ammonia complex at 10K, Brucker and Kelly<sup>47</sup> observed a fluorescence excitation band around 400 nm that resembles the present absorption band. These authors attributed this band to HF anion (**A**), (**Chart 3.1.**) formed as a result of proton transfer from 3HF to (NH<sub>3</sub>)<sub>n</sub> cluster in the ground state.

We have also noticed that, in one of the earlier reports,<sup>43</sup> it is mentioned that the absorption and emission spectra of the anion, **A**, generated in alkaline (KOH) methanolic solution of HF are very similar to the spectra we have observed in alcoholic media. Taking into consideration these investigations and our present observation we assign the 410 nm absorbing species to **A** that emits at 480 nm. This implies that HF undergoes solvent mediated deprotonation reaction in alcoholic media in the ground state. This phenomenon has been illustrated in **Scheme 3.1.**



The extent of anion formation in alcoholic media has been evaluated by estimating the equilibrium constant,  $K_a$ , by monitoring the changes in the absorbance at 410 nm, following addition of methanol to an acetonitrile solution of HF. Using data from **Fig. 3.3.** and the molar extinction coefficient of **A** at 410 nm as  $1.44 \times 10^4 \text{ M}^{-1}\text{cm}^{-1}$  (estimated from the absorbance at 410 nm in excess KOH added alcoholic solution of known concentration of HF), the  $K_a$  value has been estimated to be  $2.9 \times 10^{-7}$  (See **Appendix 1**). This suggests that the extent of ionisation of HF is rather small.

In this context, we would like to take into account an earlier report of anion formation of HF in neutral medium.<sup>43</sup> The formation of **A** in a neutral solvent, formamide, was attributed to a greater hydrogen bond donating ability of this solvent compared to that of others such as acetonitrile or alcohol.<sup>43</sup> However, though hydrogen bond donating ability of formamide is greater than that of acetonitrile, most of the alcohols are stronger hydrogen bond donor compared to formamide.<sup>49</sup> Hence, anion should also have been formed in the alcoholic media. Moreover, according to the explanation offered, **A** should have been formed in water, known to be the strongest hydrogen bond donor.

Since we have observed the anion **A** in alcoholic media, we examined how the proton abstracting ability of the alcohols compares with that of the other solvents, where the 410 nm absorption band could not be observed. We have also considered, whether it is possible for the alcohol molecules to abstract proton from HF in the ground state. That the proton abstracting ability of the alcohols is superior to other solvents is evident from **Table 3.1.**, in which the hydrogen bond donating and accepting abilities of some of the solvents pertinent to this investigation are collected from the literature.<sup>49</sup> The proton abstracting ability of the solvents, as assessed from the hydrogen bond acceptor basicity

parameter,  $\beta$ ,<sup>50</sup> increases in the following order: acetonitrile < ethyl acetate  $\approx$  diethyl ether < alcohols. We note that formamide, where anion formation has been observed previously, has a  $\beta$  value of 0.55, higher than that of acetonitrile, ether and ethyl acetate. In order to address the second question of whether the alcohols can abstract a proton from HF, we take note of the fact that aromatic hydroxy compounds are in general stronger acids compared to aliphatic hydroxy compounds. Since HF contains an electron withdrawing carbonyl group adjacent to the hydroxy group, it can be expected to be an even stronger acid, making the generation of anion possible in alcoholic media. Perhaps, the most important question that needs to be answered here is why the anion disappears in the presence of water. It is evident from **Table 3.1.** that the hydrogen bond acceptor basicity ( $\beta$ ) of water is not as good as that of the alcohols and also, the hydrogen bond donor acidity ( $\alpha$ ) of water is the highest among all the solvents. It is, therefore, quite likely that the equilibrium, shown in **Scheme 3.1.** is displaced towards the left in the presence of water. It is for the same reason, that the anion formation could not be observed in 2,2,2-trifluoroethanol, a solvent with a high  $\alpha$  value, but with a  $\beta$  value of zero (*vide Table 3.1.*).

Though we have unambiguously established that the anionic form (**A**) of HF, generated by ground state proton transfer reaction in alcoholic media, is responsible for the long-wavelength absorption band, we find that the intensities of the 410 nm band in various alcoholic solvents do not commensurate with the hydrogen bond acceptor basicity ( $\beta$ ) values. Instead, the intensities are closely related to the hydrogen bond donating ability ( $\alpha$ ) of the solvents.

**Table 3.1. Kamlet-Taft's hydrogen bond donor acidity ( $\alpha$ ) and hydrogen bond acceptor basicity ( $\beta$ ) parameters,<sup>a</sup> collected from ref. 49.**

Solvents	$\beta$	$\alpha$
Diethyl ether	0.47	0.00
Ethyl acetate	0.45	0.00
Acetonitrile	0.31	0.19
Formamide	(0.55) <sup>b</sup>	0.71
2-Propanol	(0.95)	0.76
Ethanol	(0.77)	0.83
Methanol	(0.62)	0.93
Water	0.47 <sup>c</sup>	1.17
2,2,2-Trifluoroethanol	0.00	1.51

<sup>a</sup>Vide ref. 50; <sup>b</sup>values in the parenthesis are less certain;  
<sup>c</sup>from ref. 51.

This observation implies that the formation of anion in neutral solvents is governed by two factors. First, formation of a hydrogen-bonded complex between HF and the solvent, where the solvent acts as a hydrogen bond donor. This is followed by abstraction of the hydroxy proton of HF, where the hydrogen bond acceptor basicity ( $\beta$ ) of the solvent plays a decisive role. While the first step may not be favoured by an increase in temperature, the second step that involves the abstraction of proton from HF is expected to be facilitated by an increase in temperature. The observed temperature dependence implies that the influence of temperature is more pronounced for the second step.



### 3.4. Conclusion

We have identified a new long-wavelength absorption band of 3-hydroxyflavone in alcoholic media. A detailed study of the influence of various factors on the absorption and fluorescence behaviour reveals that the new absorption is due to the anionic form of the molecule generated in the ground state via solvent mediated deprotonation of the 3-hydroxy group.

### 3.5. References

- (1) Klopffer, W. *Adv. Photochem.* **1977**, 10, 311.
- (2) Huppert, D.; Gutman, M.; Kaufmann, M. J. *Adv. Chem. Phys.* **1981**, 47, 643.
- (3) Kasha, M. *J. Chem. Soc., Faraday Trans. 2* **1986**, 82, 2379.
- (4) Barbara, P. F.; Walsh, P. K.; Brus, L. E. *J. Phys. Chem.* **1989**, 93, 29.
- (5) Special issue (Spectroscopy and Dynamics of Elementary Proton Transfer in Polyatomic Systems, Barbara, P. F.; Trommsdorff, H. D., Eds.) *Chem. Phys.* **1989**, 136, 153-360.
- (6) Special Issue (M. Kasha Festschrift) *J. Phys. Chem.* **1991**, 95, 10220-10524.
- (7) Chou, P. T. *J. Chin. Chem. Soc.* **2001**, 48, 651.
- (8) Scheiner, S. *J. Phys. Chem. A* **2000**, 104, 5898.
- (9) Arnaut, L. G.; Formosinho, S. J. *J. Photochem. Photobiol. A : Chem.* **1993**, 75, 1.
- (10) Douhal, A.; Lahmani, F.; Zewail, A. *Chem. Phys.* **1996**, 207, 477.
- (11) Aquino, A. J. A.; Lischka, H.; Christof, H. *J. Phys. Chem. A* **2005**, 109, 3201.
- (12) Agmon, N. *J. Phys. Chem. A* **2005**, 109, 13.
- (13) Sengupta, P. K.; Kasha, M. *Chem. Phys. Lett.* **1979**, 68, 382.
- (14) Woolfe, G. J.; Thistlethwaite, P. J. *J. Am. Chem. Soc.* **1981**, 103, 6916.
- (15) Itoh, M.; Tokumara, K.; Tanimoto, Y.; Okada, Y.; Takeuchi, H.; Obi, K.; Tanaka, I. *J. Am. Chem. Soc.* **1982**, 104, 4146.
- (16) Strandjord, A. J. G.; Courtney, S. H.; Friedrich, D. M.; Barbara, P. F. *J. Phys. Chem.* **1983**, 87, 1125.
- (17) Strandjord, A. J. G.; Barbara, P. F. *Chem. Phys. Lett.* **1983**, 98, 21.
- (18) McMorrow, D.; Kasha, M. *J. Am. Chem. Soc.* **1983**, 105, 5133.
- (19) Sytnik, A.; Gormin, D.; Kasha, M. *Proc. Natl. Acad. Sci. USA* **1994**, 91, 11968.
- (20) McMorrow, D.; Kasha, M. *J. Phys. Chem.* **1984**, 88, 2235.
- (21) Strandjord, A. J. G.; Barbara, P. F. *J. Phys. Chem.* **1985**, 89, 2355.
- (22) Strandjord, A. J. G.; Smith, D. E.; Barbara, P. F. *J. Phys. Chem.* **1985**, 89, 2362.
- (23) Schwartz, B. J.; Peteanu, L. A.; Harris, C. B. *J. Phys. Chem.* **1992**, 96, 3591.
- (24) Ameer-Beg, S.; Ormson, S. M.; Brown, R. G.; Matousek, P.; Towrie, M.; Nibbering, E. T. J.; Foggy, P.; Neuwahl, F. V. R. *J. Phys. Chem. A* **2001**, 105, 3709.

- (25) Bader, A. N.; Ariese, F.; Gooijer, C. *J. Phys. Chem. A* **2002**, 106, 2844.
- (26) Swinney, T. C.; Kelley, D. F. *J. Chem. Phys.* **1993**, 99, 211.
- (27) Itoh, H.; Tanimoto, Y.; Tokumara, K. *J. Am. Chem. Soc.* **1983**, 105, 3339.
- (28) Dick, B.; Ernsting, N. P. *J. Phys. Chem.* **1987**, 91, 4261.
- (29) Itoh, H.; Fujiwara, Y.; Sumitani, M.; Yoshihara, K. *J. Phys. Chem.* **1986**, 90, 5672.
- (30) Brucker, G. A.; Swinney, T. C.; Kelly, D. F. *J. Phys. Chem.* **1991**, 95, 3190.
- (31) Premvardhan, L. L.; Peteanu, L. A. *J. Phys. Chem. A* **1999**, 103, 7506.
- (32) Chou, P. T.; McMorow, D.; Aartsma, T. J.; Kasha, M. *J. Phys. Chem.* **1984**, 88, 4596.
- (33) Brewer, W. E.; Studer, S. L.; Chou, P. T.; Orton, E. *Chem. Phys. Lett.* **1989**, 158, 345.
- (34) Sarkar, M.; Sengupta, P. K. *Chem. Phys. Lett.* **1991**, 179, 68.
- (35) Salman, O. A.; Drickamer, H. G. *J. Chem. Phys.* **1981**, 75, 572.
- (36) McMorow, D.; Kasha, M. *Proc. Natl. Acad. Sci. USA* **1984**, 81, 3375.
- (37) Ernsting, N. P.; Dick, B. *Chem. Phys.* **1989**, 136, 181.
- (38) Khan, A. U.; Kasha, M. *Proc. Natl. Acad. Sci. USA* **1983**, 80, 1767.
- (39) Ormson, S. M.; LeGourrierec, D.; Brown, R. G.; Foggi, P. *Chem. Commun.* **1995**, 2133.
- (40) Rulliere, C.; Declémy, A. *Chem. Phys. Lett.* **1987**, 134, 64.
- (41) Seipol, J.; Kolos, R. *Chem. Phys. Lett.* **1990**, 167, 445.
- (42) Dick, B. *J. Phys. Chem.* **1990**, 94, 5752.
- (43) Perthenopoulos, D. A.; Kasha, M. *Chem. Phys. Lett.* **1990**, 173, 303.
- (44) Ormson, S. M.; Brown, R. G.; Vollmer, F.; Rettig, W. *J. Photochem. Photobiol. A : Chem.* **1994**, 81, 65.
- (45) McMorow, D.; Dzigan, T. P.; Aartsma, T. J. *Chem. Phys. Lett.* **1984**, 103, 492.
- (46) Brucker, G. A.; Kelley, D. F. *J. Phys. Chem.* **1987**, 91, 2856.
- (47) Brucker, G. A.; Kelley, D. F. *J. Phys. Chem.* **1989**, 93, 5179.
- (48) Taft, R. W.; Kamlet, M. J. *J. Am. Chem. Soc.* **1976**, 98, 2886.
- (49) Reichardt, C. *Solvents and Solvent Effects in Organic Chemistry*; VCH: Weinheim, Germany, 1988.
- (50) Kamlet, M. J.; Abboud, J. L.; Abraham, M. H.; Taft, R. W. *J. Org. Chem.* **1983**, 48, 2877.
- (51) Marcus, Y. *J. Phys. Chem.* **1987**, 91, 4422.

### Dynamic Stokes' Shift of Fluorescence: Solvation Dynamics in Room Temperature Ionic Liquids

---

This chapter describes the time-dependent Stokes' shift studies of dipolar probes in two different RTILs; viz., [bmim][BF<sub>4</sub>] and [bmpy][Tf<sub>2</sub>N]. In [bmim][BF<sub>4</sub>], the solvation has been reported to be biphasic in nature, and the average solvation time has been noted to be dependent on the probe molecule employed. We have reinvestigated the probe dependency employing a different probe C102. An ultrafast component of solvation, which could not be time-resolved, is observed in imidazolium RTIL, but not in ammonium or phosphonium RTILs. With a view to finding out whether the cationic component of the RTIL is responsible for this ultrafast component, we have studied the solvation phenomenon in a new RTIL based on pyrrolidinium cation.

---

#### 4.1. Introduction

Solvation is an important phenomenon in chemistry and biology and has been a topic of considerable interest for more than a couple of decades.<sup>1-30</sup> Time-dependent Stokes' shift of the fluorescence spectrum of the dipolar probes in polar media can be quantitatively measured, following their excitation with an ultra-short laser pulse, to obtain information on the reorganisation dynamics of the solvent molecules around the newly created dipole of the solute.

Recent studies on solvation dynamics in RTILs have indicated the non-exponential or biphasic nature and slowness of the solvation dynamics.<sup>31-41</sup> Of the two observable components of the dynamics faster component is in picosecond time scale and the slower component is in the nanosecond time scale. For moderately viscous imidazolium RTILs, the faster component varies

from 125 to 280 ps whereas the slower component varies from 0.65 to 3.98 ns.<sup>32,33</sup> The average solvation time is found to be consistent with the viscosity of the RTIL. The results presented in **Table 1.2.** highlight some of these major findings. These studies have also shown that nearly 50 % of the total expected spectral relaxation was missed in the measurements having a time resolution of 25 ps.<sup>31-33</sup> This implies that a substantial portion of the solvation dynamics is ultrafast and occurs within 25 ps, the time resolution of the instrument, despite the high viscosity of these RTILs.

Interestingly, this ultrafast solvation component could not be observed in ammonium and phosphonium RTILs.<sup>37,41</sup> This observation has been rationalised proposing that the ultrafast component of the dynamics in imidazolium RTILs arises due to small amplitude motions of one or more cations in close contact with the solute and is facilitated by coplanar arrangements of the solute with imidazolium nearest neighbours.<sup>36</sup> The polarizability of the cations is also considered to be responsible for the fast component.<sup>40</sup> Clearly, there is disagreement on the origin of the ultrafast components. There is also dispute on how fast the ultrafast component is. It was reported earlier that the ultrafast component is shorter than 5 ps.<sup>41</sup> However, with subpicosecond time resolution measurement, it has been suggested recently that the ultrafast time constant is around 40-70 ps.<sup>40</sup>

A number of theoretical studies have been carried out in order to understand the mechanism of solvation.<sup>42-48</sup> Shim et al. have found a subpicosecond component of the dynamics, which they have assigned to the anion translation.<sup>42</sup> Kobrak et al. have shown that collective cation and anion motions are responsible for the fast component.<sup>46</sup>

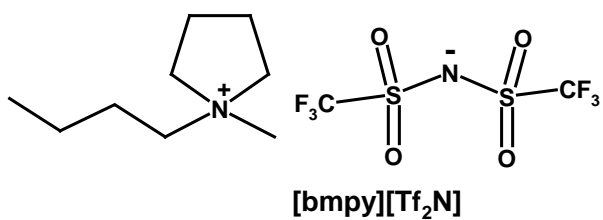
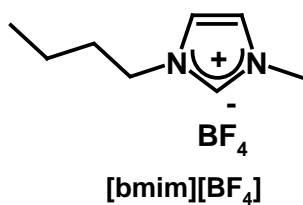
We have utilised several solvation probes like C153, C102, PRODAN, AP in the time-dependent Stokes' shift studies. The idea behind using a number of probes for the study of solvation dynamics is to examine whether the solvation time is dependent on the nature of the probe molecule. Among different solvation probes, C153 is the most extensively used. However, all these molecules have a rigid structure. Also, the  $S_0 \leftrightarrow S_1$  transition for all the probes is uncomplicated by other nearby transition or interfering reactions. As can be seen from **Table 4.1.**, these molecules display a large change in the dipole moment on electronic excitation and consequently, exhibit significant Stokes' shift on increasing the polarity of the solvent. Moreover, the excited state lifetime of these molecules is significantly high.

**Table 4.1. Change in dipole moment and excited state lifetime values of solvation probes.**

Probe	$\Delta\mu$ (D)	$\tau$ (ns)
C153	4.9 – 5.4 <sup>a</sup>	5.6 <sup>d</sup>
C102	3.0 – 3.8 <sup>a</sup>	3.3 <sup>d</sup>
PRODAN	4.4 – 5.0 <sup>b</sup>	3.2 <sup>e</sup>
AP	3.0 – 3.7 <sup>c</sup>	14.0 <sup>f</sup>

a:ref. 49 ; b:ref. 50; c:ref. 51 ; d:ref. 52 ; e:ref. 53 ; f:ref. 51.

## RTILs:



## Polarity and Solvation Probes:

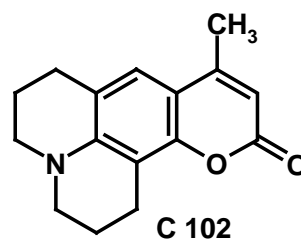
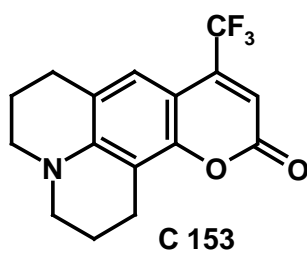
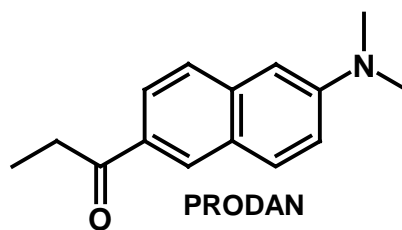
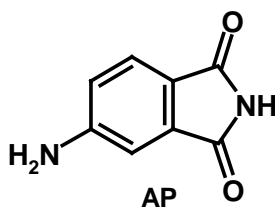
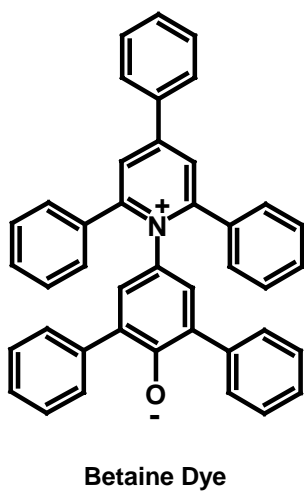
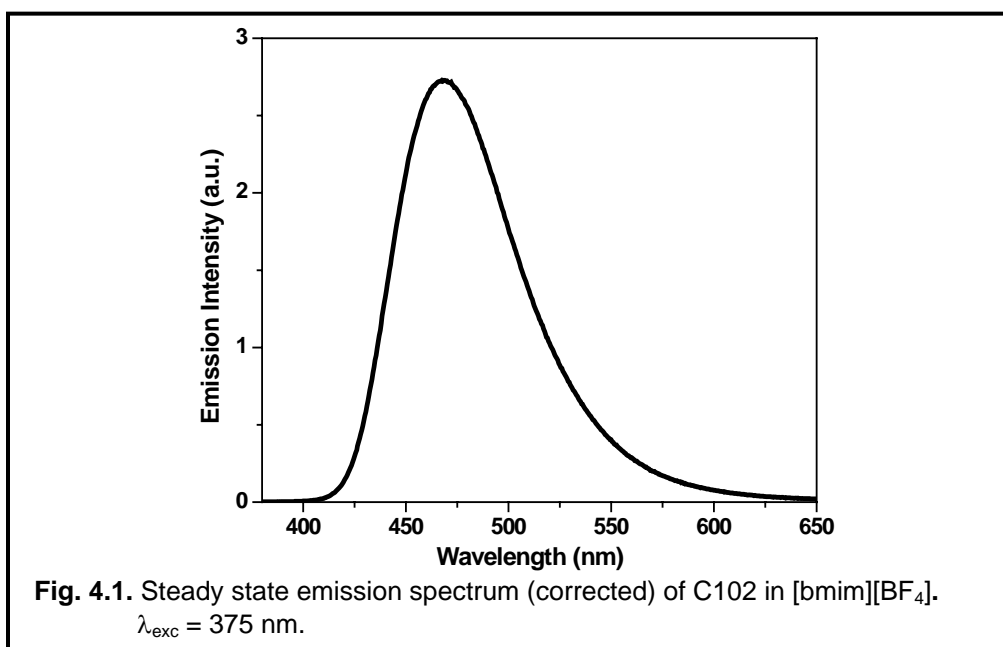


Chart 4.1. Two RTILs and the probes employed in the study.

## 4.2. Solvation dynamics in [bmim][BF<sub>4</sub>] employing C102

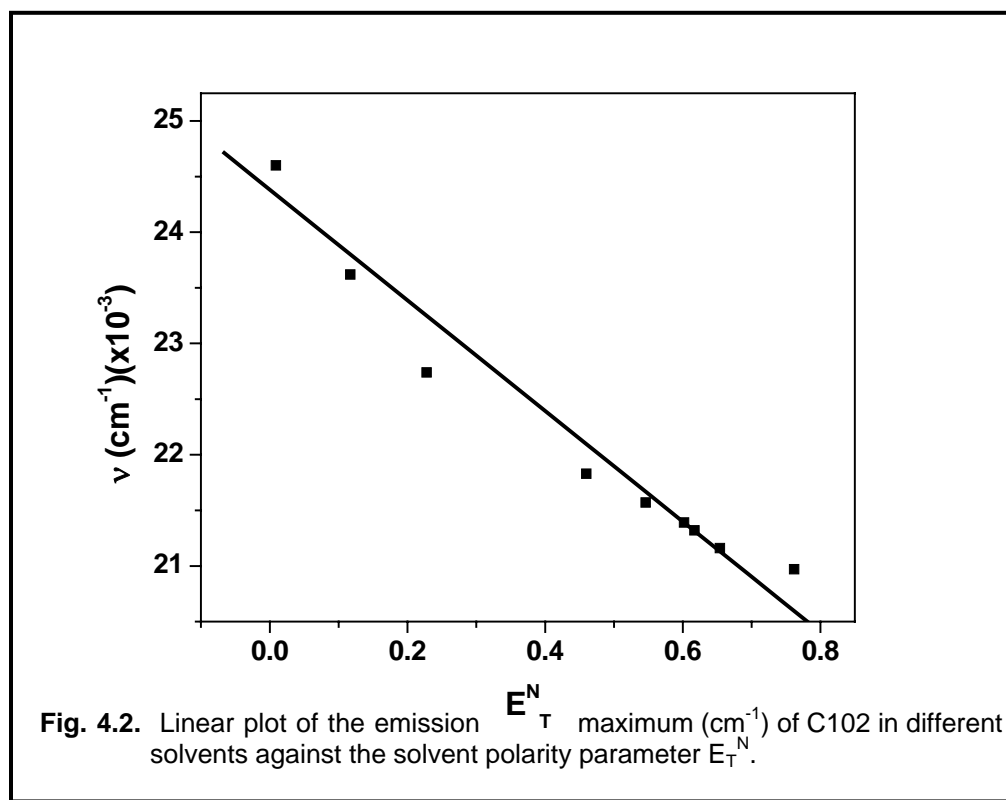
### 4.2.1. Steady state fluorescence studies

The steady state emission spectrum of C102 in [bmim][BF<sub>4</sub>] (**Chart 4.1.**) is shown in **Fig. 4.1**. The emission maximum appears at 468 nm. In view of the intramolecular charge transfer nature of the fluorescent state, C102 exhibits broad fluorescence band whose location is dependent on the polarity of the media.



Taking into consideration the linear dependence of the wavenumber corresponding to the steady state fluorescence maximum ( $\bar{\nu}_{flu}^{max}$ ) on the Reichardt's solvent polarity parameter,  $E_T(30)$ ,<sup>54</sup> the polarity of this RTIL has been estimated to be 50.4 in the  $E_T(30)$  scale of the polarity. This value suggests that [bmim][BF<sub>4</sub>] is more polar than acetonitrile ( $E_T(30)$  of 45.6), but less polar

than methanol ( $E_T(30)$  of 55.4). The polarity of this RTIL in  $E_T^N$  scale (See **Fig. 4.2.**) has been measured to be 0.6.

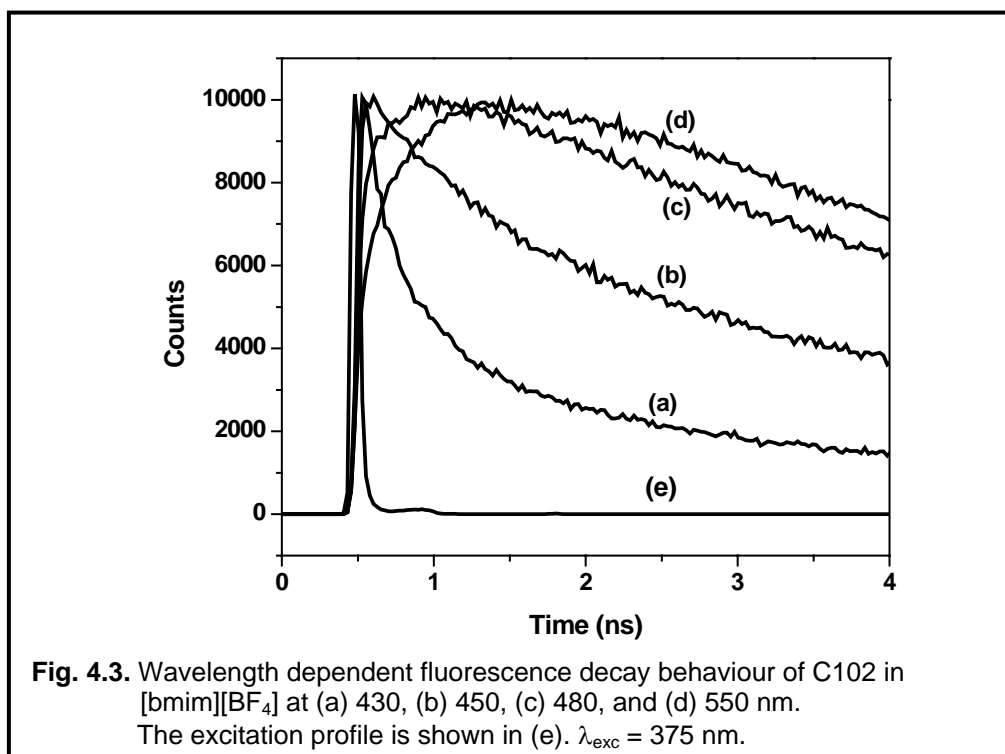


This finding is consistent with that obtained previously from the analysis of the fluorescence behaviour of other probe molecules.<sup>31,32,55</sup> Moreover, the present estimate of the polarity of [bmim][BF<sub>4</sub>] is in fairly good agreement with that obtained by Muldoon et al. from the absorption maximum of the betaine dye.<sup>56</sup>

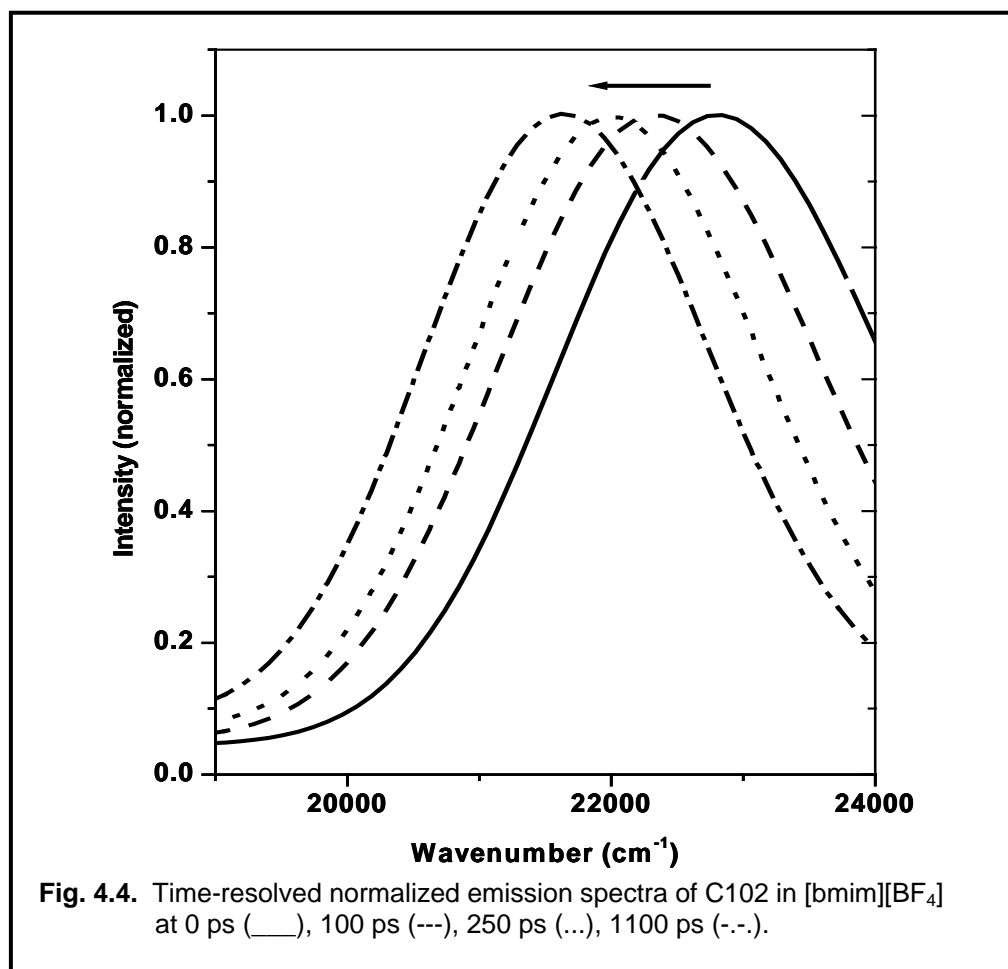


#### 4.2.2. Time-resolved fluorescence studies

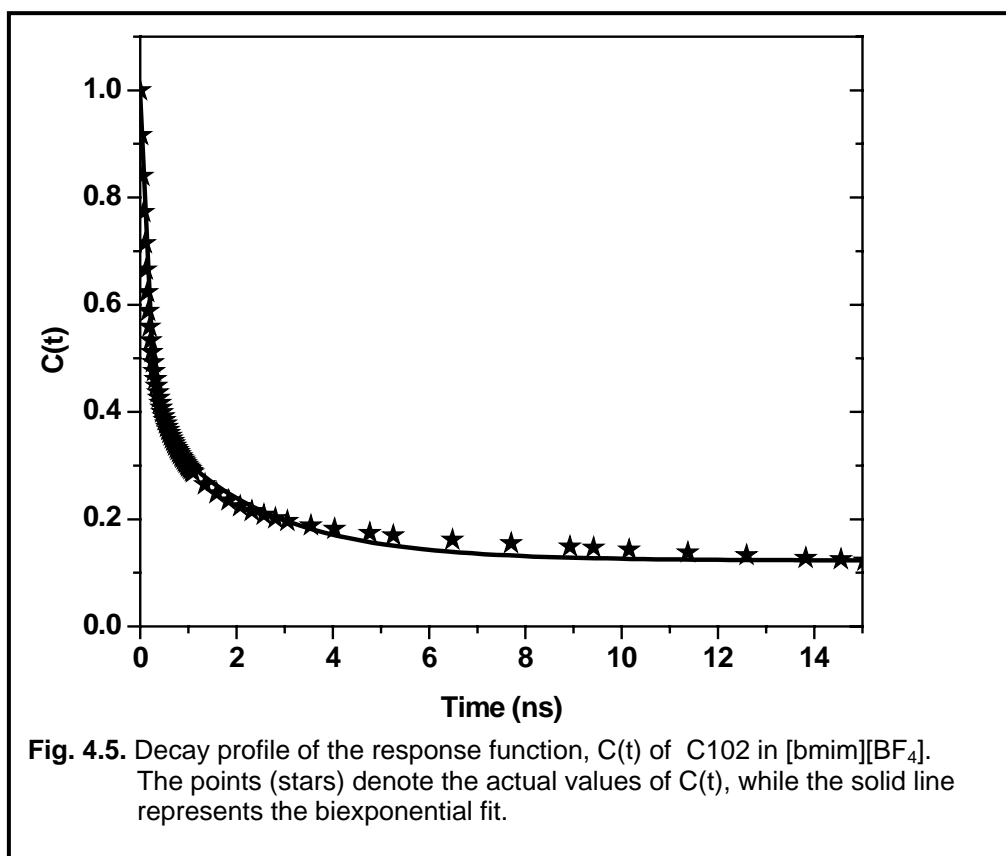
The time-resolved fluorescence behaviour of C102 has been studied at several wavelengths. The wavelength dependence of the fluorescence decay profiles is clearly evident from **Fig. 4.3**. As can be seen, when monitored at the blue side of the fluorescence spectrum, the profiles consist of a steady decay of the fluorescence intensity with time. However, when monitored at longer wavelengths, the time-profiles consist of a slow growth (rise) followed by normal decay. The rise portion of time profile is indicative of a slow relaxation of the constituent ions around the photo excited probe molecule.



The time constants thus obtained from the fits to the decay profiles change continuously, as a function of the wavelength, suggesting a continuous time-dependent shift of the spectrum rather than kinetics, which involves a few discrete states. The fitted decay profiles at various wavelengths were then normalized such that the time-integrated intensity is proportional to the intensity of the steady state fluorescence spectrum at each wavelength.



The time-dependent fluorescence spectra of C102 have been shown in **Fig. 4.4**. Having obtained the  $\bar{\nu}$  values at various times, the values of spectral shift correlation function,  $C(t)$  were calculated. The time-dependence of the  $C(t)$  values has been shown in **Fig. 4.5** along with the best fit to the data.



The data shown in the figure could be fit well to a biexponential decay function. The biexponential relaxation times thus obtained are 170 ps and 2.26 ns, with an average solvation time of 850 ps. It should be noted here that the

order of magnitude of the two time constants is however quite similar to that obtained earlier using other probe molecules (See **Table 1.2.**).

Based on the previous studies on imidazolium RTILs,<sup>31-33</sup> we attribute the two components of the dynamics as follows: the short component predominantly arises from the translational motion of the anions, having a smaller size, and the long component arises due to a collective diffusion involving both the cations and the anions. The close proximity of the ions makes this mechanism more realistic than the one involving a separate contribution of the ions.

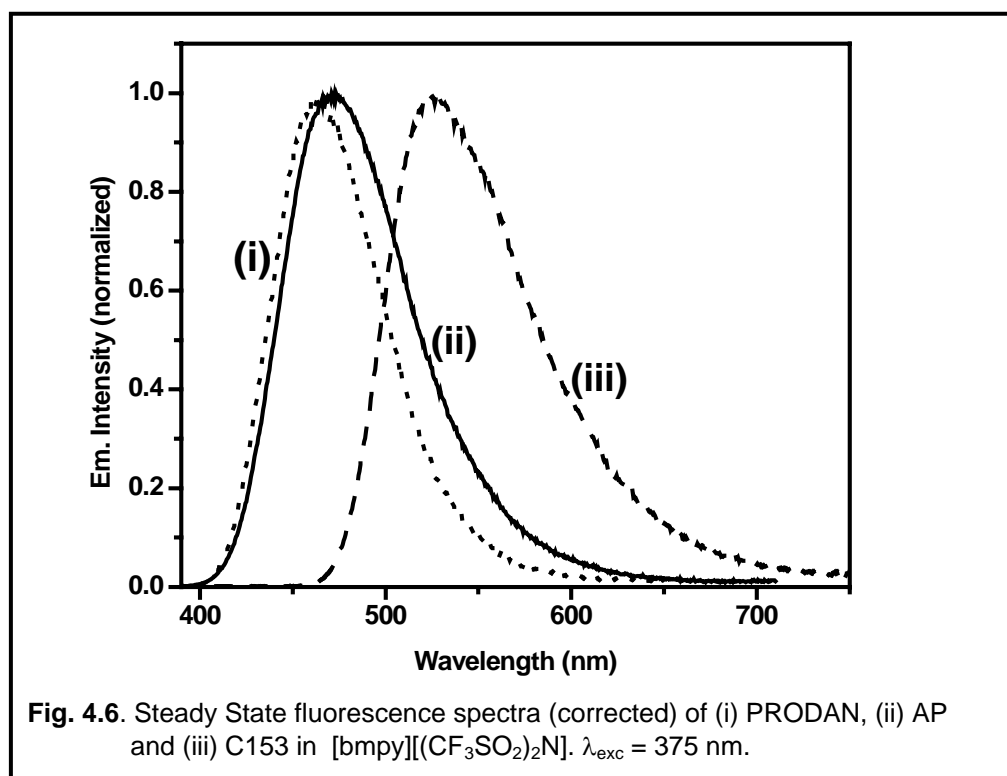
The average solvation estimated in this case, employing the solvation probe, C102, is 850 ps. Earlier studies of solvation dynamics, in this particular RTIL ([bmim][BF<sub>4</sub>]) employing other solvation probes, have shown (See **Table 1.2.**) that the average solvation time is 460 ps (C153)<sup>40</sup>, 1440 ps (PRODAN)<sup>32</sup>, and 2130 ps (C153)<sup>32</sup>. Thus, the value of the average solvation time obtained with C102 is well within the range of values obtained by various probe molecules. Therefore, the present result supports the observation made earlier in this RTIL, that the average solvation time depends on the choice of probe molecule employed.

#### 4.3. Solvation dynamics in a pyrrolidinium RTIL

We have studied the solvation phenomenon in a pyrrolidinium RTIL, [bmpy][Tf<sub>2</sub>N] (**Chart 4.1.**). The choice of this particular RTIL is based on the fact that this RTIL is structurally similar to that of ammonium salts and the cation lacks the planarity. We have also chosen three probes, viz., C153, AP and PRODAN (**Chart 4.1.**) in order to check whether there is any probe dependence.

#### 4.3.1. Steady state fluorescence studies

The steady state emission spectra of the systems in [bmpy][Tf<sub>2</sub>N] have been depicted in **Fig. 4.6.** and the wavenumbers corresponding to the emission maxima are listed in **Table 4.2.**



Since the emission spectra of the chosen systems are sensitive to the polarity of the surrounding medium, and the fact that the polarity of this RTIL was not known, it was necessary to estimate the polarity of [bmpy][Tf<sub>2</sub>N] in terms of the microscopic solvent polarity parameter,  $E_T(30)$ , from the fluorescence spectral data of the systems. An independent and direct estimation of the

polarity of this RTIL has also been made from the absorption spectral data of the betaine dye (**Chart 4.1.**).

**Table 4.2. Wavenumbers corresponding the fluorescence maxima of the systems in [bmpy][Tf<sub>2</sub>N] and the estimated E<sub>T</sub>(30) values of the medium.**

Probe	$\bar{\nu}_f$ (cm <sup>-1</sup> )	E <sub>T</sub> (30) value of the medium as indicated by the $\bar{\nu}_f$ value
C153	19010	47.3
AP	21185	47.4
PRODAN	21505	45.9
Betaine dye	-	50.1 <sup>a</sup>

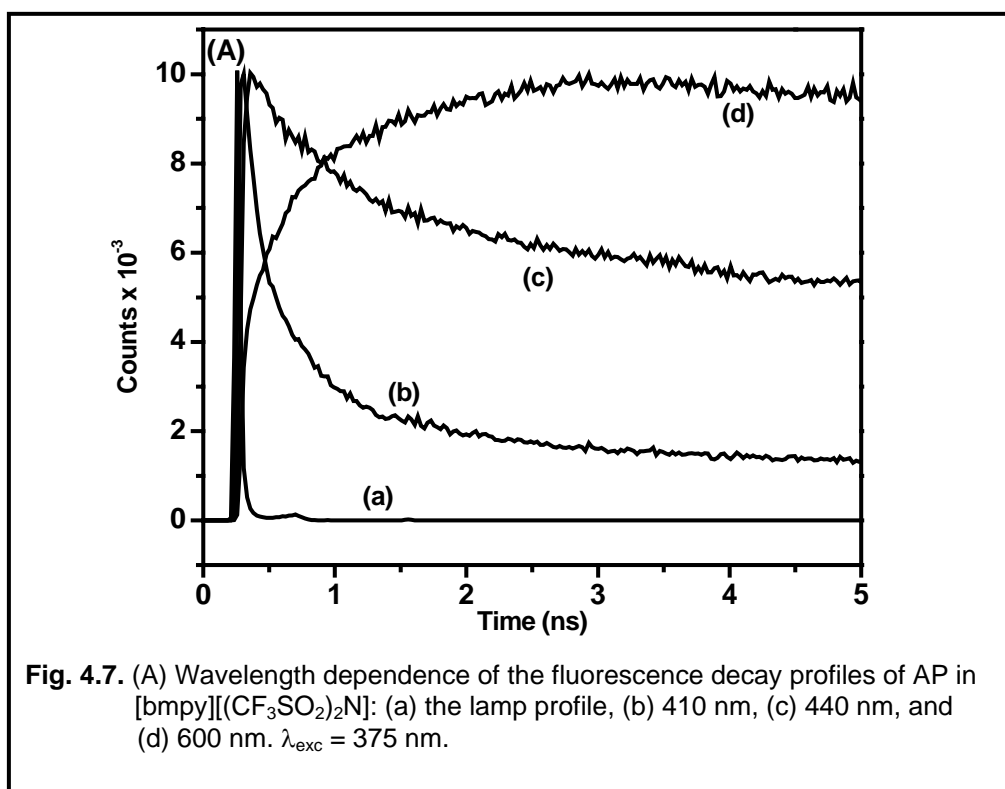
<sup>a</sup>This value is directly measured from the longest wavelength absorption maximum of the betaine dye in the RTIL.

While estimating the polarity of the medium from the fluorescence measurements, the  $\bar{\nu}_f$  values of the systems were measured in several conventional solvents of known E<sub>T</sub>(30) values. The linear correlation of  $\bar{\nu}_f$  and E<sub>T</sub>(30) and the measured  $\bar{\nu}_f$  value of the probe molecule in [bmpy][Tf<sub>2</sub>N] allowed evaluation of the microscopic solvent polarity parameter, E<sub>T</sub>(30) of this particular RTIL. Different E<sub>T</sub>(30) values obtained by this procedure using three probe molecules and the one directly obtained from the longest wavelength absorption maximum of the betaine dye are collected in **Table 4.2.** It can be seen that the measured E<sub>T</sub>(30) values vary between 45.9 (obtained with PRODAN) and 50.1 (obtained by direct measurement with the betaine dye). Based on these measurements, an average E<sub>T</sub>(30) value of 47.7 can be considered as an

indicator of the polarity of this RTIL. An inspection of the  $E_T(30)$  values of the conventional solvents reveals that the present RTIL is as polar as 1-decanol, which also has an  $E_T(30)$  value of 47.7. It is also evident that the polarity of this pyrrolidinium RTIL is comparable to that of the other imidazolium RTILs. In fact, the  $E_T(30)$  value of [bmpy][Tf<sub>2</sub>N] is found to be identical to that of [emim][Tf<sub>2</sub>N].

#### 4.3.2. Time resolved fluorescence studies

The fluorescence decay profiles of all three probes, which were measured at several wavelengths across the emission spectra, have been found to be strongly dependent on the monitoring wavelength. A typical behaviour of this type for all the probes, have been illustrated in **Fig. 4.7**.



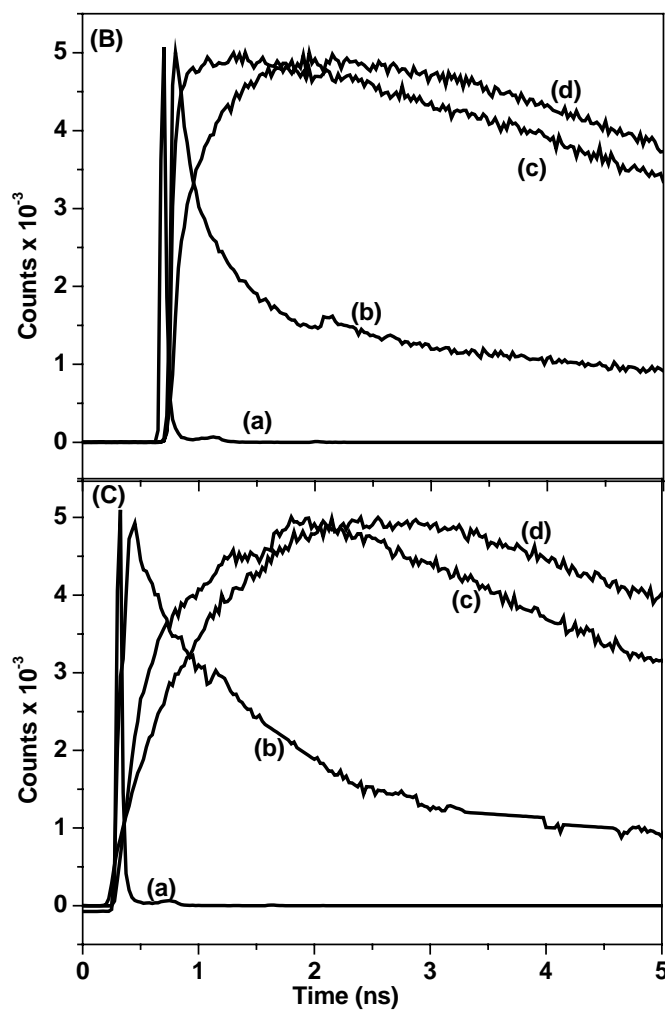
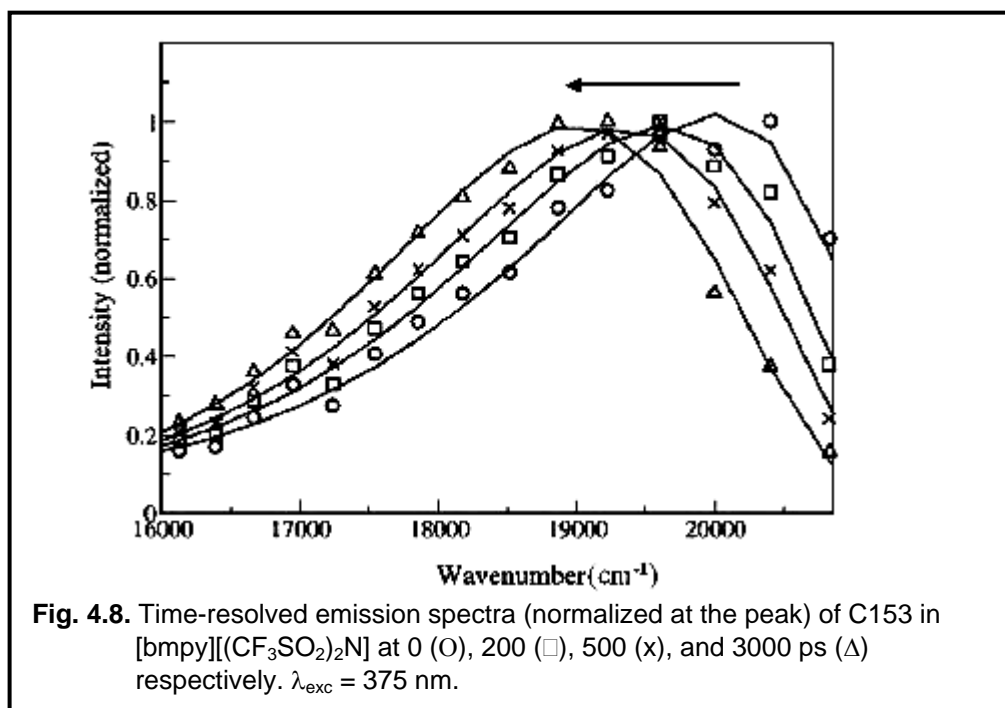


**Fig. 4.7.** Wavelength dependence of the fluorescence decay profiles of **(B)** C153 (a) the lamp profile, (b) 480 nm, (c) 520 nm, and (d) 650 nm; and **(C)** PRODAN in [bmpy][(CF<sub>3</sub>SO<sub>2</sub>)<sub>2</sub>N] (a) Lamp (b) 410 nm (b) 460 nm, (c) 600 nm.  $\lambda_{\text{exc}} = 375$  nm.



For all the systems, the decay profile consisted of a monotonous decrease of the fluorescence intensity with time when monitored at short wavelength region of the fluorescence spectrum. On the other hand, for longer monitoring wavelength, the profile comprised of an initial rise followed by decay of the intensity. This type of wavelength dependent fluorescence decay behaviour of the systems, whose fluorescence properties are well known, suggests that solvation of the photo-generated excited states is a slow process in [bmpy][Tf<sub>2</sub>N]. This behaviour is quite similar to that observed in case of imidazolium RTILs.



The time-resolved emission spectra (TRES) of the systems, constructed from the fitted decay profiles, show progressive red shift of the fluorescence

maximum with time (**Fig. 4.8.**). The total Stokes' shift (in  $\text{cm}^{-1}$ ) observed for all three probes between  $t=0$  and  $t=\infty$  are measured from the peak positions and are collected in **Table 4.3.**

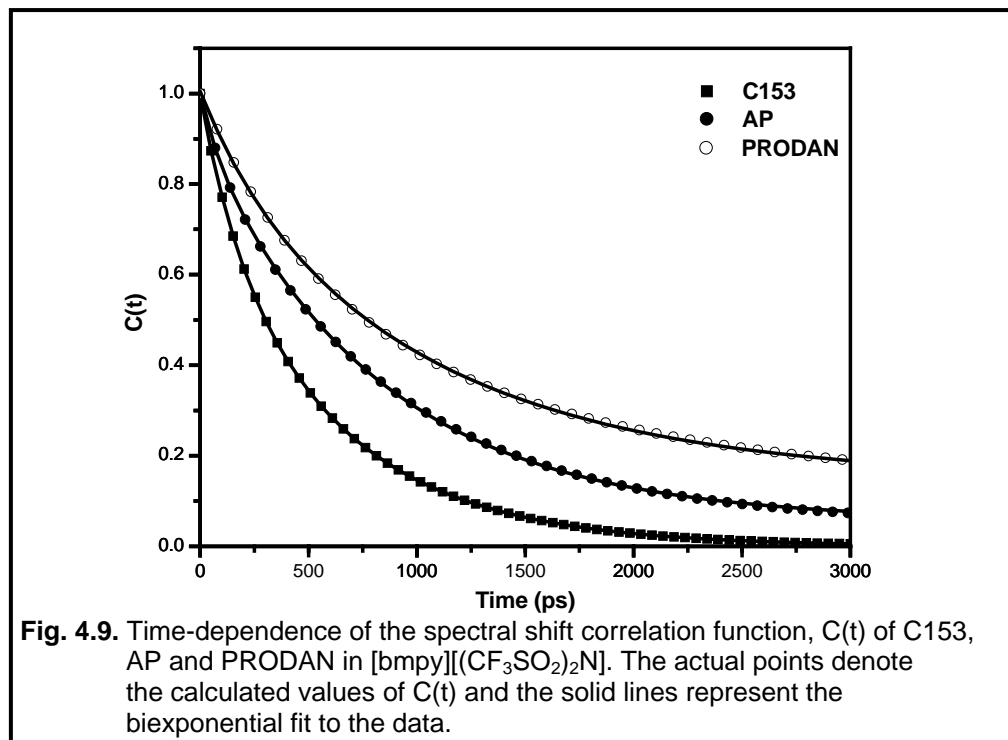
Since the polarity of [bmpy][Tf<sub>2</sub>N] is similar to that of 1-decanol, the total spectral shift is expected to be  $\sim 1770 \text{ cm}^{-1}$  for C153 according to literature.<sup>11</sup> However, the observed shift for C153 between  $t(0)$  and  $t(\infty)$  is only  $\sim 1000 \text{ cm}^{-1}$  (**Table 4.3.**). This implies that a significant portion ( $\sim 45\%$ ) of the solvation occurs in a timescale faster than the effective time resolution (25 ps) of the present instrumental setup and is being missed here. It should be noted here that a similar ultrafast component of the dynamics has been observed in imidazolium RTILs, but not in ammonium or phosphonium RTILs.

The time constant of the observable portion of solvation is obtained from the peak frequencies by constructing the spectral shift correlation function,  $C(t)$ . The time-dependence of the calculated  $C(t)$  values and the fit to the biexponential function, have been shown in **Fig. 4.9.** The relaxation times obtained from the fits are collected in **Table 4.3.** The results can be summarized as follows.

The observable dynamics in this RTIL also, is biphasic in nature. The short component, which has relatively smaller amplitude, varies between 115 and 440 ps. The longer component on the other hand varies between 610 and 1395 ps. The average solvation time varies between 500 and 1025 ps, depending on the probe molecule employed.

Having observed a similar biphasic solvation dynamics in imidazolium RTILs, we attributed the fast component to the anion and the slower component to the collective motion of both anion and cation, after taking into consideration the literature available on the dynamics in molten salts and the amplitude of the two components.<sup>31-33</sup> Considering the present state of knowledge (both theory

and experiment), no unambiguous assignment of the various components of the dynamics is possible. We, therefore, refrain from commenting on the individual components and instead, concentrate on the general trends.



An important point that should not be neglected here is the missed ultrafast component of the dynamics. An ultrafast component has been observed previously in the case of imidazolium RTILs,<sup>31-33</sup> but not in the cases of ammonium or phosphonium RTILs<sup>37,41</sup>. It has been reported that the ultrafast component of dynamics in imidazolium RTILs arises due to small amplitude motions of one or more cations in close contact with the solute and is facilitated by coplanar arrangements of the solute with imidazolium nearest neighbours.<sup>36</sup> The existence of this ultrafast component in the present RTIL, where the

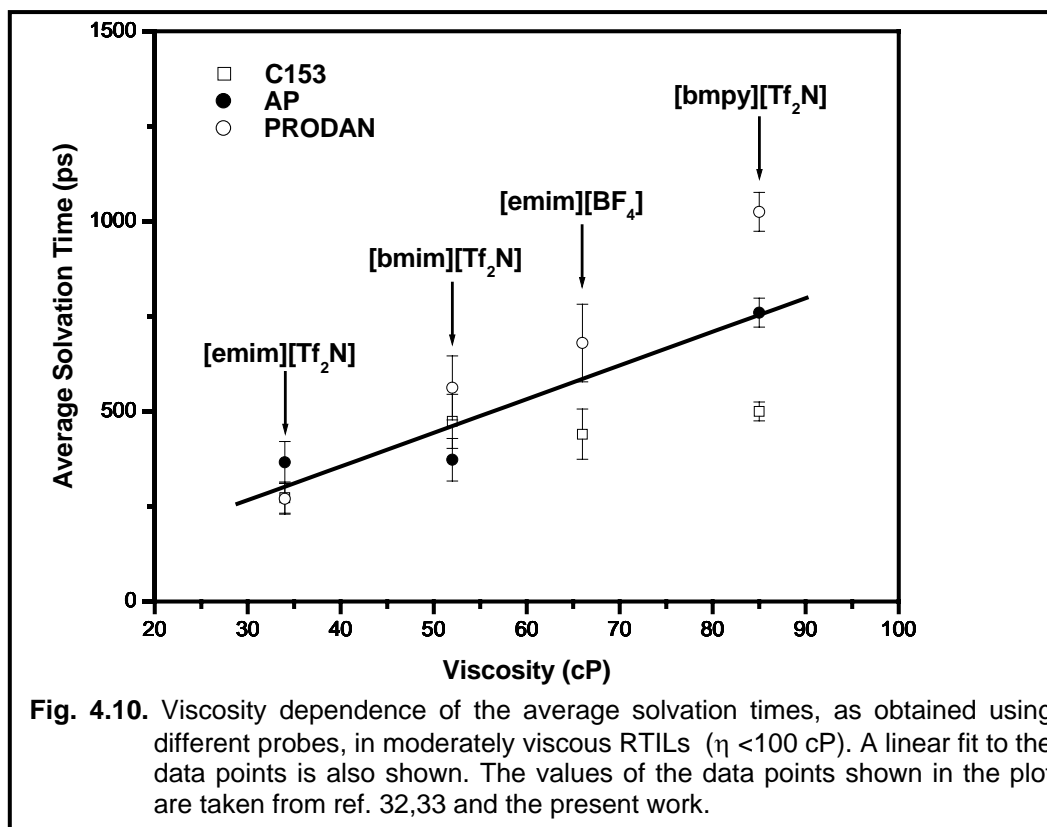
pyrrolidinium ion is structurally similar to the ammonium ion, is devoid of  $\pi$ -bonds, and thus lacks planarity, is unexpected. Since some of the earlier interpretations offered for the ultrafast component involved the planarity<sup>36</sup> or the polarizability of the cation,<sup>40</sup> a reassignment for this component seems necessary in the light of the present results as the pyrrolidinium cation is nonplanar and much less polarizable compared to imidazolium cation.

**Table 4.3. Relaxation parameters<sup>a</sup> of the three probes in [bmpy][Tf<sub>2</sub>N].**

Probe	$\tau_1$ (ps)	$\tau_2$ (ps)	$a_1$	$a_2$	$\langle\tau\rangle$ (ps) <sup>b,c</sup>	Observed shift [ $\bar{\nu}(\infty) - \bar{\nu}(0)$ ] (cm <sup>-1</sup> )
<b>C153</b>	170	610	25	75	500	1000
<b>AP</b>	115	855	12	88	765	1050
<b>PRODAN</b>	440	1395	40	60	1025	1110

<sup>a</sup>  $\tau_1$  and  $\tau_2$  are the two components of the dynamics having amplitudes of  $a_1$  and  $a_2$  respectively. <sup>b</sup> average relaxation time defined as,  $\langle\tau\rangle = a_1\tau_1 + a_2\tau_2$ , where ( $a_1 + a_2 = 1$ ).  
<sup>c</sup>  $\pm 5$  %.

The solvation time in viscous RTILs is expected to be dependent on the viscosity of the medium. Previous studies have indicated that for moderately viscous RTILs, the average solvation time is linearly dependent on the viscosity of the medium. **Fig. 4.10.** shows a plot of the various solvation times (as measured by us with different probe molecules) versus the viscosity of the medium for relatively less viscous RTILs.



For RTILs with viscosity values higher than 100 cP, (such as [bmim][BF<sub>4</sub>] and [bmim][PF<sub>6</sub>]), as has been noted previously, a substantial deviation from the linearity could be observed. Since the viscosity of the present RTIL is 85 cP (at 25<sup>0</sup>C),<sup>57</sup> the present data falls within the linear portion of the plot. The measured solvation time is, thus found to be consistent with the viscosity of this pyrrolidinium RTIL.

Another point that requires attention is the dependence of the average solvation time on the probe molecule. Earlier reports have highlighted the probe dependence of the solvation times. While in our previous studies we did observe

some variation of solvation time with the probe molecule, the extent of variation was not so appreciable (see **Table 4.4.** or **Fig. 4.10.**).

**Table 4.4.** Average solvation times (in ps) of different probes in different RTILs.

RTIL	C153	AP	PRODAN	Reference
[emim][Tf <sub>2</sub> N]	280	370	270	33
[bmim][Tf <sub>2</sub> N]	480	380	560	33
[emim][BF <sub>4</sub> ]	440	-	680	32
[bmim][BF <sub>4</sub> ]	2130	-	1440	32
[bmim][PF <sub>6</sub> ]	1000	1600	1800	36
[bmpy][Tf <sub>2</sub> N]	500	765	1025	This work

In the present case, the solvation times differ by a factor of more than two. The various solvation times measured for different RTILs with different probe molecules have been collected in **Table 4.4.** to determine whether any particular trend is apparent from this data. It can be seen from the table, that the average solvation time in [emim][Tf<sub>2</sub>N], is the lowest with PRODAN and highest with AP. However, in [bmim][Tf<sub>2</sub>N], the trend is exactly the opposite, i.e. the lowest value is obtained with AP and the highest with PRODAN. In [bmim][PF<sub>6</sub>], the average solvation time was found to be lowest for C153 and highest for PRODAN, which is though similar to the trend observed in the present case of [bmpy][Tf<sub>2</sub>N]. Thus, the numbers collected in **Table 4.4.** suggest that there is no definite pattern of the variation of the solvation time with the probe molecule.

#### **4.4. Conclusion**

The present study with C102 confirms the non-exponential nature of the solvation dynamics in [bmim][BF<sub>4</sub>]. When the spectral shift correlation function is fit to biexponential function, the two time constants obtained are of the order of hundreds of picosecond and thousands of picosecond. The average solvation time obtained with C102 is found to lie between the values estimated using other probes. Thus, this result supports the presence of probe dependent solvation times in imidazolium RTILs.

The polarity experienced by different dipolar probe molecules in [bmpy][Tf<sub>2</sub>N] is found comparable to that of 1-decanol. An ultrafast component of the dynamics, which could be observed in imidazolium RTILs but not in ammonium and phosphonium RTILs, has been detected in this pyrrolidinium RTIL, even though the pyrrolidinium ion resembles the ammonium ion structurally. This observation points to the necessity of a reassignment of the origin of ultrafast component of the dynamics. The average solvation time estimated from the observable part of the dynamics is found consistent with the viscosity of the medium. A significant probe dependence of the average solvation time is observable in this pyrrolidinium RTIL. However, no definite pattern of variation of the solvation time with the probe molecule could be identified.

#### **4.5. References**

- (1) Bagchi, B.; Oxtoby, D. W.; Fleming, G. R. *Chem. Phys.* **1984**, 86, 257.
- (2) Bagchi, B. *Annu. Rev. Phys. Chem.* **1989**, 40, 115.
- (3) Bagchi, B. *Chem. Rev.* **2005**, 105, 3197.
- (4) Fleming, G. R.; Cho, M. *Annu. Rev. Phys. Chem.* **1996**, 47, 109.

- (5) Hutterer, R.; Schneider, F. W.; Lanig, H.; Hof, M. *Biochim. Biophys. Acta* **1997**, 1323, 195.
- (6) Sykora, J.; Kapusta, P.; Fidler, V.; Hof, M. *Langmuir* **2002**, 18, 571.
- (7) Sykora, J.; Mudogo, V.; Hutterer, R.; Nepras, M.; Vanerka, J.; Kapusta, P.; Fidler, V.; Hof, M. *Langmuir* **2002**, 18, 9276.
- (8) Koti, A. S. R.; Krishna, M. M. G.; Periasamy, N. *J. Phys. Chem. A* **2001**, 105, 1767.
- (9) Rossky, P. J.; Simon, J. D. *Nature* **1994**, 370, 263.
- (10) Jimenez, R.; Fleming, G. R.; Kumar, P. V.; Maroncelli, M. *Nature* **1994**, 369, 471.
- (11) Horng, M. L.; Gardecki, J. A.; Papazyan, A.; Maroncelli, M. *J. Phys. Chem.* **1995**, 99, 17311.
- (12) Horng, M. L.; Gardecki, J. A.; Maroncelli, M. *J. Phys. Chem. A* **1997**, 101, 1030.
- (13) van der Zwan, G.; Hynes, J. T. *J. Phys. Chem.* **1985**, 89, 4181.
- (14) Nandi, N.; Bhattacharyya, K.; Bagchi, B. *Chem. Rev.* **2000**, 100, 2013.
- (15) Castner, E. W.; Maroncelli, M.; Fleming, G. R. *J. Chem. Phys.* **1987**, 86, 1090.
- (16) Castner, E. W.; Fleming, G. R.; Bagchi, B.; Maroncelli, M. *J. Chem. Phys.* **1988**, 89, 3519.
- (17) Chapman, C. F.; Fee, R. S.; Maroncelli, M. *J. Phys. Chem.* **1990**, 94, 4929.
- (18) Chapman, C. F.; Maroncelli, M. *J. Phys. Chem.* **1991**, 95, 9095.
- (19) Chapman, C. F.; Fee, R. S.; Maroncelli, M. *J. Phys. Chem.* **1995**, 99, 4811.
- (20) Su, S. G.; Simon, J. D. *J. Phys. Chem.* **1986**, 90, 6475.
- (21) Su, S. G.; Simon, J. D. *J. Phys. Chem.* **1987**, 91, 2693.
- (22) Jarzeba, W.; Barbara, P. F. *Adv. Photochem.* **1990**, 15, 1.
- (23) Bhattacharyya, K.; Bagchi, B. *J. Phys. Chem. A* **2000**, 104, 10603.
- (24) Bhattacharyya, K. *Acc. Chem. Res.* **2003**, 36, 95.
- (25) Pal, S. K.; Peon, J.; Zewail, A. *Proc. Natl. Acad. Sci. USA* **2002**, 99, 1763.
- (26) Pal, S. K.; Peon, J.; Bagchi, B.; Zewail, A. *J. Phys. Chem. B* **2002**, 106, 12376.
- (27) Pal, S. K.; Zhao, L.; Zewail, A. *Proc. Natl. Acad. Sci. USA* **2003**, 100, 8113.
- (28) Bart, E.; Meltsin, A.; Huppert, D. *J. Phys. Chem.* **1994**, 98, 3295.
- (29) Bart, E.; Meltsin, A.; Huppert, D. *J. Phys. Chem.* **1994**, 98, 10819.
- (30) Bart, E.; Meltsin, A.; Huppert, D. *J. Phys. Chem.* **1995**, 99, 9253.
- (31) Karmakar, R.; Samanta, A. *J. Phys. Chem. A* **2002**, 106, 4447.
- (32) Karmakar, R.; Samanta, A. *J. Phys. Chem. A* **2002**, 106, 6670.
- (33) Karmakar, R.; Samanta, A. *J. Phys. Chem. A* **2003**, 107, 7340.
- (34) Saha, S.; Mandal, P. K.; Samanta, A. *Phys. Chem. Chem. Phys.* **2004**, 6, 3106.
- (35) Ingram, J. A.; Moog, R. S.; Ito, N.; Biswas, R.; Maroncelli, M. *J. Phys. Chem. B* **2003**, 107, 5926.
- (36) Ito, N.; Arzhantsev, S.; Maroncelli, M. *Chem. Phys. Lett.* **2004**, 396, 83.
- (37) Ito, N.; Arzhantsev, S.; Heitz, M.; Maroncelli, M. *J. Phys. Chem. B* **2004**, 108, 5771.
- (38) Chakrabarty, D.; Hazra, P.; Chakraborty, A.; Seth, D.; Sarkar, N. *Chem. Phys. Lett.* **2003**, 381, 697.



- (39) Chakrabarty, D.; Chakraborty, A.; Seth, D.; Sarkar, N. *J. Phys. Chem. A* **2005**, *109*, 1764.
- (40) Chowdhury, P. K.; Halder, M.; Sanders, L.; Calhoun, T.; Anderson, J. L.; Armstrong, D. W.; Song, X.; Petrich, J. W. *J. Phys. Chem. B* **2004**, *108*, 10245.
- (41) Arzhantsev, S.; Ito, N.; Heitz, M.; Maroncelli, M. *Chem. Phys. Lett.* **2003**, *381*, 278.
- (42) Shim, Y.; Duan, J.; Choi, M. Y.; Kim, H. J. *J. Chem. Phys.* **2003**, *119*, 6411.
- (43) Margulis, C. J.; Stern, H. A.; Berne, B. J. *J. Phys. Chem. B* **2002**, *106*, 12017.
- (44) Popolo, M. G. D.; Lynden-Bell, R. M.; Kohanoff, J. *J. Phys. Chem. B* **2005**, *109*, 5895.
- (45) Lynden-Bell, R. M.; Kohanoff, J.; Popolo, M. G. D. *Faraday Discuss.* **2005**, *129*, 57.
- (46) Kobrak, M. N.; Znamenskiy, V. *Chem. Phys. Lett.* **2004**, *395*, 127.
- (47) Shim, Y.; Choi, M. Y.; Kim, H. J. *J. Chem. Phys.* **2005**, *122*, 044510.
- (48) Shim, Y.; Choi, M. Y.; Kim, H. J. *J. Chem. Phys.* **2005**, *122*, 044511.
- (49) Samanta, A.; Fessenden, R. W. *J. Phys. Chem. A* **2000**, *104*, 8577.
- (50) Samanta, A.; Fessenden, R. W. *J. Phys. Chem. A* **2000**, *104*, 8972.
- (51) Soujanya, T.; Fessenden, R. W.; Samanta, A. *J. Phys. Chem.* **1996**, *100*, 3507.
- (52) Gones, G. I.; Jackson, W. R.; Choi, C.; Bergmark, W. R. *J. Phys. Chem.* **1985**, *89*, 294.
- (53) Balter, A.; Nowak, W.; Pawelkiewicz, W.; Kowalczyk, A. *Chem. Phys. Lett.* **1988**, *143*, 565.
- (54) Reichardt, C. *Solvents and Solvent Effects in Organic Chemistry*, VCH: Weinheim, Germany, 1988.
- (55) Aki, S. N. V. K.; Brennecke, J. F.; Samanta, A. *Chem. Commun.* **2001**, 413.
- (56) Muldoon, M. J.; Gordon, C. M.; Dunkin, I. R. *J. Chem. Soc., Perkin Trans. 2* **2001**, 433.
- (57) MacFarlane, D. R.; Meakin, P.; Sun, J.; Amini, N.; Forsyth, M. *J. Phys. Chem. B* **1999**, *103*, 4164.

### Excitation Wavelength Dependent Fluorescence Behaviour of Some Dipolar Molecules in Room Temperature Ionic Liquids

---

This chapter depicts the unusual steady state fluorescence behaviour of several dipolar molecules in three imidazolium room temperature ionic liquids, viz., [bmim][BF<sub>4</sub>], [emim][BF<sub>4</sub>] and [bmim][PF<sub>6</sub>]. Various parameters of the fluorescent probes as well as the RTILs have been carefully examined in order to determine the factors that contribute to this kind of behaviour, generally not observed in conventional media.

---

#### 5.1. Introduction

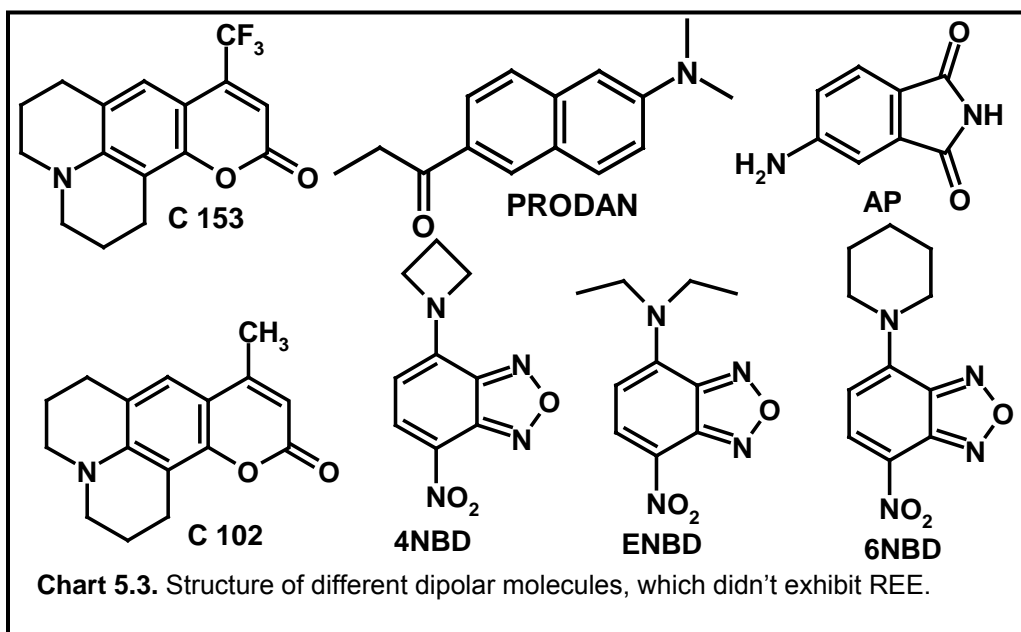
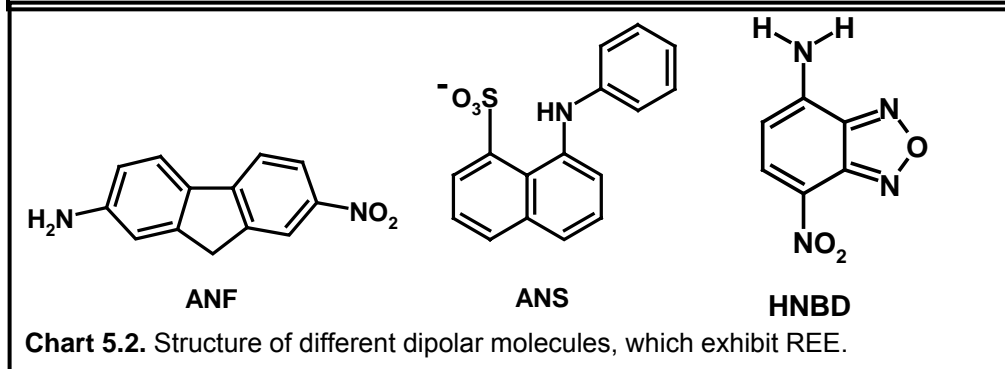
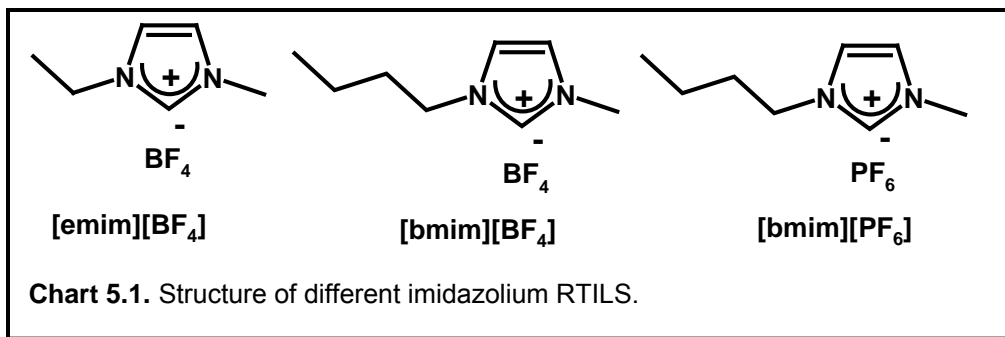
The utility driven realisation of RTILs as environmentally benign media has already been documented through a large variety of reactions in these liquids.<sup>1-6</sup> however, a little work exploring the potential of these media in photophysical and photochemical studies has so far been undertaken.<sup>7-24</sup> A vast majority of the photophysical studies carried out till date have been directed towards estimating the polarity of these liquids using various solvatochromic absorption and fluorescence probes.<sup>8,9,15,21,25</sup> These studies have indicated that the imidazolium cation based RTILs are more polar than acetonitrile but less polar than methanol; to be precise, their polarity is similar to those of the branched chain short alcohols. On the other hand, picosecond time-resolved fluorescence studies on various dipolar systems in these media have revealed a time-dependent Stokes' shift of the fluorescence maximum of the molecules in the picosecond-nanosecond time domain, suggesting that solvation is rather a

slow process in RTILs when compared to that in conventional molecular solvents such as acetonitrile or methanol.<sup>8,9,11-14,20,24</sup> However, these studies have so far indicated that the interaction between the ionic constituents of the RTILs and the solubilized molecules does not give rise to any unusual fluorescence response of the latter and that the RTILs behave very much like the conventional solvents.

During the course of our photophysical studies in RTILs, on dipolar fluorescent molecules, we observed that 2-amino-7-nitrofluorene (ANF) exhibits an excitation wavelength dependent steady state fluorescence in RTILs, a behaviour that could be termed as unusual for the following reasons. (i) The literature suggests that ANF does not exhibit excitation wavelength dependent behaviour in conventional molecular solvents,<sup>26</sup> (ii) other dipolar molecules previously examined in RTILs do not exhibit this kind of behaviour,<sup>8,9,24</sup> and (iii) the observed behaviour is contrary to what is prescribed by the famous Kasha's rule.<sup>27</sup> With a view to understanding the origin of this behaviour, we have undertaken the investigation on several electron-donor-acceptor (EDA) molecules in three different RTILs (**Chart 5.1.**) of different polarity and viscosity. The fluorescence behaviour of those dipolar probes, which show excitation wavelength dependent fluorescence spectra in RTILs, has also been examined in a viscous molecular solvent, glycerol, in order to determine whether it is only viscosity or any other specific effect that governs this unusual behaviour. The molecules studied in this work have been clubbed into two groups; the first group of molecules shown in **Chart 5.2.** does exhibit unusual excitation wavelength dependent fluorescence response; whereas, the second group of systems, put together in **Chart 5.3.** does not show this effect.

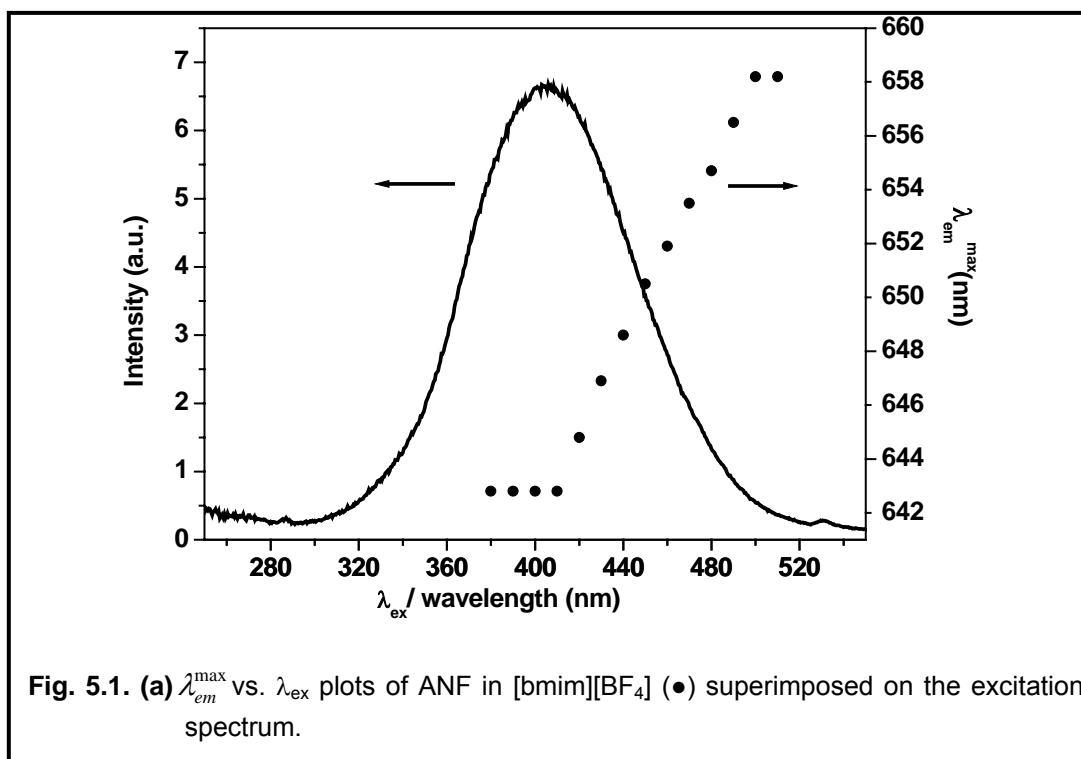
The shift of fluorescence maximum of some systems towards longer wavelength with an increase in the excitation wavelength is known for some time.<sup>28-30</sup> Extensive investigations in different media employing a variety of fluorophores, have revealed that this phenomenon could be observed frequently in frozen media such as low temperature glasses, highly viscous media, or in polymer matrices.<sup>31-33</sup> (See Section 1.4.3. for detail) Although different acronyms have been put forward to describe this phenomenon, we would like to use the acronym REE throughout the thesis. REE has quite well been exploited by several researchers for studies in biological systems and an excellent recent review on this topic is available.<sup>31</sup> Different excited state reactions can contribute to REE.<sup>34-38</sup> (See Section 1.4.3. for detail) This phenomenon can also be observed in different media.<sup>38-45</sup> (See Section 1.4.3. for detail) It is now well understood that that this type of unusual excitation wavelength dependent emission behaviour does not really violate fundamental principles such as the Kasha's rule. Rather, it arises from the operation in some specific conditions whereby the molecules in the ensemble are distributed in different interaction energy domain with the surrounding molecules. Different reasons that control the REE phenomenon can briefly be stated as follows.

The probe molecules with large change in dipole moment values ( $\Delta\mu$ ), and short fluorescence lifetime are the most suitable candidates to exhibit REE. The larger the polarity and nuclear polarizability of the medium, the stronger is the interaction of the solvent with the probe molecule and hence, greater is the chance to observe REE. The more viscous is the medium, the slower is the intermolecular excited state relaxation process and hence, higher is the possibility to observe REE.



## 5.2. Results

Absorption behaviour exhibited by ANF in RTILs, is very much similar to that in conventional solvents<sup>26,46,47</sup>. In [bmim][BF<sub>4</sub>], when ANF is excited at the blue side (say, at 360 - 380 nm) of the absorption maximum, the fluorescence emission maximum ( $\lambda_{em}^{max}$ ) of ANF in [bmim][BF<sub>4</sub>] is observed to be at 643 nm (**Fig. 5.1.(a)**). Interestingly, it can be seen from this figure, as the excitation wavelength is progressively shifted towards the red side of the absorption maximum, a small but steady shift of the fluorescence maximum is clearly observable. The variation of the emission maximum ( $\lambda_{em}^{max}$ ) of ANF in [bmim][BF<sub>4</sub>] on the excitation wavelength ( $\lambda_{ex}$ ) has been shown in **Fig. 5.1.(b)**.



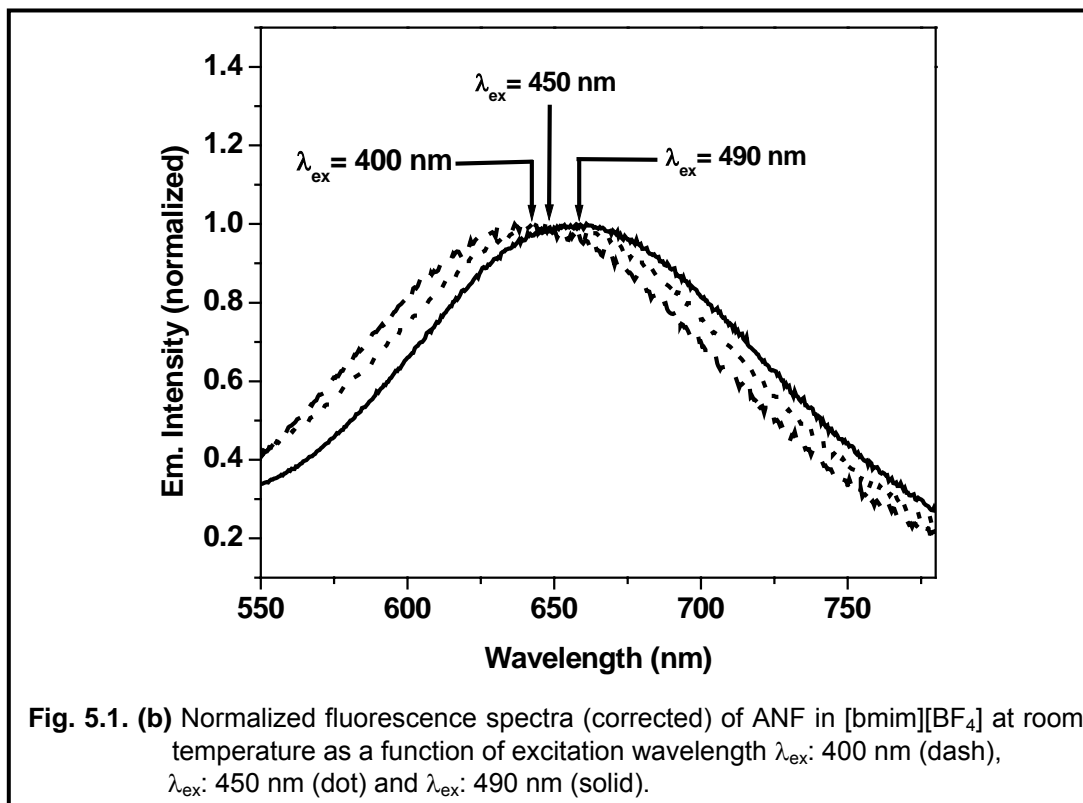


**Fig. 5.1. (b)** Normalized fluorescence spectra (corrected) of ANF in [bmim][BF<sub>4</sub>] at room temperature as a function of excitation wavelength  $\lambda_{ex}$ : 400 nm (dash),  $\lambda_{ex}$ : 450 nm (dot) and  $\lambda_{ex}$ : 490 nm (solid).

The extent of the shift, as measured from  $\lambda_{em}^{max}$  (**Fig. 5.1. (a)**), is around 14 nm in [bmim][BF<sub>4</sub>]. This sort of excitation wavelength dependent emission shift has also been observed in two other RTILs, although the extent of the shift is different in different RTILs. In two other RTILs, viz., [emim][BF<sub>4</sub>] and [bmim][PF<sub>6</sub>], the observable shift magnitudes are respectively 10 and 16 nm. The  $\lambda_{em}^{max}$  vs.  $\lambda_{ex}$  plots of ANF in the two RTILs are shown in **Fig. 5.2**. The shift magnitude of the  $\lambda_{em}^{max}$  values in three RTILs at room temperature has been collected in **Table 5.1** for comparison.

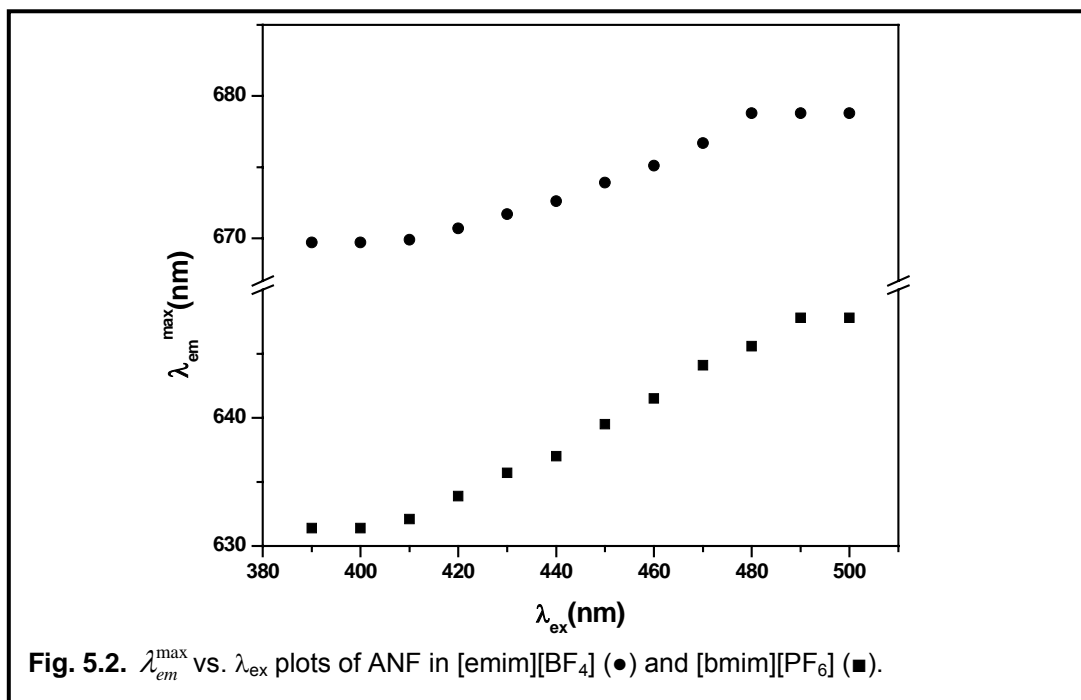


**Table 5.1.** Shift magnitude (in nm)<sup>a</sup> of the fluorescence maximum observed for dipolar probes in different media<sup>b</sup>.

	[emim][BF <sub>4</sub> ] (66.5 cP) <sup>c</sup>	[bmim][BF <sub>4</sub> ] (154 cP) <sup>c</sup>	[bmim][PF <sub>6</sub> ] (371 cP) <sup>c</sup>	Glycerol (900 cP) <sup>c</sup>
<b>ANF</b>	10	14	16	30
<b>ANS</b>	30	35	28	2
<b>HNBD</b>	14	16	13	3

<sup>a</sup> $\pm 1$  nm; <sup>b</sup>the observed shift values (nm) for ENBD, 4NBD, 6NBD, C102, C153, AP, and PRODAN in [bmim][BF<sub>4</sub>] are 1.0, 3.5, 2.0, 5.0, 1.5, 2.5, and 4.5 respectively. <sup>c</sup>The bracketed quantities are the viscosities of these media at 25°C. These values for the RTILs have been obtained from ref.5 and that for glycerol from ref.48.



In order to obtain an understanding of the plausible reason(s) for the observation of such a behaviour, we have carefully examined the excitation wavelength dependence (if any) for several other commonly employed dipolar probe molecules (shown in **Chart 5.2.** and **Chart 5.3.**). While all the systems shown in **Chart 5.3.** show normal fluorescence behaviour (with very little or negligible excitation wavelength dependence), we could identify, in addition to ANF, two more systems, HNBD and ANS (**Chart 5.2.**), which also exhibit appreciable excitation wavelength dependent shift of the fluorescence maximum (**Fig. 5.3. (a, b)** and **Fig. 5.4. (a, b)**). The shift magnitude observed for these two systems in the various RTILs has been listed in **Table 5.1.**

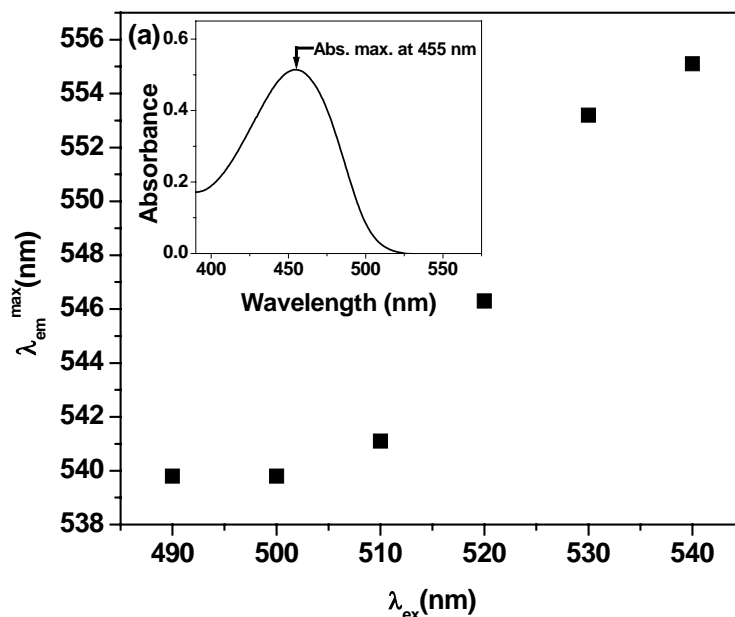


**Fig. 5.3. (a)**  $\lambda_{em}^{max}$  vs.  $\lambda_{ex}$  plots of HNBD in [bmim][BF<sub>4</sub>]. The corresponding absorption spectrum is shown as an insert.

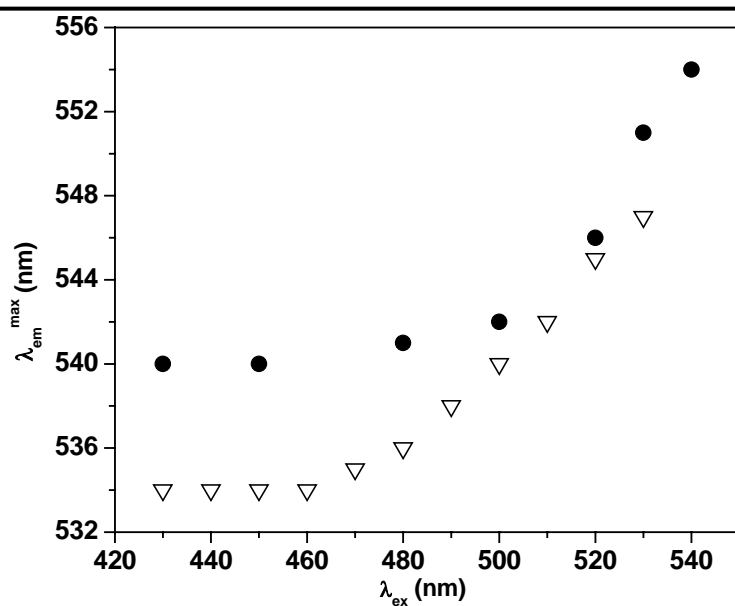


Fig. 5.3. (b)  $\lambda_{em}^{max}$  vs.  $\lambda_{ex}$  plots of HNBD in [emim][BF<sub>4</sub>] (•) and [bmim][PF<sub>6</sub>] (▽).

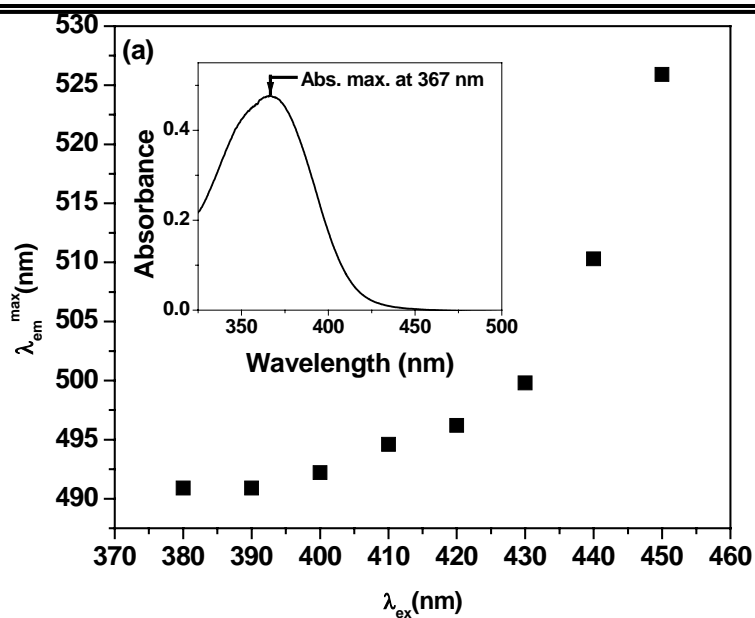
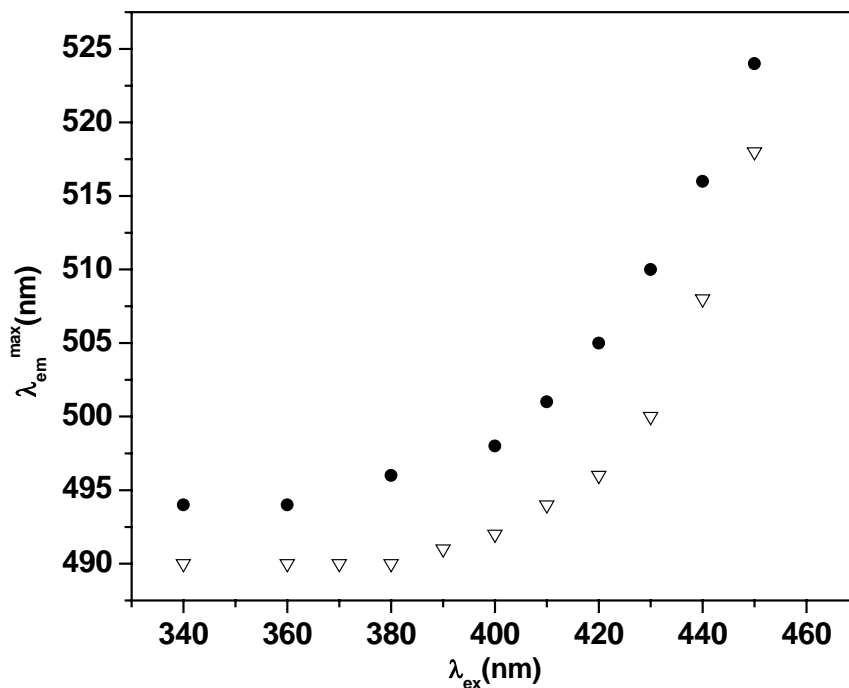
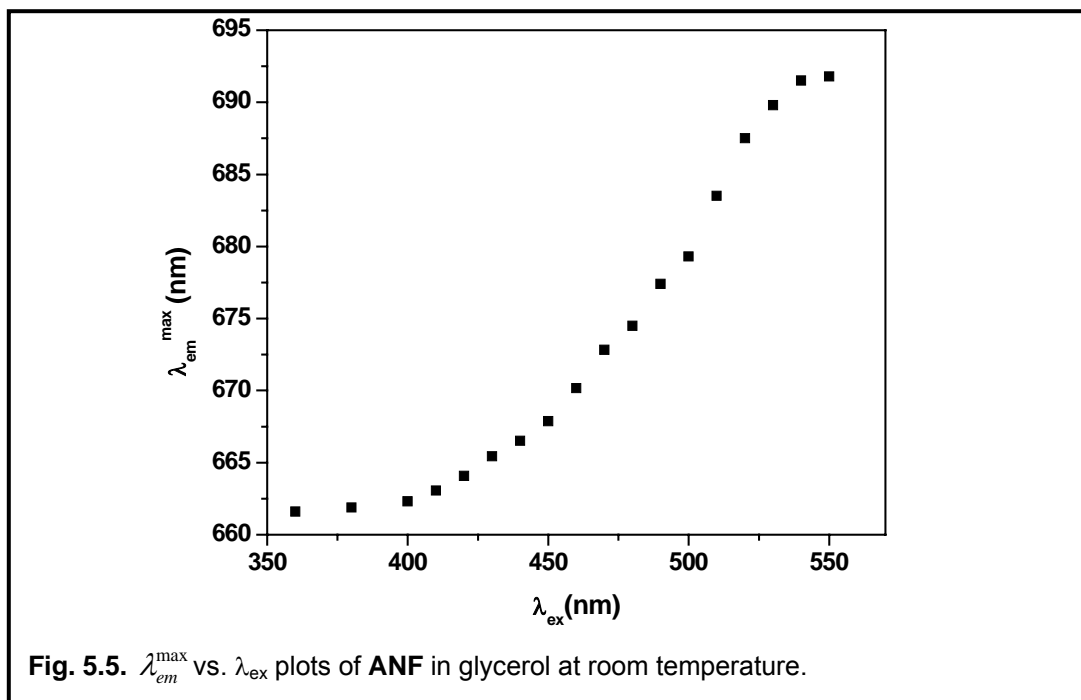


Fig. 5.4. (a)  $\lambda_{em}^{max}$  vs.  $\lambda_{ex}$  plots of ANS in [bmim][BF<sub>4</sub>]. The corresponding absorption spectrum is shown as an insert.

In order to determine whether specific interaction between the probe molecules and RTILs or the high viscosity controls the REE, we have also examined the excitation wavelength dependence of  $\lambda_{em}^{max}$  for ANF, ANS and HNBD in a viscous conventional molecular solvent, glycerol. As can be seen from **Fig. 5.5.**, ANF exhibits a more pronounced excitation wavelength dependence in relatively more viscous solvent glycerol, while the other two probes do not show any significant excitation dependent shift of the fluorescence maximum in this medium.



**Fig. 5.4. (b)**  $\lambda_{em}^{max}$  vs.  $\lambda_{ex}$  plots of ANS in [emim][BF<sub>4</sub>](●) and [bmim][PF<sub>6</sub>](▽).



### 5.3. Discussion

#### 5.3.1. Case of ANF

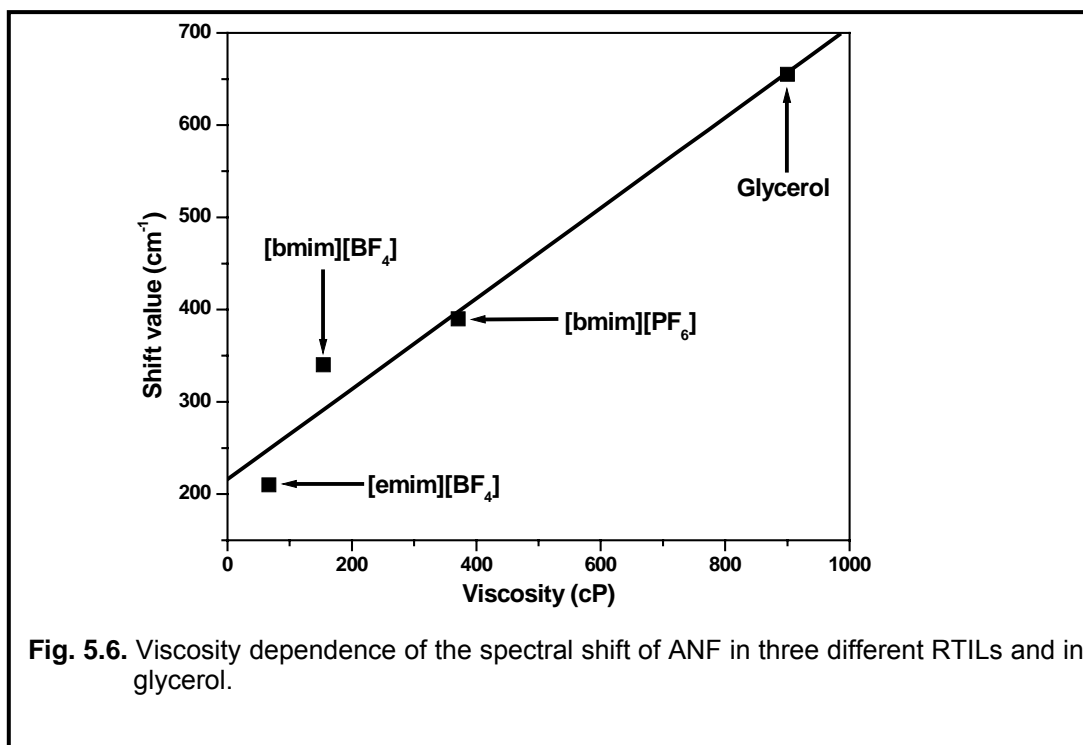
We would like to find out why ANF exhibits considerable REE in RTILs whereas the other dipolar systems such as AP, PRODAN, C153, and C102 do not. First, it is known that the extent of inhomogeneous broadening of the absorption spectrum, which permits the initial photoselection of energetically different species, depends on the change of the dipole moment on electronic excitation ( $\Delta\mu$ ).<sup>31</sup> As reported earlier, the estimated  $\Delta\mu$  is 25 D for ANF,<sup>26,46,47</sup> whereas, for C153, C102, AP and PRODAN, the values are 4.9 - 5.4,<sup>49</sup> 3.0 - 3.8,<sup>49</sup> 3.0 - 3.7,<sup>50</sup> and 4.4 - 5.0 D,<sup>51</sup> respectively. From this consideration, ANF

clearly appears to be better suited to exhibit REE compared to the other EDA systems previously employed in the study in RTILs.

The second factor, which is even more important than the first one, is that ANF has a very short fluorescence lifetime ( $\tau_f$ ) compared to the other systems (vide **Table 5.2.**). The  $\tau_f$  value of ANF in 2-propanol is reported to be <50 ps.<sup>46</sup> Our own measurement yielded a lifetime value of only ~100 ps in [bmim][BF<sub>4</sub>]. As we have discussed in the earlier chapter, recent studies on solvation dynamics suggest that solvation in imidazolium based RTILs is rather a slow process. The slow component of the solvent relaxation time in [bmim][BF<sub>4</sub>] is between 3.3 and 3.9 ns and the average solvation time is around 1.4 – 2.1 ns.<sup>8</sup> Since the solvent relaxation time ( $\langle\tau_{sol}\rangle$ ) around the photoexcited molecule is an order of magnitude higher than the  $\tau_f$  value of ANF, it is quite understandable why unrelaxed fluorescence, which gives rise to the excitation wavelength dependent emission behaviour in RTILs, could be observed in the case of ANF, even in the steady state. As the  $\tau_f$  values of AP (14 ns),<sup>50</sup> C153 (5.6 ns),<sup>52</sup> C102 (3.3 ns),<sup>52</sup> and PRODAN (3.2 ns)<sup>53</sup> in acetonitrile are higher than the  $\langle\tau_{sol}\rangle$  value of the solvent, the fluorescence occurs from a fully solvated state in these molecules and thus there is no chance of unrelaxed emission and hence no REE.

That the excitation wavelength dependent emission behaviour in [bmim][BF<sub>4</sub>], or in other two RTILs, is not due to any specific interaction between the RTILs and ANF, but is mainly due to incomplete solvation of the fluorescent state in these viscous medium, is evident from the fact that ANF does exhibit an excitation wavelength dependent shift of  $\lambda_{em}^{max}$  in a highly viscous conventional molecular solvent, glycerol also (**Fig. 5.5.**). As the plot in **Fig. 5.6.** shows, the magnitude of spectral shift is linearly related to the viscosity of the media and thus specific interaction with the RTILs is not responsible for REE. In essence, it

is the incomplete solvation in the viscous media that is primarily responsible for the observed excitation wavelength dependent spectral shift of ANF.



### 5.3.2. Case of ANS and HNBD

Both ANS and HNBD are known to exhibit REE in biological systems.<sup>44,45,54-56</sup> Thus, the excitation wavelength dependent fluorescence behaviour of these two probes in RTILs may not be surprising. However, that the case of ANS and HNBD is distinctly different from that of ANF is evident from the fact that (i) unlike ANF, both ANS and HNBD do not show much REE in a higher viscous solvent, glycerol and (ii) the  $\tau_f$  values of ANS and HNBD (8.4 and 9.6 ns respectively in [bmim][BF<sub>4</sub>]) are significantly larger than the average solvation

time of 1.4 – 2.1 ns in RTILs. Both these observations establish that the slow solvation (compared to  $\tau_f$ ) of the fluorescence state, which gives rise to REE in ANF, is not responsible for REE in ANS and HNBD. Obviously other factors contribute to REE for ANS and HNBD.

In case of negatively charged ANS, it is the electrostatic interaction which is expected to dominate the other interactions and probably plays the most significant role in creating a distribution of energetically different molecules in the ground state, which allows their photoselection. Previous reports on ANS in micellar media<sup>57,58</sup> corroborate this view of ours. Two factors could be responsible for the slow relaxation of the excited state; retardation of solvation due to the electrostatic forces induced by charged ANS and/or an inefficient energy transfer process between the energetically different species.

**Table 5.2. Fluorescence lifetime of the different systems studied.**

Systems	Media	$\tau_f$ (ns)	Reference
<b>ANF</b>	[bmim][BF <sub>4</sub> ]	0.1	This work
<b>ANS</b>	[bmim][BF <sub>4</sub> ]	8.4	This work
<b>HNBD</b>	[bmim][BF <sub>4</sub> ]	9.6	This work
<b>ENBD</b>	Acetonitrile	0.27	59
<b>4NBD</b>	Acetonitrile	9.96	59
<b>6NBD</b>	Acetonitrile	0.16	59
<b>C102</b>	Acetonitrile	3.3	52
<b>C153</b>	Acetonitrile	5.6	52
<b>AP</b>	Acetonitrile	14	50
<b>PRODAN</b>	Acetonitrile	3.2	53

Among the four structurally similar NBD derivatives we have studied, since only HNBD exhibits the shift of  $\lambda_{em}^{max}$  (not ENBD or 6NBD, which possess subnanosecond fluorescence lifetime (vide **Table 5.2.**), the origin of the excitation wavelength dependent spectral shift in HNBD has to be something different from slow solvation. Examination of the absorption characteristics of these four NBD derivatives reveals that, the full width at half maximum (FWHM) value of the first intramolecular charge transfer (ICT) band is the largest for HNBD in [bmim][BF<sub>4</sub>] (**Table 5.3.**). Also, the spectral width of this band of HNBD in RTILs is relatively larger than that in other solvents including glycerol (**Table 5.4.**).

**Table 5.3. FWHM values (in cm<sup>-1</sup>)<sup>a</sup> of the lowest energy absorption band of the NBD derivatives in [bmim][BF<sub>4</sub>].**

System	FWHM
<b>4 NBD</b>	2730
<b>6 NBD</b>	2700
<b>ENBD</b>	2990
<b>HNBD</b>	3900

<sup>a</sup>  $\pm 100 \text{ cm}^{-1}$

**Table 5.4. FWHM values (in cm<sup>-1</sup>)<sup>a</sup> of the first absorption band of HNBD in different solvents.**

Solvent	FWHM
AN	3400
MeOH	3200
Glycerol	3000
<b>[bmim][BF<sub>4</sub>]</b>	3900

<sup>a</sup>  $\pm 100 \text{ cm}^{-1}$



From the structural viewpoint, what makes HNBD unique among the rest of the systems of this group is that it possesses free amino hydrogen atoms and hence, this probe can enter into hydrogen bonding interaction utilising the hydrogen atoms. Since all the other NBD derivatives lack this type of interaction with the solvents, the spectral width of the ICT band for these systems is significantly narrower compared to HNBD. It is thus evident that hydrogen-bonding interaction between the RTIL and HNBD, where the latter plays the role of H-bond donor, provides the ground state inhomogeneity and hence facilitates the initial photoselection. Since the amino group of HNBD can form hydrogen bonding with the anionic part of the RTILs, it provides the ground state inhomogeneity. In fact, in addition to the electrostatic effects, hydrogen-bonding interaction of ANS, which contains  $-NH$  moiety, with the RTILs may also contribute to inhomogeneous broadening and slow excited state dynamics. This observation is supported by the fact that, between the two [bmim] salts used in this study, the hydrogen bond accepting ability, judged from the reported hydrogen bond basicity parameter ( $\beta$ ), is higher for [bmim][BF<sub>4</sub>] than [bmim][PF<sub>6</sub>].<sup>60,61</sup> Perhaps this is why the magnitude of the excitation wavelength dependent shift of the emission maximum is larger in [bmim][BF<sub>4</sub>] although [bmim][PF<sub>6</sub>] is a more viscous solvent. As far as the excited state relaxation is concerned, an inefficient energy transfer between the energetically different molecules, as has been stated earlier, presumably contributes to the excitation wavelength dependent fluorescence behaviour in these cases.

#### 5.4. Conclusion

An excitation wavelength dependent shift of the fluorescence emission spectra of some dipolar molecules has been observed in RTILs. This observation not only suggests that there exists a distribution of ground state molecules

differing in their interaction energies with the RTILs, but also implies that the excited state relaxation processes such as solvation and energy transfer are significantly slower in these media. While the ground state heterogeneity, which allows photoselection of the molecules is always present for these systems, even in conventional fluid media, it is the slow rate of the excited state processes, which governs the excitation wavelength dependent fluorescence behaviour in RTILs. Since the measured  $\lambda_{em}^{max}$  values of the dipolar systems are routinely used for the estimation of the polarity of the RTILs, the observation that these values can be excitation wavelength dependent suggests that proper care is extremely necessary, while choosing the probe molecules for these measurements.

## 5.5. References

- (1) Welton, T. *Chem. Rev.* **1999**, 99, 2071.
- (2) Dupont, J.; Souza, R. F. D.; Suarez, P. A. Z. *Chem. Rev.* **2002**, 102, 3667.
- (3) Wasserscheid, P.; Keim, W. *Angew. Chem., Int. Ed.* **2000**, 39, 3772.
- (4) *Ionic Liquids in Synthesis*; Welton, T. W., P., Ed.; VCH-Wiley: Weinheim, 2002.
- (5) Seddon, K. R.; Stark, A.; Torres, M. J. In *Clean Solvents: Alternative Media for Chemical Reactions and Processing*; Abraham, M., Moens, L., Eds.; ACS Symposium Series 819: Washington DC, 2002.
- (6) *Ionic Liquids, Industrial Applications for Green Chemistry*; Rogers, R. D.; Seddon, K. R., Eds.; ACS Symposium Series 818: Washington DC, 2002.
- (7) Karmakar, R.; Samanta, A. *J. Phys. Chem. A* **2002**, 106, 4447.
- (8) Karmakar, R.; Samanta, A. *J. Phys. Chem. A* **2002**, 106, 6670.
- (9) Karmakar, R.; Samanta, A. *J. Phys. Chem. A* **2003**, 107, 7340.
- (10) Karmakar, R.; Samanta, A. *Chem. Phys. Lett.* **2003**, 376, 638.
- (11) Arzhantsev, S.; Ito, N.; Heitz, M.; Maroncelli, M. *Chem. Phys. Lett.* **2003**, 381, 278.
- (12) Ito, N.; Arzhantsev, S.; Maroncelli, M. *Chem. Phys. Lett.* **2004**, 396, 83.
- (13) Ito, N.; Arzhantsev, S.; Heitz, M.; Maroncelli, M. *J. Phys. Chem. B* **2004**, 108, 5771.
- (14) Chowdhury, P. K.; Halder, M.; Sanders, L.; Calhoun, T.; Anderson, J. L.; Armstrong, D. W.; Song, X.; Petrich, J. W. *J. Phys. Chem. B* **2004**, 108, 10245.
- (15) Aki, S. N. V. K.; Brennecke, J. F.; Samanta, A. *Chem. Commun.* **2001**, 413.
- (16) Grodkowski, J.; Neta, P. *J. Phys. Chem. A* **2002**, 106, 5468.

- (17) Skrzypczak, A.; Neta, P. *J. Phys. Chem. A* **2003**, *107*, 7800.
- (18) Wishart, J. F.; Neta, P. *J. Phys. Chem. B* **2003**, *107*, 7261.
- (19) Saha, S.; Mandal, P. K.; Samanta, A. *Phys. Chem. Chem. Phys.* **2004**, *6*, 3106.
- (20) Chakrabarty, D.; Hazra, P.; Chakraborty, A.; Seth, D.; Sarkar, N. *Chem. Phys. Lett.* **2003**, *381*, 697.
- (21) Muldoon, M. J.; Gordon, C. M.; Dunkin, I. R. *J. Chem. Soc., Perkin Trans. 2* **2001**, 433.
- (22) Fletcher, K. A.; Pandey, S. *J. Phys. Chem. B* **2003**, *107*, 13532.
- (23) Fletcher, K. A.; Pandey, S. *Langmuir* **2004**, *20*, 33.
- (24) Ingram, J. A.; Moog, R. S.; Ito, N.; Biswas, R.; Maroncelli, M. *J. Phys. Chem. B* **2003**, *107*, 5926.
- (25) Bonhote, P.; Dias, A.; Papageorgiou, N.; Kalyanasundaram, K.; Gratzel, M. *Inorg. Chem.* **1996**, *35*, 1168.
- (26) Halliday, L. A.; Topp, M. R. *J. Phys. Chem.* **1978**, *82*, 2415.
- (27) Birks, J. B. *Photophysics of Aromatic Molecules*; Wiley-Inter-science: London, 1970.
- (28) Galley, W. C.; Purkey, R. M. *Proc. Natl. Acad. Sci. USA* **1970**, *67*, 1116.
- (29) Rubinov, A. N.; Tomin, V. *Opt. Spekt.* **1970**, *29*, 1082.
- (30) Weber, G.; Shinitzky, M. *Proc. Natl. Acad. Sci. USA* **1970**, *65*, 823.
- (31) Demchenko, A. P. *Luminescence* **2002**, *17*, 19.
- (32) Demchenko, A. P. In *Topics in Fluorescence Spectroscopy*; Lakowicz, J. R., Ed.; Plenum Press: New York, 1991; Vol. 3.
- (33) Lakowicz, J. R.; Nakamoto, S. K. *Biochemistry* **1984**, *23*, 3013.
- (34) Al-Hassan, K. A.; Rettig, W. *Chem. Phys. Lett.* **1986**, *126*, 273.
- (35) Demchenko, A. P.; Sytnik, A. S. *Proc. Natl. Acad. Sci. USA* **1991**, *88*, 9311.
- (36) Demchenko, A. P.; Sytnik, A. S. *J. Phys. Chem.* **1991**, *95*, 10518.
- (37) Demchenko, A. P. *Biochim. Biophys. Acta* **1994**, *1209*, 149.
- (38) Al-Hassan, K. A.; Azumi, T. *Chem. Phys. Lett.* **1988**, *150*, 344.
- (39) Zvinevich, Y. B.; Nemkovich, N. A.; Rubinov, A. N. *Zh. Prikl. Spekt.* **1993**, *58*, 237.
- (40) Rawat, S.; Mukherjee, S.; Chattopadhyay, A. *J. Phys. Chem. B* **1997**, *101*, 1922.
- (41) Rawat, S.; Chattopadhyay, A. *J. Fluoresc.* **1999**, *9*, 233.
- (42) Demchenko, A. P. *Ukr. Biochim. Zh.* **1981**, *53*, 22.
- (43) Al-Hassan, K. A.; El-Bayoumi, M. A. *J. Polymer Sci. B* **1987**, *25*, 495.
- (44) Chattopadhyay, A.; Mukherjee, S. *Biochemistry* **1993**, *32*, 3804.
- (45) Chattopadhyay, A.; Mukherjee, S. *J. Phys. Chem. B* **1999**, *103*, 8180.
- (46) Halliday, L. A. T., M. R. *Chem. Phys. Lett.* **1977**, *48*, 40.
- (47) Ruthmann, J.; Kovalenko, S. A.; Ernsting, N. P.; Ouw, D. *J. Chem. Phys.* **1998**, *109*, 5466.
- (48) Osborne, A. D.; Winkworth, A. C. *Chem. Phys. Lett.* **1982**, *85*, 513.
- (49) Samanta, A.; Fessenden, R. W. *J. Phys. Chem. A* **2000**, *104*, 8577.
- (50) Soujanya, T.; Fessenden, R. W.; Samanta, A. *J. Phys. Chem.* **1996**, *100*, 3507.
- (51) Samanta, A.; Fessenden, R. W. *J. Phys. Chem. A* **2000**, *104*, 8972.

- (52) Gones, G. I.; Jackson, W. R.; Choi, C.; Bergmark, W. R. *J. Phys. Chem.* **1985**, 89, 294.
- (53) Balter, A.; Nowak, W.; Pawelkiewicz, W.; Kowalczyk, A. *Chem. Phys. Lett.* **1988**, 143, 565.
- (54) Lakowicz, J. R. *Principles of Fluorescence Spectroscopy*, 2nd ed.; Plenum Press: New York, 1999.
- (55) Wong, M.; Thomas, J. K.; Gratzel, M. *J. Am. Chem. Soc.* **1976**, 98, 2391.
- (56) DeToma, R. P.; Easter, J. H.; Brand, L. *J. Am. Chem. Soc.* **1976**, 98, 5001.
- (57) Wehry, E. L. In *Practical Fluorescence*; Guilbault, G. G., Ed.; Marcel Dekker, Inc: New York, 1990; pp 139.
- (58) Gratzel, M.; Thomas, J. K. In *Modern Fluorescence Spectroscopy*; Wehry, E. L., Ed.; Plenum Press: New York, 1976; Vol. 2; pp 172.
- (59) Saha, S.; Samanta, A. *J. Phys. Chem. A* **1998**, 102, 7903.
- (60) Crowhurst, L.; Mawdsley, P. R.; Perez-Arlandis, J. M.; Salter, P. A.; Welton, T. *Phys. Chem. Chem. Phys.* **2003**, 5, 2790.
- (61) Anderson, J. L.; Ding, J.; Welton, T.; Armstrong, D. W. *J. Am. Chem. Soc.* **2002**, 124, 14247.

### **Concluding Remarks**

---

This chapter summarizes the results of the investigations delineated in the thesis. The scope of further studies based on the findings of the present work and recent literature has also been outlined.

---

#### **6.1. Overview**

The work embodied in the thesis had been undertaken in accordance with the plan of studying different photophysical processes in conventional solvents and RTILs. The photophysical processes that have been explored in this study are the intramolecular proton transfer, and charge transfer, and solvation dynamics. Various instrumental techniques and methodologies like IR, NMR, UV-Vis absorption, steady-state and time-resolved fluorescence, and theoretical calculations have been used in this study for the characterisation of the systems and the media and understanding of the photophysical processes. The objectives of the various projects undertaken and the results obtained from these investigations have been outlined below.

The intramolecular proton transfer phenomenon in HF, one of the most extensively studied systems, has been reinvestigated in protic solvents. Although steady-state and time-resolved fluorescence properties of HF in aprotic media are fairly well understood, the mechanism of the proton transfer reaction in HF in hydrogen bond donating solvents is far from clear. Though fluorescence measurements have indicated the formation of complexes of various stoichiometries between HF and the protic solvent molecules, specific complexes

with well-characterised photophysical behaviour have not been clearly demonstrated.

In neat alcohols and in acetonitrile-methanol mixture, we have identified for the first time a broad long wavelength absorption band with maximum ~ 410 nm. We found that selective excitation of this band did not produce either the characteristic fluorescence of the 'normal' form or the tautomer; instead, an emission characterized by a structureless band having maximum ~ 480 nm was observed. These absorption and emission bands disappear completely in the presence of water. We also found that at higher temperatures the species responsible for the 410 nm absorption band is produced at higher concentration. Furthermore, the methoxy derivative of HF did not produce the above absorption and emission features. Based on these control experiments and the literature, we have attributed the long-wavelength absorption band of HF to its anionic form, which is generated in the alcoholic media by solvent mediated deprotonation of the 3-hydroxy group of the molecule in the ground state.

The growing concern for increasing air and water pollution by volatile organic solvents has led to the realization of the importance of solvent free synthesis, use of water, supercritical carbon dioxide, different fluoruous phases, and RTILs as alternative reaction media and has given birth to '**Green Chemistry**' as a new vibrant area.

Since little is known about the photophysical behaviour of solutes in RTILs we have studied some photo-processes in these media. A large amount of time has been devoted to the synthesis and purification of the RTILs, used as media. Although the preparatory steps were somewhat straightforward, the purification process was time consuming and laborious.

### *Concluding Remarks*

In order to examine the probe dependence of the solvation dynamics in RTILs, the steady-state and time-resolved fluorescence behaviour of C102 has been investigated in [bmim][BF<sub>4</sub>]. From the steady-state fluorescence maximum of C102 in [bmim][BF<sub>4</sub>], the polarity of this RTIL has been estimated to be 50.4 in the E<sub>T</sub>(30) scale, suggesting that [bmim][BF<sub>4</sub>] is more polar than acetonitrile but less polar than methanol. The solvation dynamics has been found to be biphasic in nature consisting of picosecond and nanosecond components. The average solvation time obtained using this probe molecule is 850 ps. Earlier studies of solvation dynamics, in [bmim][BF<sub>4</sub>], have shown that the average solvation time is dependent on the probe molecule. The various solvation times estimated are as follows: 460 ps (C153), 1440 ps (PRODAN), and 2130 ps (C153). Thus, the average solvation time obtained with C102 is well within the range of values obtained by various probe molecules, reported earlier. Therefore, the present result supports the observation made earlier, that the average solvation time is dependent on the probe molecule employed. However, at this stage it is not possible to explain the nature of the probe dependence of the solvation dynamics.

While the imidazolium RTILs are being explored for quite some time, very little is known about the pyrrolidinium RTILs. We have studied both steady state and picosecond time-resolved fluorescence behaviour of three electron donor-acceptor molecules, viz., C153, AP, and PRODAN in a pyrrolidinium RTIL, [bmpy][Tf<sub>2</sub>N]. One specific reason of studying solvation dynamics in this medium was to find out whether there is any ultrafast component of solvation. Different probes have been used in order to find out whether there is any probe dependence of solvation. Since polarity of this RTIL was not known we wanted to measure the same. The steady-state fluorescence spectral data of the systems

suggest that the microenvironment around these probe molecules is similar to that in 1-decanol and that the polarity of this RTIL is comparable to that of the imidazolium RTILs. The dynamics of solvation, suggests that almost half of the relaxation is too rapid to be measured for this RTIL, using the present setup having a time resolution of 25 ps. This observation implies that earlier speculation, which attributed this ultrafast component of solvation to the planarity and polarisability of the cationic component, is not correct. The observable components of the dynamics in this particular RTIL consist of a shorter component of 115-440 ps (with smaller amplitude) and a longer component of 610-1395 ps (with higher amplitude). The average solvation time is found to be consistent with the viscosity of this particular RTIL. The dynamics of solvation is found to be dependent on the probe molecule and more than two-fold variation of the solvation time depending on the probe molecule could however be observed. No correlation of the average solvation time with the probe molecule could be drawn.

Spectral and temporal fluorescence studies had earlier indicated that the interaction between the dipolar probes and RTILs does not give rise to any unusual behaviour. However, during the course of our studies we found that the steady-state fluorescence behaviour of ANF to be excitation wavelength dependent in [bmim][BF<sub>4</sub>]. In order to determine the origin of this excitation wavelength dependent behaviour, we have studied the fluorescence behaviour of several dipolar molecules in three imidazolium RTILs, viz., [bmim][BF<sub>4</sub>], [emim][BF<sub>4</sub>], and [bmim][PF<sub>6</sub>] as a function of the excitation wavelength. While a large majority of these systems show normal fluorescence behaviour without any excitation wavelength dependence, a few systems surprisingly exhibit fairly strong excitation wavelength dependent fluorescence behaviour in these media.



### *Concluding Remarks*

The excitation wavelength dependent shift of the fluorescence maximum has been measured to be between 10 and 35 nm. ANF showed excitation wavelength dependent emission behaviour in a conventional viscous solvent, glycerol also. The excitation wavelength dependent shift of the fluorescence maximum is found to be linearly related to the viscosity of the medium. This excitation wavelength dependent fluorescence behaviour observed on red edge excitation of ANF is attributed to short excited state lifetime of ANF compared to the average solvation time in RTILs. Essentially, it is the incomplete solvation that gives rise to the excitation wavelength dependent fluorescence behaviour of ANF in RTILs.

The REE phenomenon is also observed in the case of two other probe molecules, ANS and HNBD. ANS and HNBD, form a distribution of energetically different species in the ground state, due to their ability to interact with RTILs through coulombic and hydrogen bonding network respectively. It is shown that the existence of a distribution of energetically different species in the ground state coupled with a slow rate of either or both the excited state relaxation processes, viz., solvation and energy transfer, are responsible for the excitation wavelength dependent fluorescence behaviour for these systems in RTILs.

### **6.2. Future prospects**

We have shown that the hydrogen bond donating and accepting ability of the solvents can play a major role in dictating the photophysical behaviour of a system. The observation of new absorption and emission features in the case of a molecular system, which is one of the most extensively studied systems, implies that it is possible to obtain a wealth of informations by careful examination of other systems that have not been looked into in such detail.

Although a number of solvation dynamics studies have already been carried out in RTILs, there are several issues that remain unanswered. Neither the origin of the ultrafast component of the dynamics nor is the time-constant of this component known at present. There is still disagreement on what the two observable components of the dynamics represent. The probe dependence of the solvation dynamics is another aspect that is far from clear. Therefore, it is necessary that further studies be undertaken to address these aspects of solvation dynamics. The mechanism of solvation dynamics in RTILs can be understood fully when additional solvation data on a variety of RTILs and probe molecules are obtained under identical experimental conditions.

Theoretical simulation studies on the dynamical behaviour of the RTILs are absolutely essential in this regard. It is only when definite information on the time scales of the ionic constituents of the various RTILs are available from these simulation studies, perhaps one will be in a position to understand the time-resolved Stokes' shift data of the molecules.

One must not forget that the ionic constituents of the RTILs are highly associated. Experimental results have demonstrated clearly that a high percentage of the ions exist in the associated form. One can therefore expect contributions to the solvation dynamics from these associated species, which could be an ion-pair or higher order ionic aggregates.

While the excitation wavelength dependent fluorescence behaviour of some dipolar systems in RTILs is an interesting observation, it is a matter of concern too. For example, one of the most common utilities of the fluorescence studies in RTILs has been the measurement of the polarity of these media from the wavenumber corresponding to the fluorescence maximum. However, when

### *Concluding Remarks*

this quantity dependent on the excitation wavelength, one does not know which value to use for these measurements.

The usage of the RTILs depends largely on how transparent these substances are in the optical region. Since the recent reports suggest that the imidazolium RTILs possess significant absorption in the UV region, it becomes necessary to look for RTILs that are more transparent.

## Appendix 1

### Estimation of equilibrium constant of formation of anion of HF in alcoholic solvents

Let us assume that the molecule HF is HP where H stands for proton and P stands for the probe itself. 'A' stands for the alcohol molecule.  $P^-$  is the anion of HF and  $AH^+$  is the protonated alcoholic species. Let us consider the equilibrium as follows:

$$\begin{aligned}
 & HP + A \xrightleftharpoons{K_e} P^- + AH^+ \\
 & K_e = \frac{[P^-]_e [AH^+]_e}{[HP]_e [A]_e} \\
 & = \frac{[P^-]_e^2}{\{[HP]_0 - [P^-]_e\} \{ [A]_0 - [AH^+]_e \}} \quad [\text{Assuming } [P^-]_e = [AH^+]_e] \\
 & = \frac{[P^-]_e^2}{\{[HP]_0 - [P^-]_e\} \{ [A]_0 \}} \quad [\text{Assuming } [A]_0 \gg [AH^+]_e] \\
 & \text{Thus, } K_e \times [A]_0 = \frac{[P^-]_e^2}{\{[HP]_0 - [P^-]_e\}} \dots\dots\dots (i)
 \end{aligned}$$

Now, Optical Density (OD) at 407 nm =  $OD_{407} = \epsilon_P \times [P^-]_e$

Thus from equation (i) we get,

$$\begin{aligned} \frac{1}{K_e [A]_0} &= \frac{[HP]_0}{[P^-]_e^2} - \frac{1}{[P^-]_e} \\ &= \frac{[HP]_0 \epsilon_{P^-}^2}{OD_{407}^2} - \frac{\epsilon_{P^-}}{OD_{407}} \\ \frac{\epsilon_{HP}}{\epsilon_{P^-}^2} \frac{1}{K_e [A]_0} &= \frac{OD_{HP}}{OD_{407}^2} - \frac{\epsilon_{HP}}{\epsilon_{P^-}} \frac{1}{OD_{407}} \end{aligned}$$

On rearrangement, we get the final equation,

$$\frac{\epsilon_{HP}}{\epsilon_{P^-}^2} \frac{1}{K_e} \frac{1}{[A]_0} = \frac{OD_{HP}}{OD_{407}^2} - \frac{\epsilon_{HP}}{\epsilon_{P^-}} \frac{1}{OD_{407}} \dots\dots\dots(ii)$$

Thus, plotting the R.H.S. against  $\frac{1}{[A]_0}$ , we will get a straight line. The slope of

that straight line will be equal to  $\frac{\epsilon_{HP}}{\epsilon_{P^-}^2} \frac{1}{K_e}$ .

Thus, if the extinction coefficient of the parent molecule and the anion is known we will be able to get the value of equilibrium constant. The extinction coefficient value of parent molecule is known to be  $1.7 \times 10^4 \text{ M}^{-1} \text{cm}^{-1}$  (ref. *J. Phys. Chem.* **1983**, 87, 1127) and that of the anion was measured to be  $1.44 \times 10^4 \text{ M}^{-1} \text{cm}^{-1}$ . With different experimental sets the value of the equilibrium constant was calculated to be  $2.9 \times 10^{-7}$ .